



Supplemental Material to:

Synthesis and *in vitro* Evaluation of C7 and C8 Luteolin Derivatives as Influenza Endonuclease Inhibitors

Róbert Reiberger^{1,2†}, Kateřina Radilová^{1,3†}, Michal Král^{1,3}, Václav Zima^{1,2}, Pavel Majer¹, Jiří Brynda^{1,4}, Martin Dračinský¹, Jan Konvalinka^{1,5}, Milan Kožíšek^{1,*} and Aleš Machara^{1,*}

¹ Institute of Organic Chemistry and Biochemistry of the Academy of Sciences of the Czech Republic, Gilead Sciences and IOCB Research Center, Flemingovo n. 2, 166 10 Prague 6, Czech Republic; robert.reiberger@uochb.cas.cz (R.R.); katerina.radilova@uochb.cas.cz (K.R.); michal.kral@uochb.cas.cz (M.K.); vaclav.zima@uochb.cas.cz (V.Z.); pavel.majer@uochb.cas.cz (P.M.); jiri.brynda@uochb.cas.cz (J.B.); martin.dracinsky@uochb.cas.cz (M.D.); jan.konvalinka@uochb.cas.cz (J.K.)

² Department of Organic Chemistry, Faculty of Science, Charles University, Hlavova 8, 128 00 Prague 2, Czech Republic

³ First Faculty of Medicine, Charles University, Kateřinská 1660, 121 08 Prague 2, Czech Republic

⁴ Institute of Molecular Genetics of the Academy of Sciences of the Czech Republic, Vídeňská 1083, 140 00 Prague 4, Czech Republic

⁵ Department of Biochemistry, Faculty of Science, Charles University, Hlavova 8, 128 00 Prague 2, Czech Republic

[†] These authors contributed equally to this work

* Correspondence: milan.kozisek@uochb.cas.cz (M.K.); ales.machara@uochb.cas.cz (A.M.); Tel.: +420-220-183-479 (A.M.)

Table of Contents

AlphaScreen titration curves	3
Gel-based cleavage assay – wild type	4
Gel-based cleavage assay – comparison of wild type with I38T	6
ssDNA and ssRNA cleavage efficiency of PA-Nter WT and I38T mutant	7
Crystallographic data – Table S1	9
Conditions screening of Mannich aminomethylation	11
¹ H, ¹³ C, ¹⁹ F and ³¹ P NMR spectra	12
HPLC analysis of final compounds	79

AlphaScreen titration curves

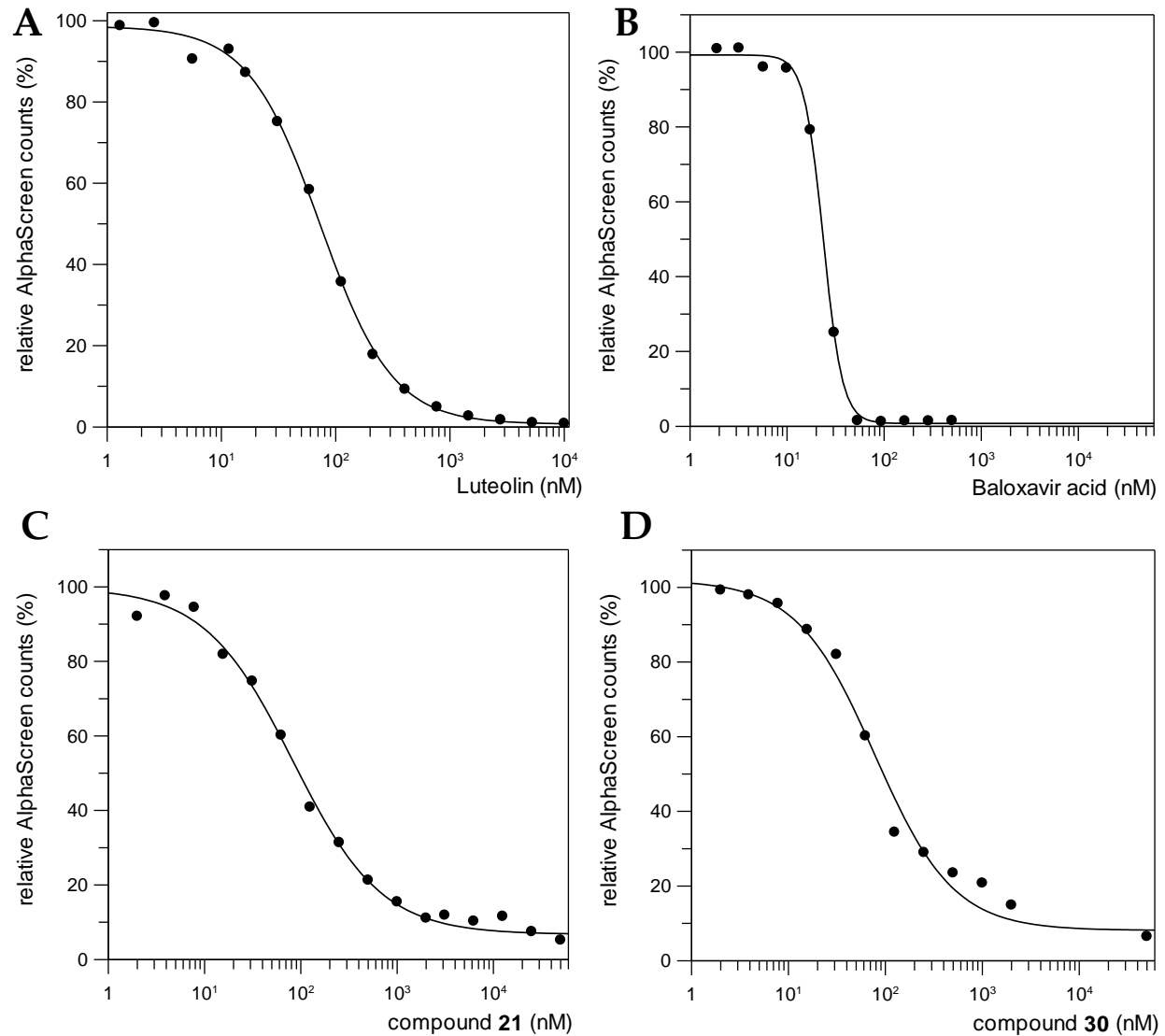
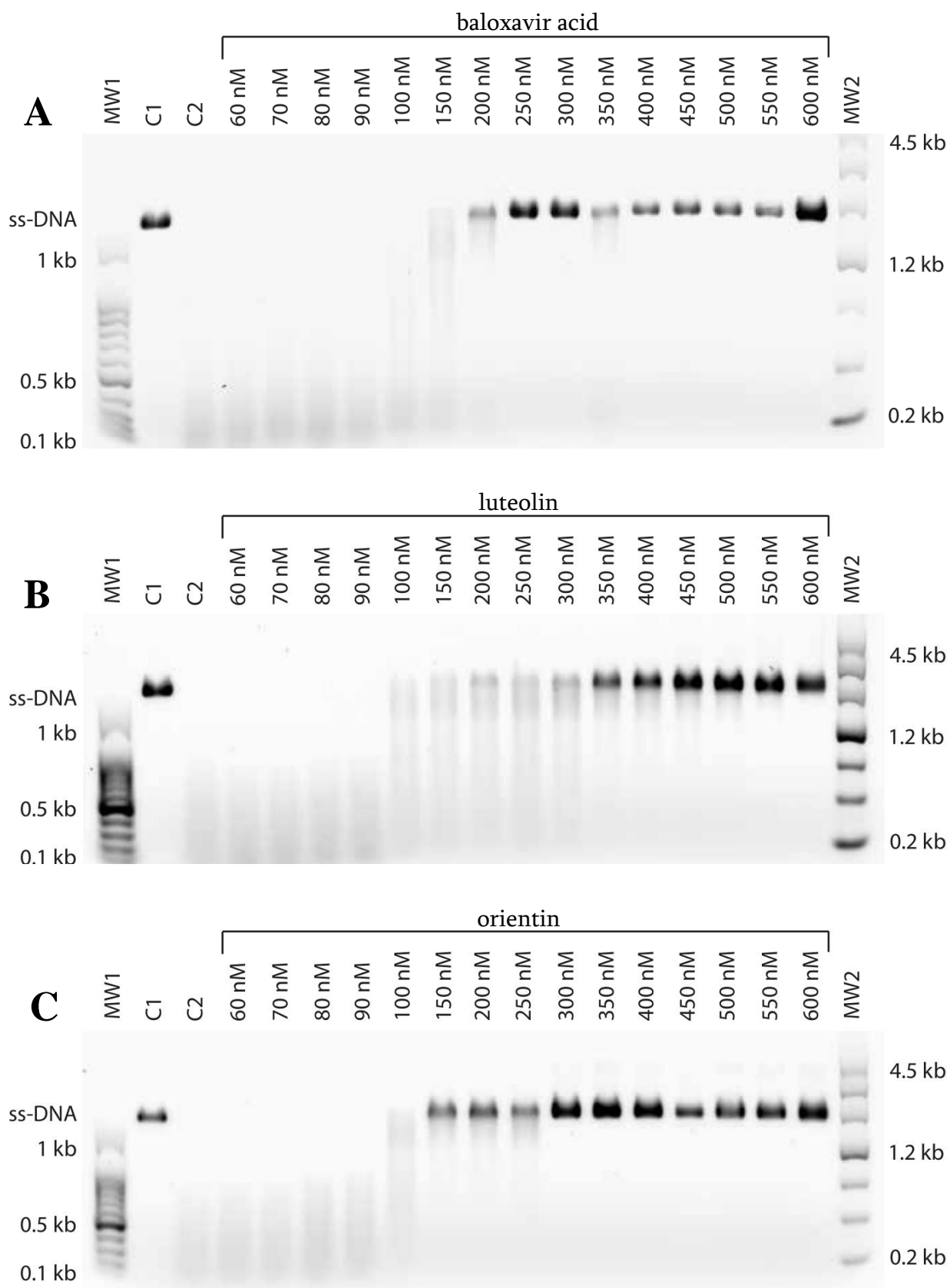


Figure S1. AlphaScreen titration curves of luteolin (A), baloxavir acid (B), compound 21 (C), and compound 30 (D).

Gel-based cleavage assay – wild type



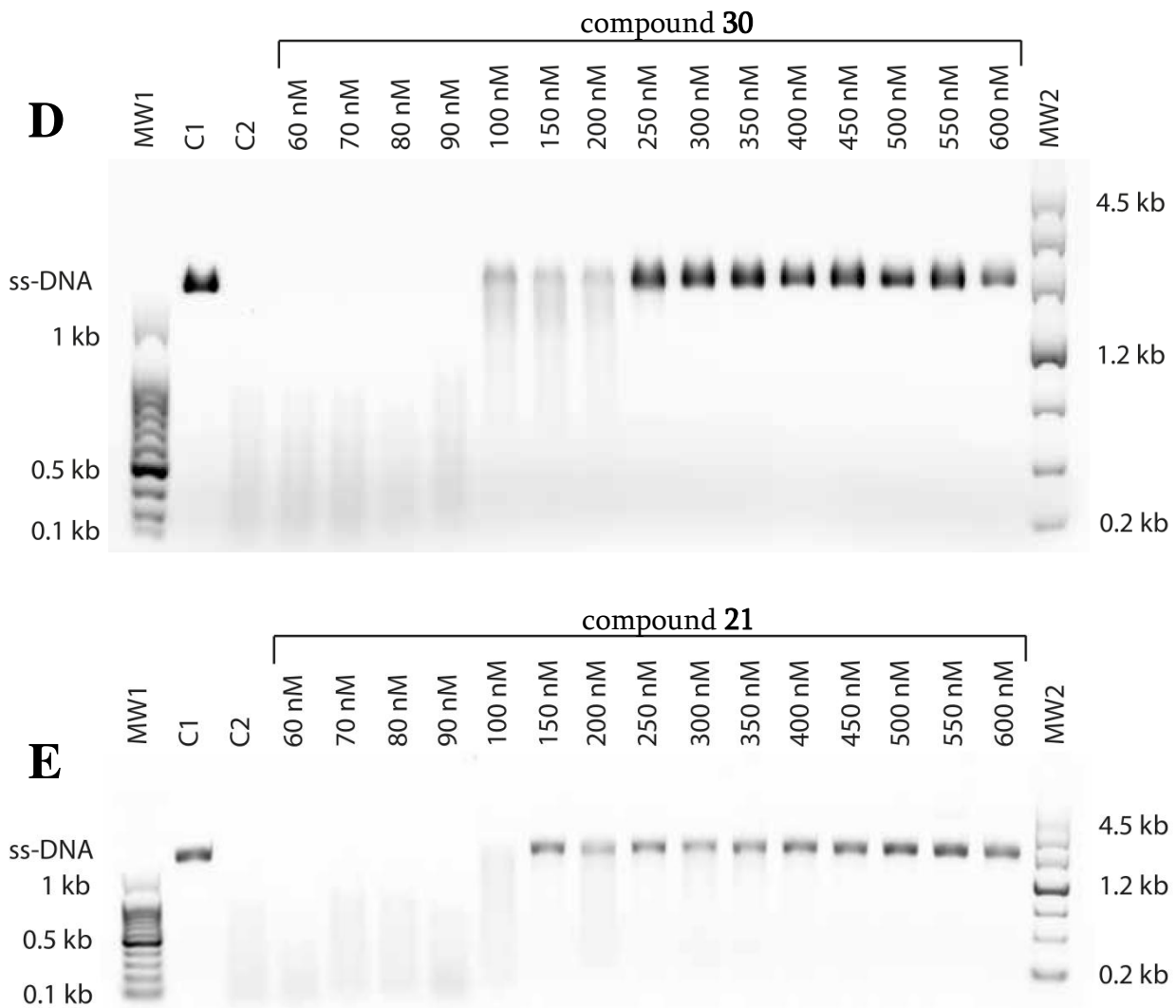


Figure S2. Inhibition of endonuclease activity by of baloxavir acid (A), luteolin (B), orientin (C), compound **30** (D), and compound **21** (E). The single-stranded DNA M13mp18 was used as substrate (lane C1). Fully cleaved substrate without any inhibitor was used as control (lane C2). The GelPilot 100bp Plus Ladder molecular weight marker (lane MW1) and the GelPilot Wide Range Ladder molecular weight marker (lane MW2) are as reference.

Gel-based cleavage assay – comparison of wild type with I38T

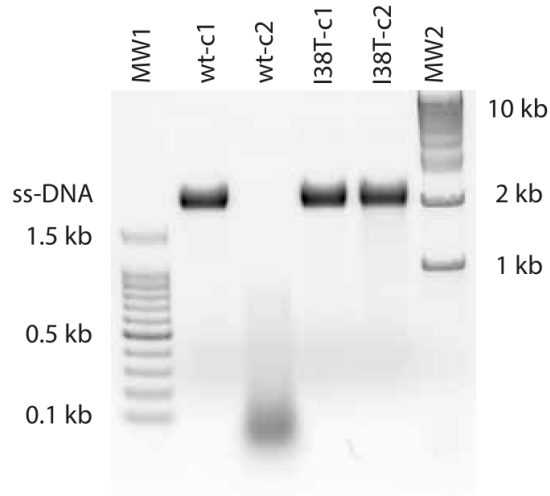


Figure S3. Endonuclease cleavage comparison of wild type and I38T mutant variant. The single-stranded DNA M13mp18 was used as substrate. The uncleaved DNA without endonuclease was used as control (lines wt-c1 and I38T-c1). The overnight cleavage of substrate by 1 μ M endonucleases (PA-Nter-wt/PA-Nter-I38T) in the presence of metal ions is shown in lines wt-c2 (for PA-Nter-wt) and I38T-c2 (for PA-Nter-I38T). The GelPilot 100bp Plus Ladder molecular weight marker (lane MW1) and the GelPilot 1 kb Ladder molecular weight marker (lane MW2) are as reference.

ssDNA and ssRNA cleavage efficiency of PA-Nter WT and I38T mutant

To detect the endonuclease activity of the PA-Nter WT and I38T, FRET-based endonuclease assay was performed in 96-well black microplate and measured with Tecan Infinite M1000 reader (Tecan, Switzerland). Two dual-labelled oligonucleotides with 5'-6-FAM (5'6-carboxyfluorescein) fluorophore and a 3'-BHQ1 quencher (3'-Black Hole Quencher 1) were used as substrates for testing the endonuclease activities and specificities. The substrate S1 of a sequence 5'(6-FAM)-dT-dC-dT-dC-dT-dA-dG-dC-dA-dG-dT-dG-dG-dC-dG-dC-3'(BHQ1) (Generi Biotech, Czech Republic) was used as ssDNA substrate, the substrate S2 of a sequence 5'(6-FAM)-rA-rA-rA-rA-rA-rA-rA-rA-rA-rA-3'(BHQ-1) (Integrated DNA Technologies, Inc., USA) was used as ssRNA substrate. Cleavage of the oligonucleotide substrate liberates the 6-FAM fluorophore from the BHQ1 quencher resulting in an increase of the fluorescent signal. FRET-based endonuclease assay was performed by incubating 1 μ M GST-PA-Nter (WT or I38T mutant) with 1 μ M substrate at 37°C in a final volume of 40 μ l in reaction buffer 25 mM Tris-HCl, pH 7.4, 150 mM NaCl, 0.05% Tween20, 1 mM MnCl₂, 10 mM MgCl₂, 1 mM 2-mercaptoethanol. Consequent to the endonuclease cleavage the fluorescent signal was measured at the wavelength of 485 nm excitation and 535 nm emission.

The PA-Nter WT enzyme cleaved both ssRNA and ssDNA substrates, with higher efficiency to the ssRNA sequence. Implementation of the I38T mutation caused change in substrate selectivity, where only the ssRNA substrate was cleaved. This result is in agreement with the gel-based cleavage assay, where ssDNA M13mp18 was cleaved only with PA-Nter WT endonuclease (Figure S3). The catalytic efficiency was significantly affected by the mutation, the activity of the mutant endonuclease was only 1.9 % of the wild-type activity (determined as a ratio of slopes of the yellow and red linear curves in Figure S4).

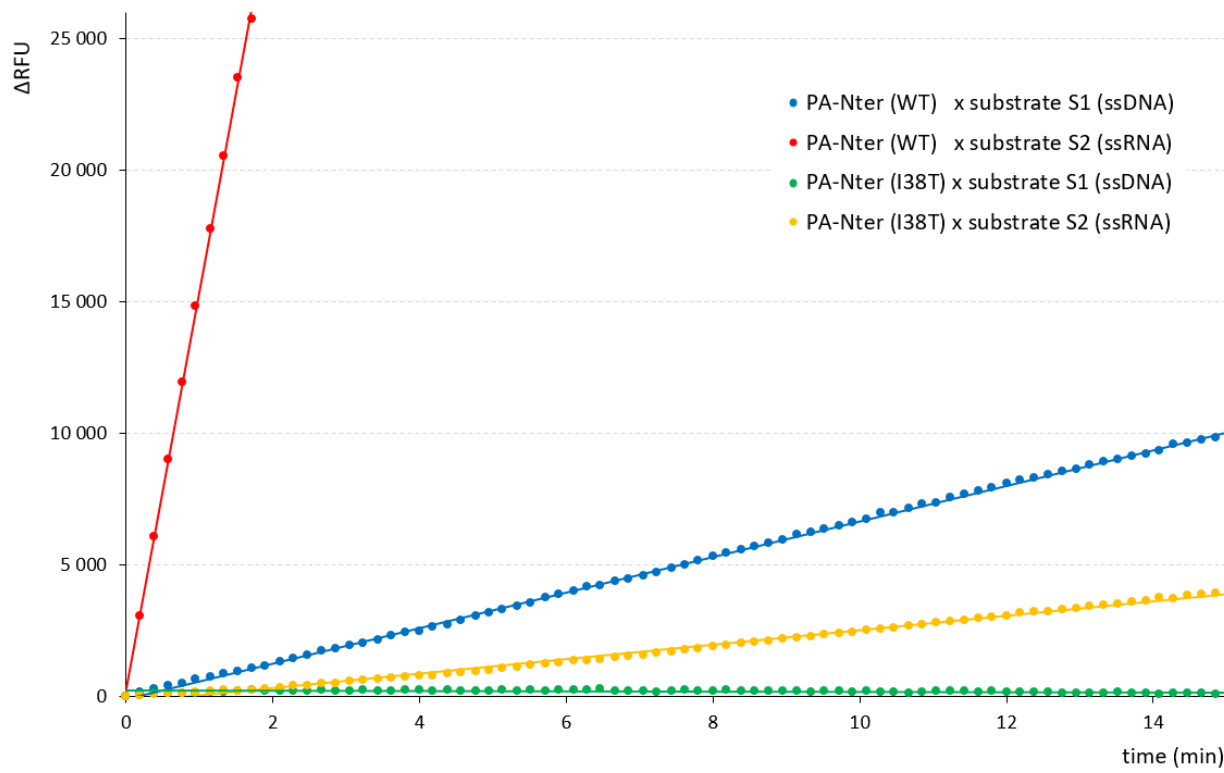


Figure S4. Detection of PA-Nter activity measured by FRET-based endonuclease assay. The enzymes were monitored for their cleavage of ssDNA substrate S1 (WT in blue, I38T in green) or ssRNA substrate S2 (WT in red, I38T in yellow).

Crystallographic data – Table S1

Table S1 – Diffraction data collection and refinement statistics:

	PA-Nter-wt	PA-Nter-I38T
Data collection statistics		
Wavelength (Å)	1.54187	1.54187
Space group	<i>P</i> 6 ₄ 22	<i>P</i> 6 ₄ 22
Cell parameters (Å, °)	74.36, 74.36, 126.46, 90.0, 90.0, 120.0	74.97, 74.97, 127.57, 90.0, 90.0, 120.0
Resolution range (Å)	50.00-1.90 (2.02-1.90)	50.00-2.20 (2.26-2.20)
Number of unique reflections	16,879 (1,211)	10,985 (770)
Multiplicity	9.3 (6.2)	6.8 (4.2)
Completeness (%)	99.5 (99.3)	90.4 (62.5)
R _{merge} ^a	9.4 (130.9)	5.9 (147.3)
CC _(1/2) (%)	99.8 (58.2)	99.2 (98.1)
Average I/σ(I)	15.29 (1.6)	15.96 (1.21)
Wilson B (Å ²)	29.27	41.7
Refinement statistics		
Resolution range (Å)	42.15-1.90 (1.95-1.90)	45.24-2.20 (2.26-2.20)
No. of reflection in working set	16,040 (1,150)	10,437 (731)
No. of reflection in the test set	845 (61)	549 (36)
R _{work} value (%) ^b	19.50 (39.2)	19.27 (31.4)
R _{free} value (%) ^c	25.05 (38.9)	26.41 (32.8)
RMSD bond length (Å)	0.01	0.01
RMSD angle (°)	1.5	1.4
Mean ADP value (Å ²)	26.5	42.1
Ramachandran plot statistics^d		
Residues in favored regions (%)	97.8	96.1
Residues in allowed regions (%)	2.2	3.9
PDB code	7NUG	7NUH

The data in parentheses refer to the highest-resolution shell for data collection statistic.

^a R_{merge} = (|I_{hkl} - ⟨I⟩|)/I_{hkl}, where the average intensity ⟨I⟩ is taken over all symmetry equivalent measurements and I_{hkl} is the measured intensity for any given reflection

^b R-value = ||F_o| - |F_c||/|F_o|, where F_o and F_c are the observed and calculated structure factors, respectively.

^c R_{free} is equivalent to R-value but is calculated for 5% of the reflections chosen at random and omitted from the refinement process.^[1]

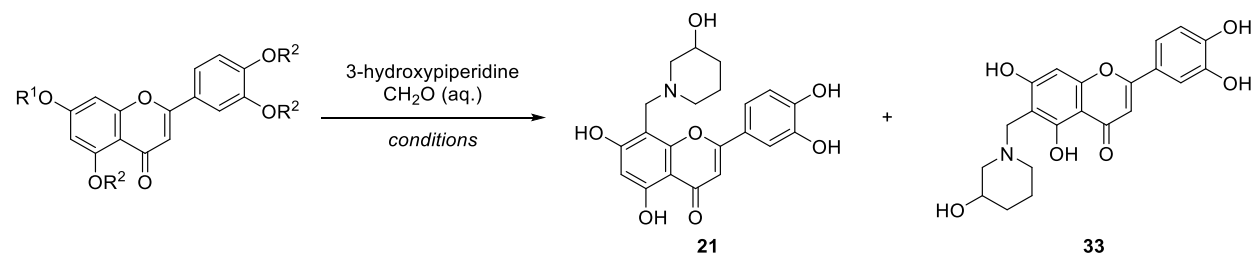
^d As determined by Molprobity.^[2]

¹ Murshudov, G. N.; Skubak, P.; Lebedev, A. A.; Pannu, N. S.; Steiner, R. A.; Nicholls, R. A.; Winn, M. D.; Long, F.; Vagin, A. A., REFMAC5 for the refinement of macromolecular crystal structures. *Acta Crystallographica Section D-Structural Biology* **2011**, 67, 355-367.

² Chen, V. B.; Arendall, W. B.; Headd, J. J.; Keedy, D. A.; Immormino, R. M.; Kapral, G. J.; Murray, L. W.; Richardson, J. S.; Richardson, D. C., MolProbity: all-atom structure validation for macromolecular crystallography. *Acta Crystallographica Section D-Structural Biology* **2010**, 66, 12-21.

Conditions screening of Mannich aminomethylation

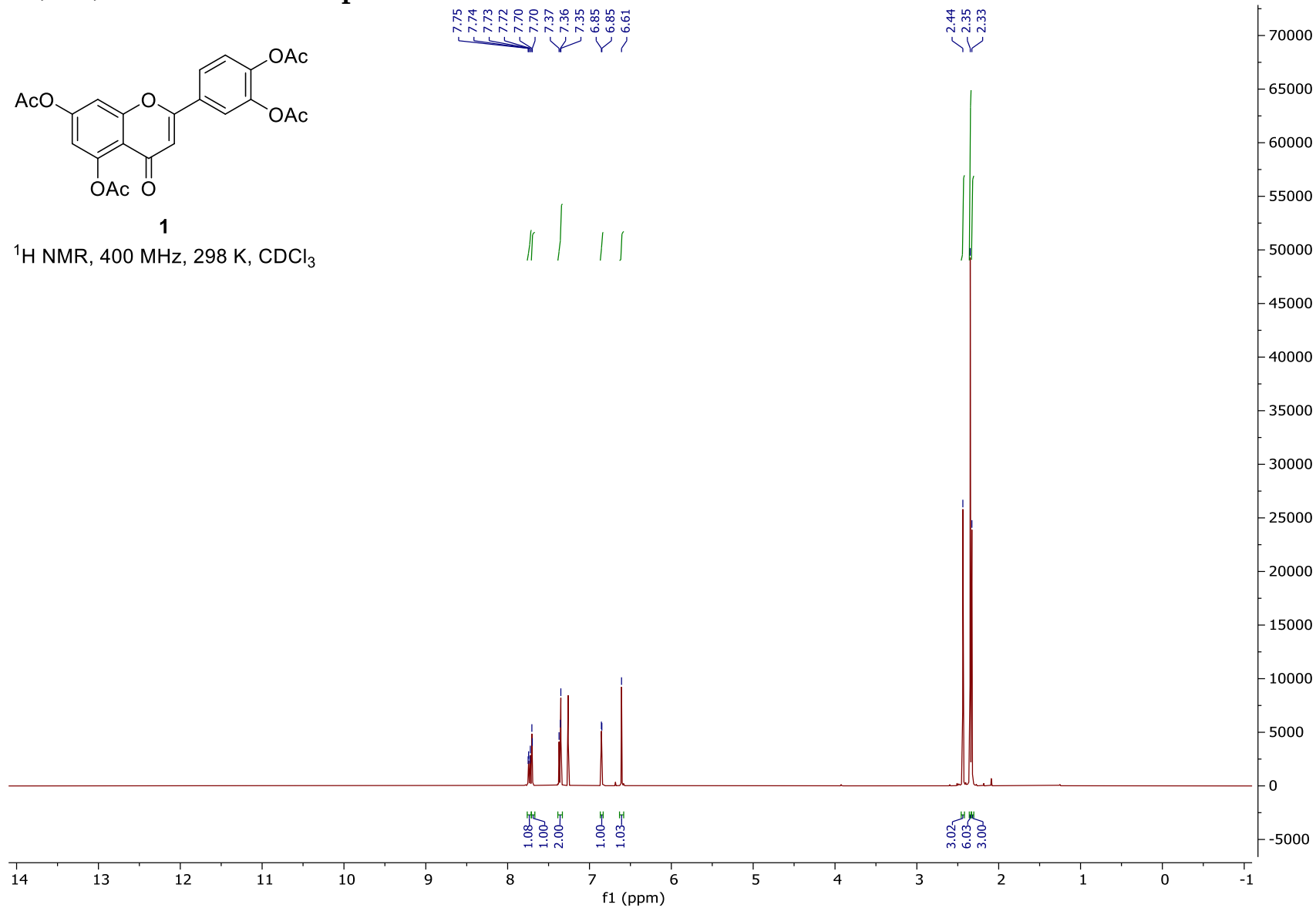
Table S2 – Conditions screening of Mannich aminomethylathion of luteolin with 3-hydroxypiperidine:

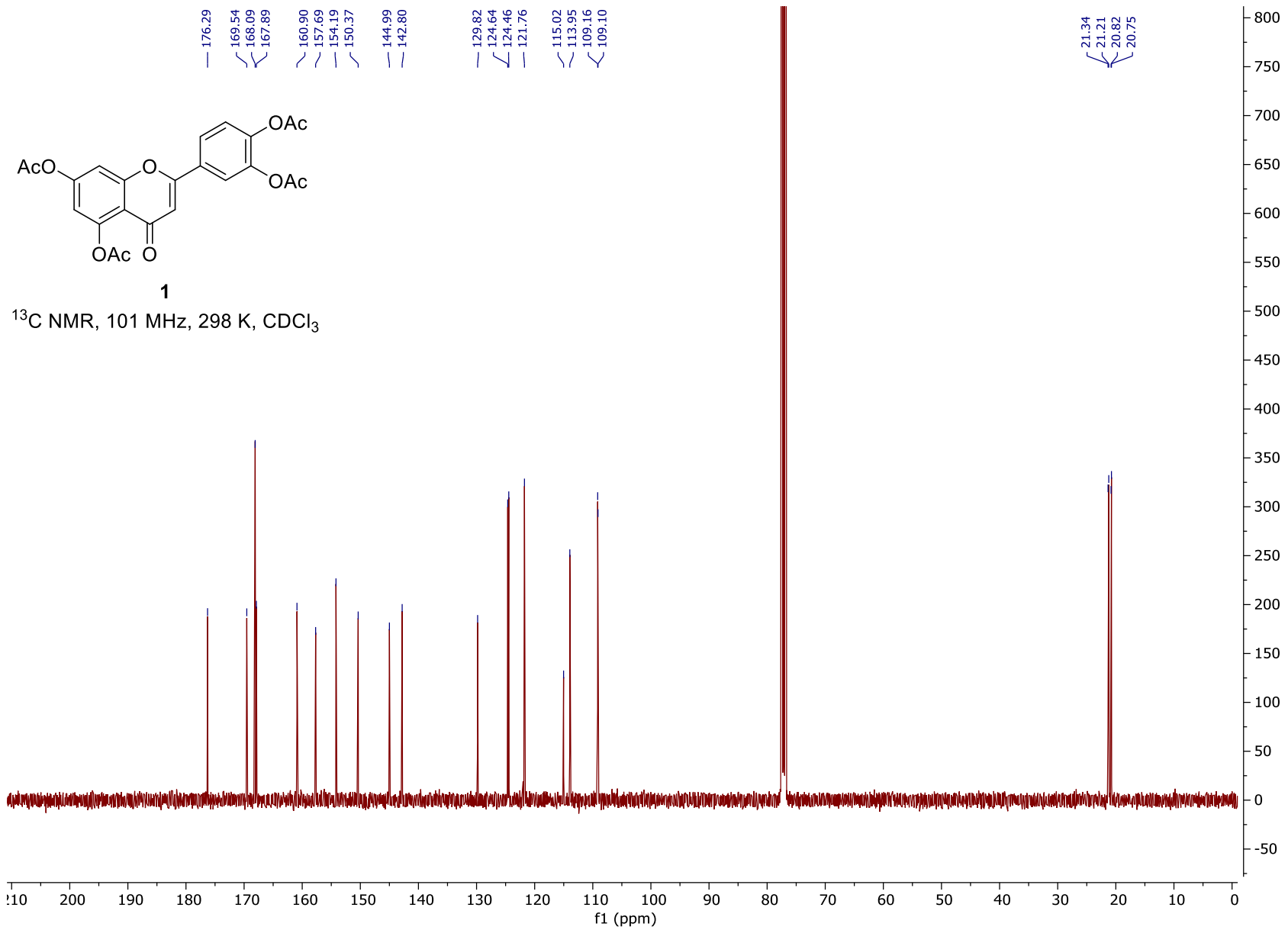


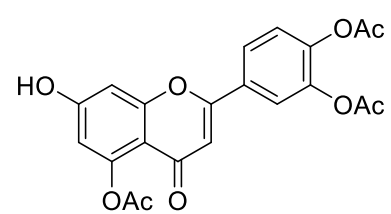
entry	R ¹	R ²	conditions	amine (eq.)	formalin (eq.)	T (°C)	conversion ^a (%)	yield 21 (%)	ratio ^a (21 : 33)
1	H	H	EtOH, 16 h	1.0	1.0	r.t	58	4 ^a	82:18
2	H	H	MeOH, 16 h	1.0	1.0	r.t	86	20 ^b	44:26
3	H	H	dmap, dioxane, 4 h	1.2	1.2	100	-	0 ^{a,d}	N/A
4	H	H	dmap, <i>i</i> -PrOH	1.2	1.2	70	-	0 ^{a,d}	N/A
5	H	H	<i>i</i> -PrOH, 5 d	1.5	0.8	35	0	0 ^{a,c}	N/A
6	H	Ac	DMF/MeOH (4:1), 14 h	2.0	2.0	r.t	-	0 ^{a,d}	N/A
7	Ac	Ac	1. CHCl ₃ , 36 h 2. 2M LiOH (aq.), MeOH	2.0	2.0	r.t	39	14 ^b	95:5
8	Ac	Ac	1. CHCl ₃ , <i>p</i> -TSA, 4 d 2. 2M LiOH (aq.), MeOH	1.5	1.5	r.t	0	0 ^{a,c}	N/A
9	Bn	Bn	CHCl ₃ , 2 d	2.0	2.0	r.t	0	0 ^{a,c}	N/A
10	MOM	MOM	EtOH, 16 h	1.0	1.0	r.t	0	0 ^{a,c}	N/A
11	MOM	MOM	CHCl ₃ , 36 h	2.0	2.0	r.t	0	0 ^{a,c}	N/A

a) Determined by UHPLC-MS. **b)** Yield obtained by multiple preparative HPLC isolation. **c)** No reaction. **d)** Full decomposition of starting material was observed. N/A = not applicable

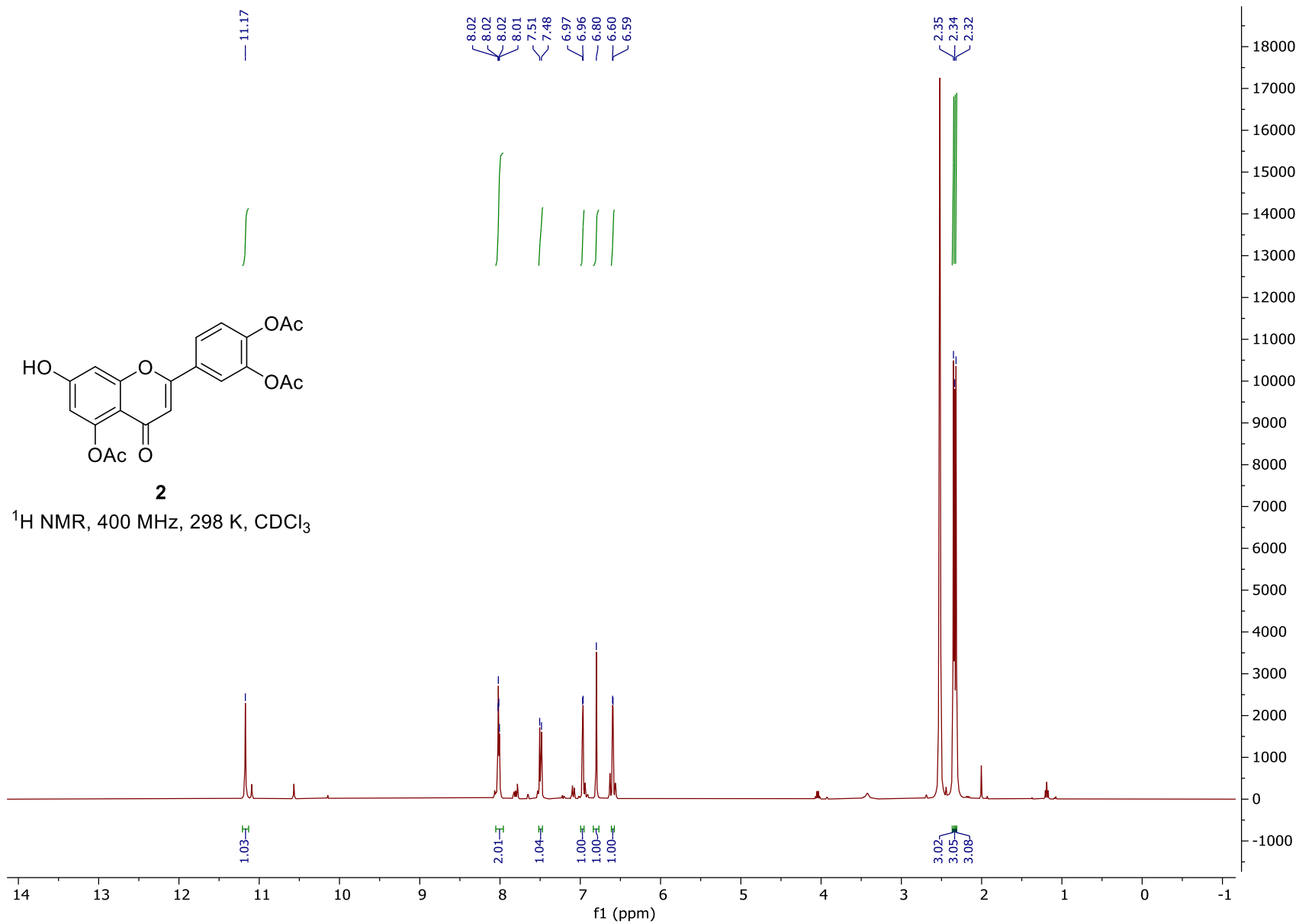
^1H , ^{13}C , ^{19}F and ^{31}P NMR spectra

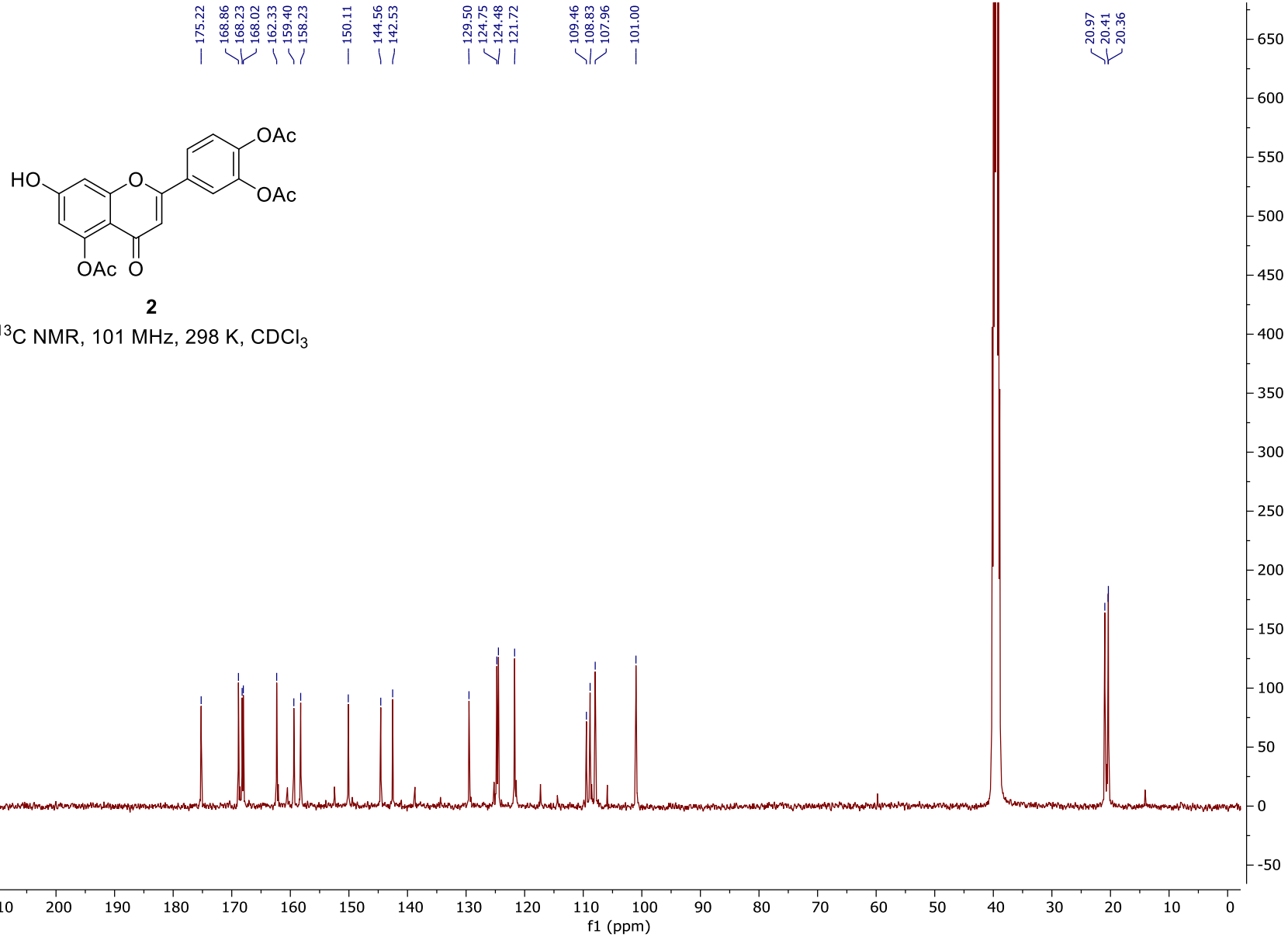


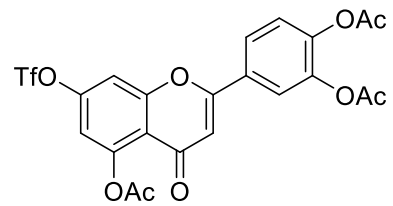




^1H NMR, 400 MHz, 298 K, CDCl_3

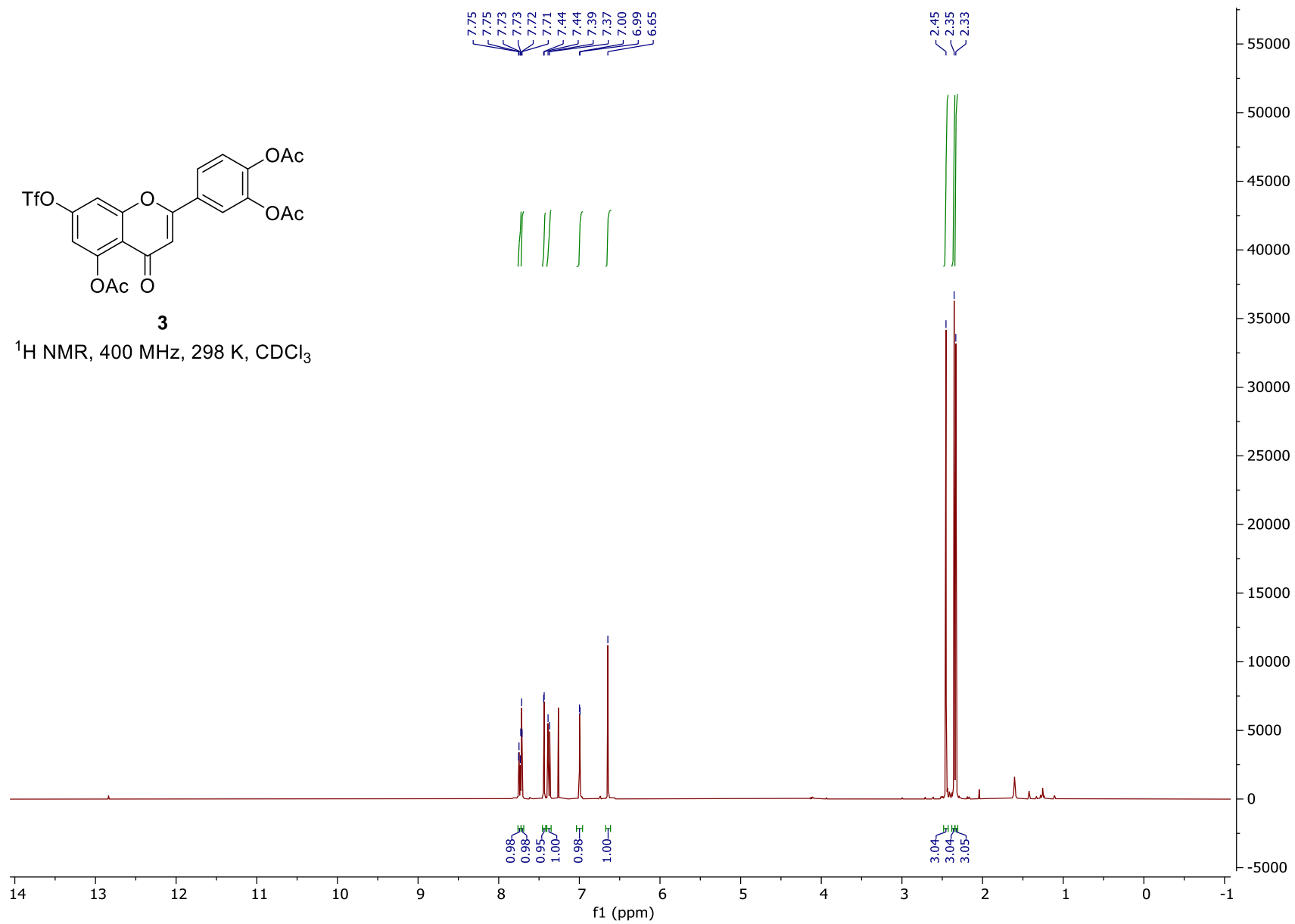


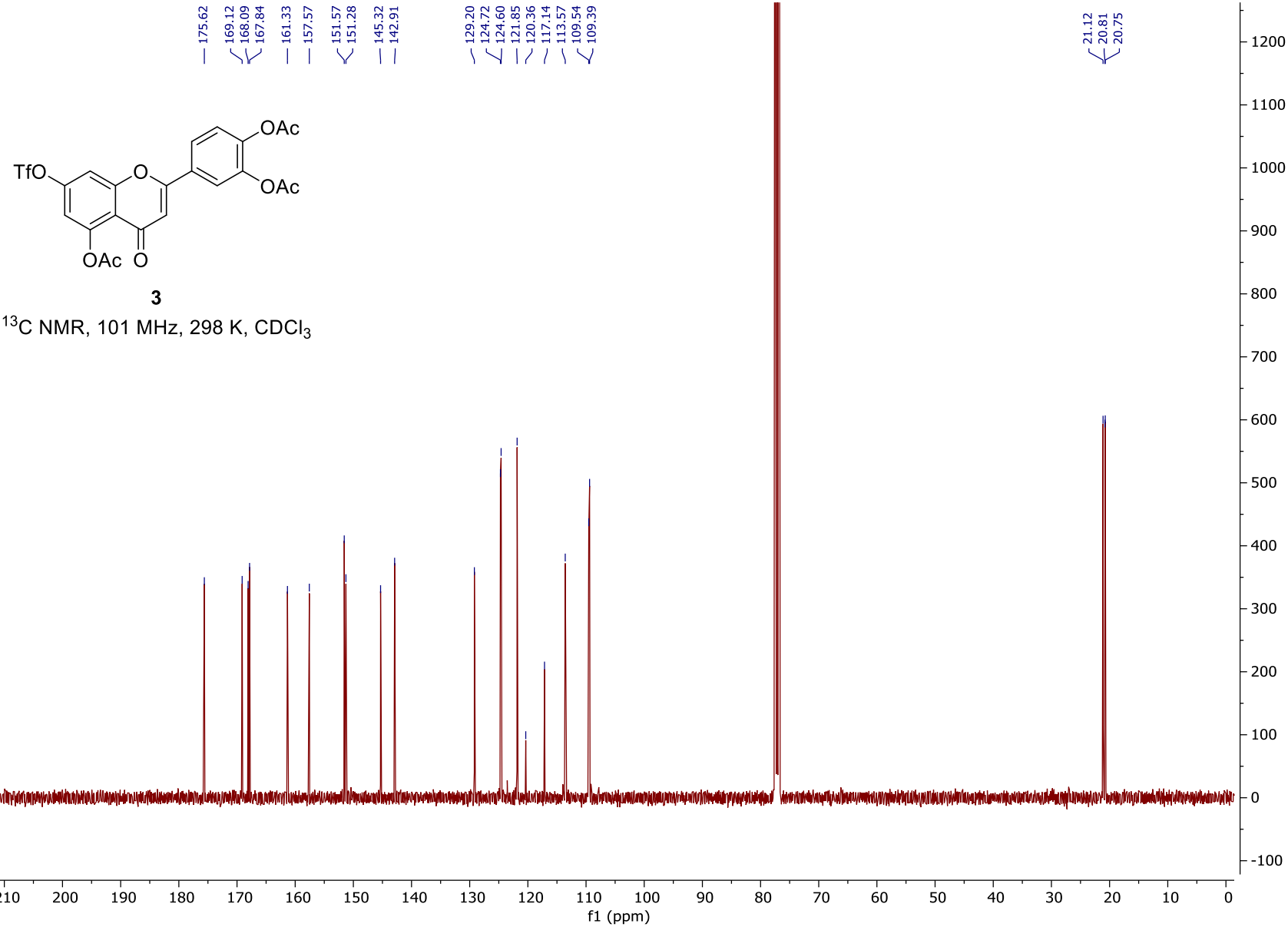


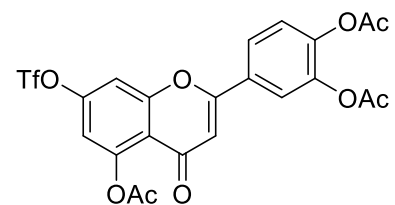


3

^1H NMR, 400 MHz, 298 K, CDCl_3

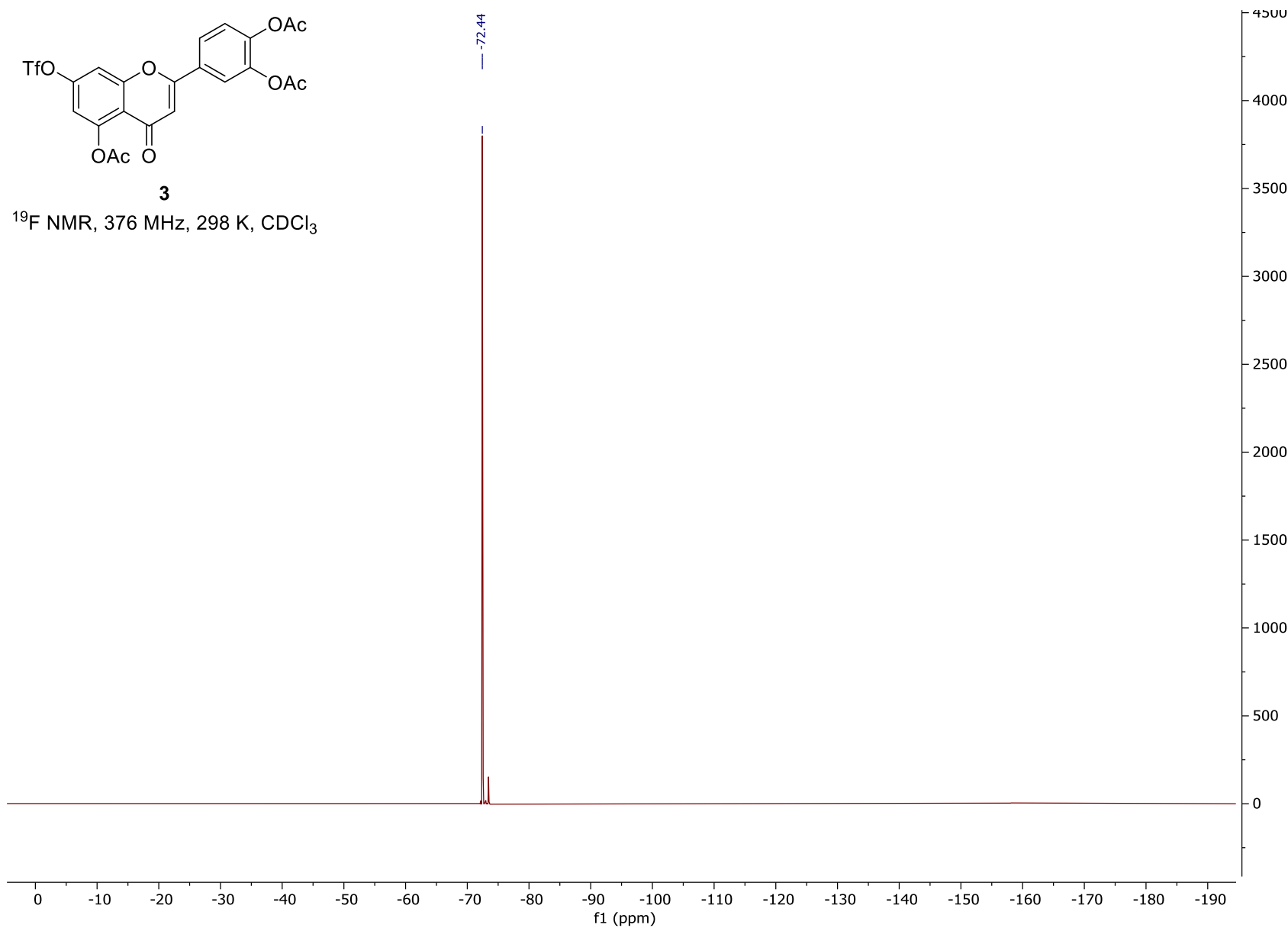


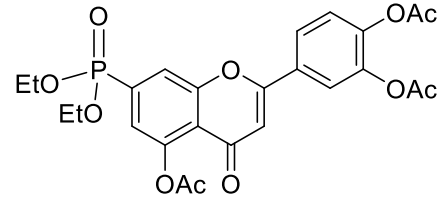




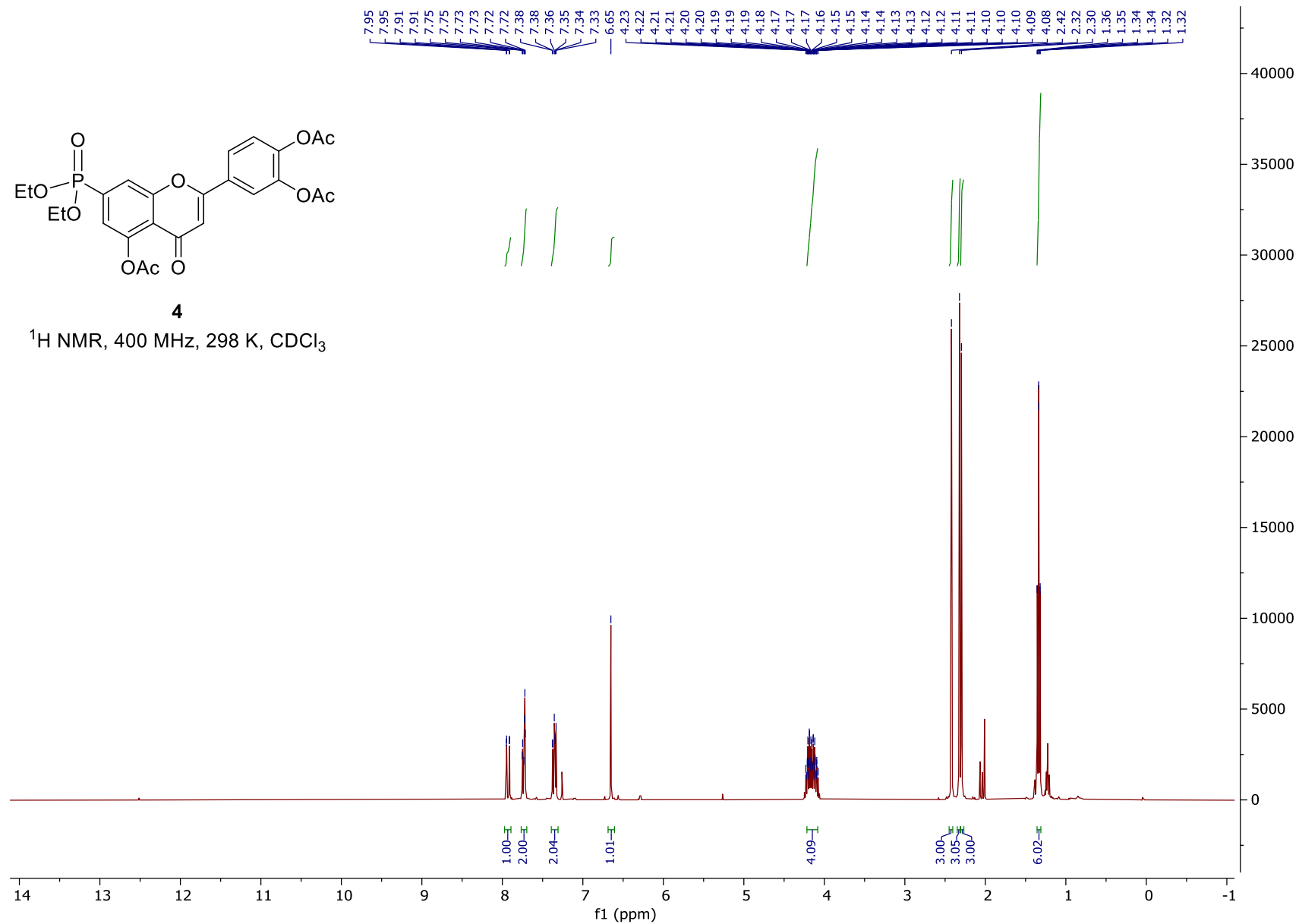
3

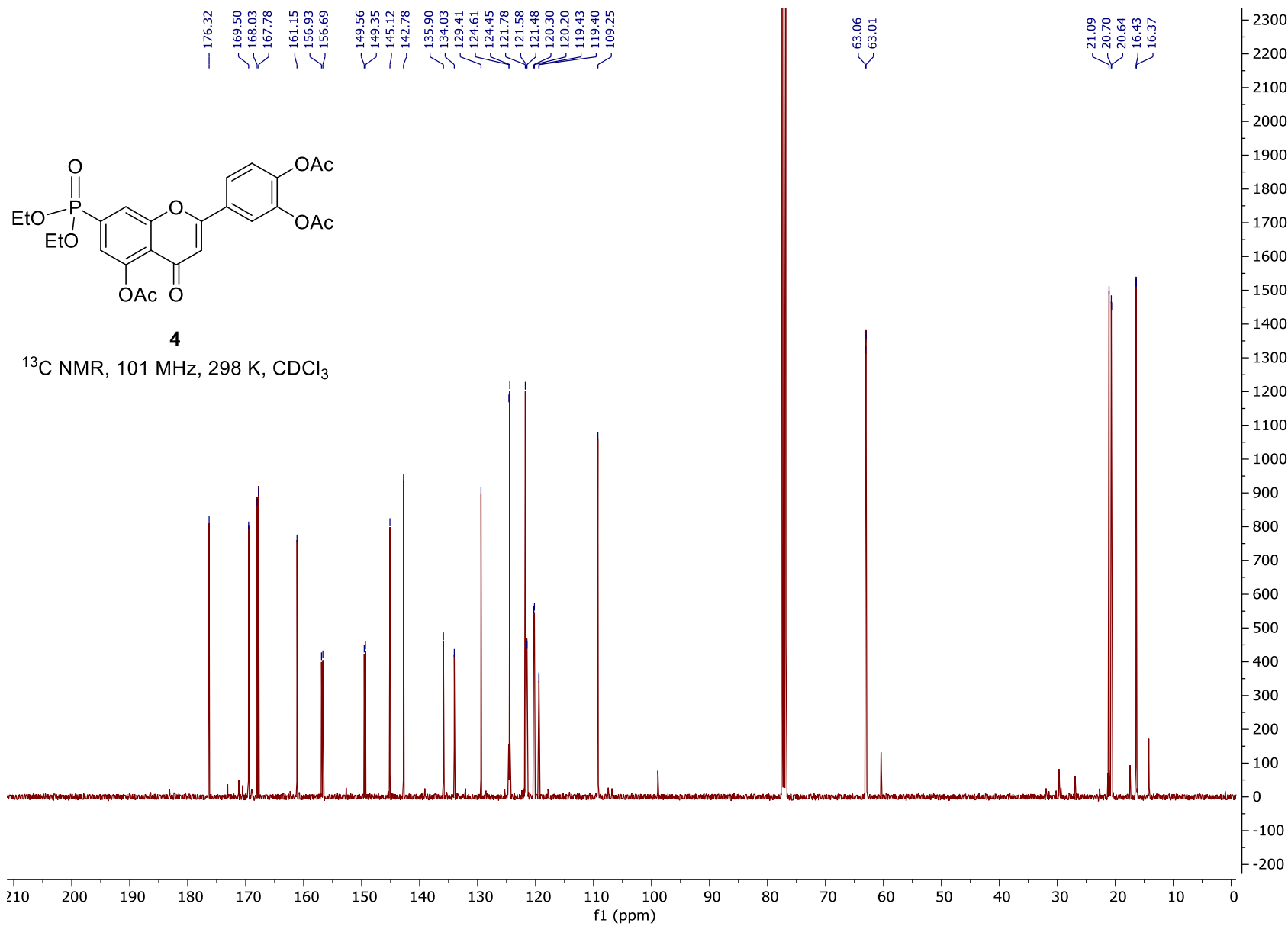
^{19}F NMR, 376 MHz, 298 K, CDCl_3

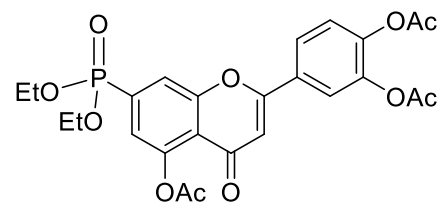




^1H NMR, 400 MHz, 298 K, CDCl_3

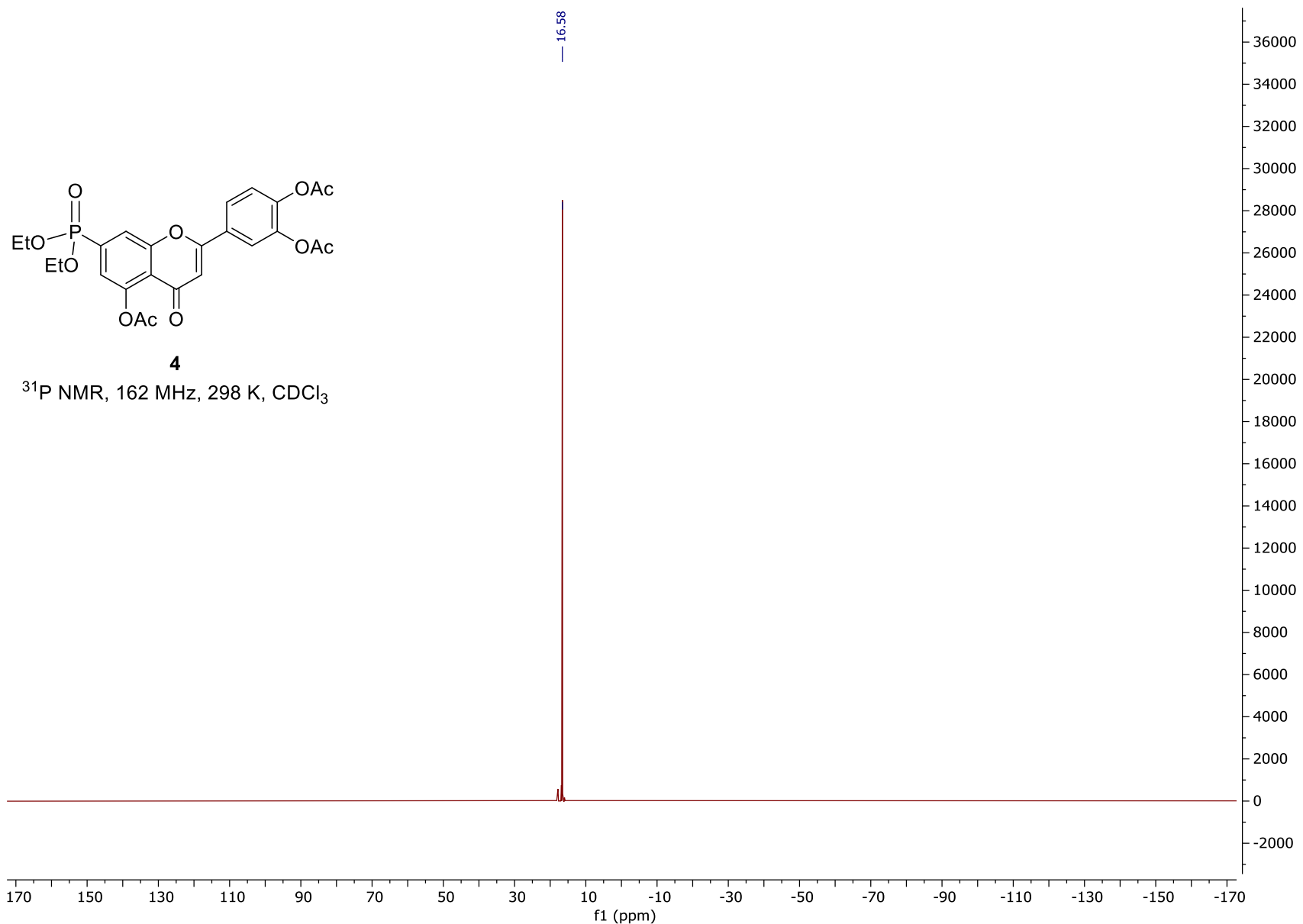


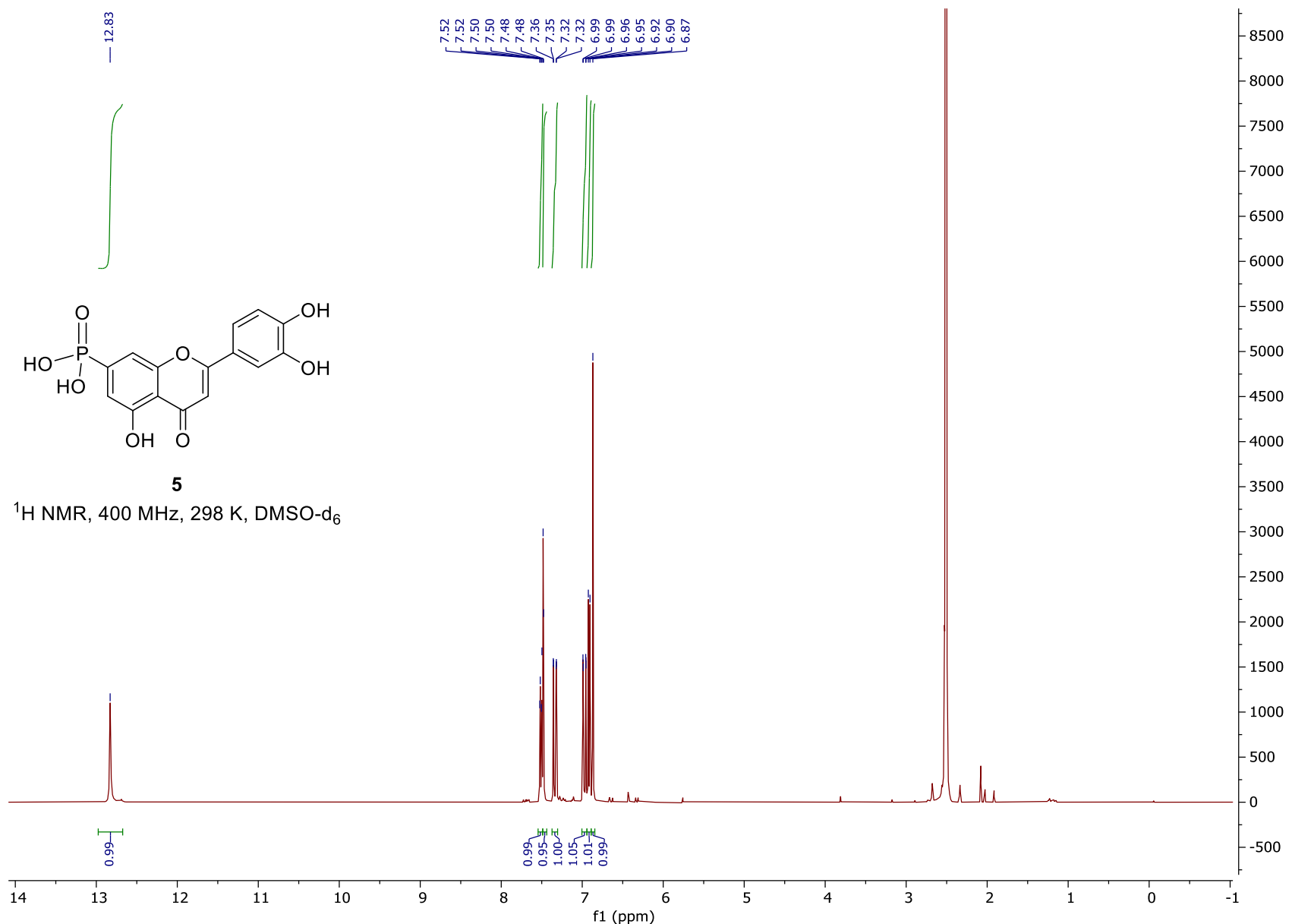


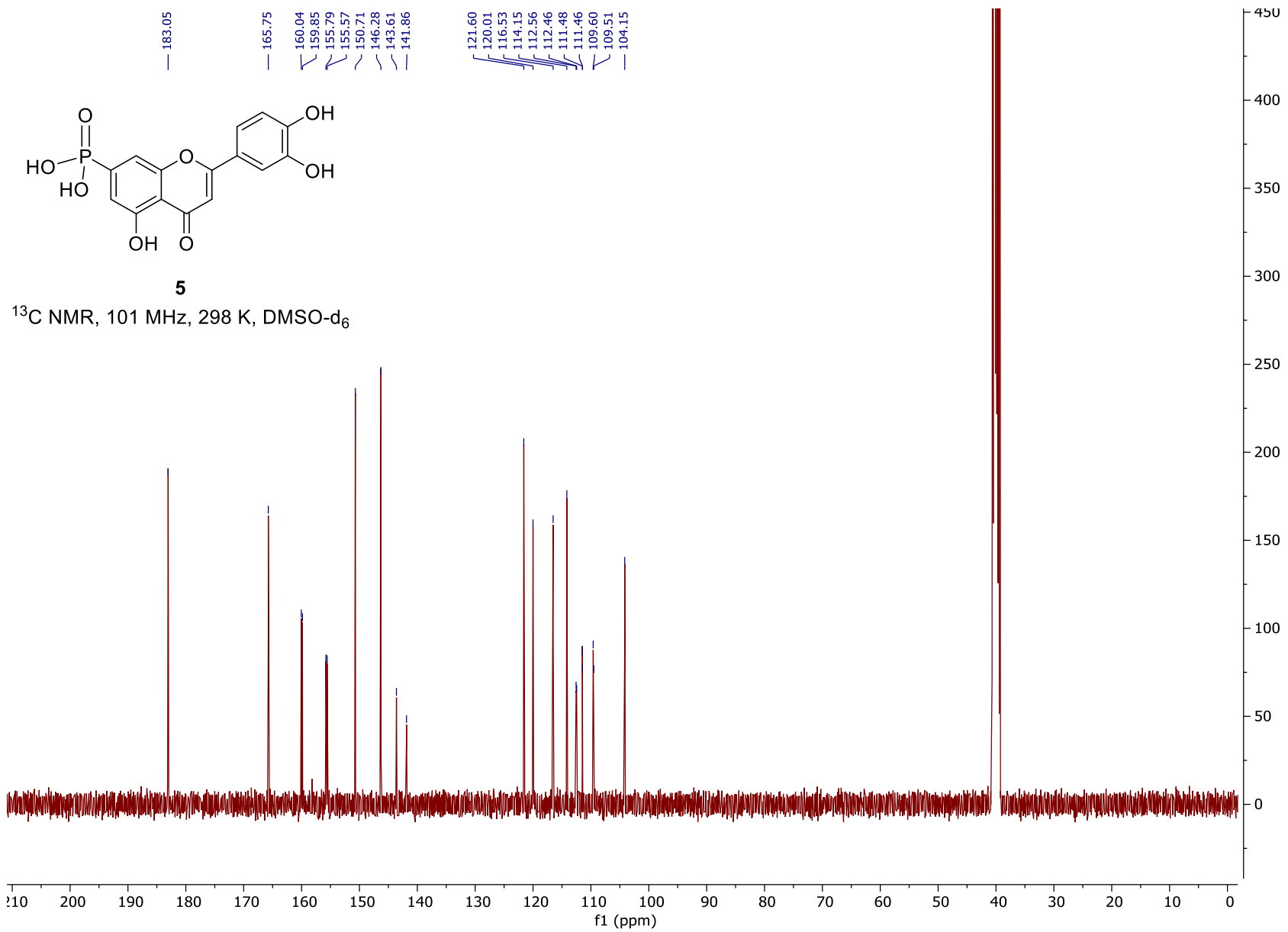


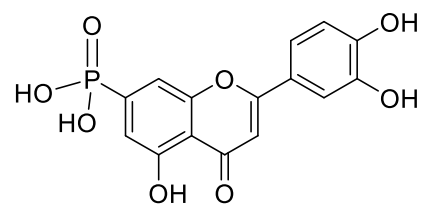
4

^{31}P NMR, 162 MHz, 298 K, CDCl_3



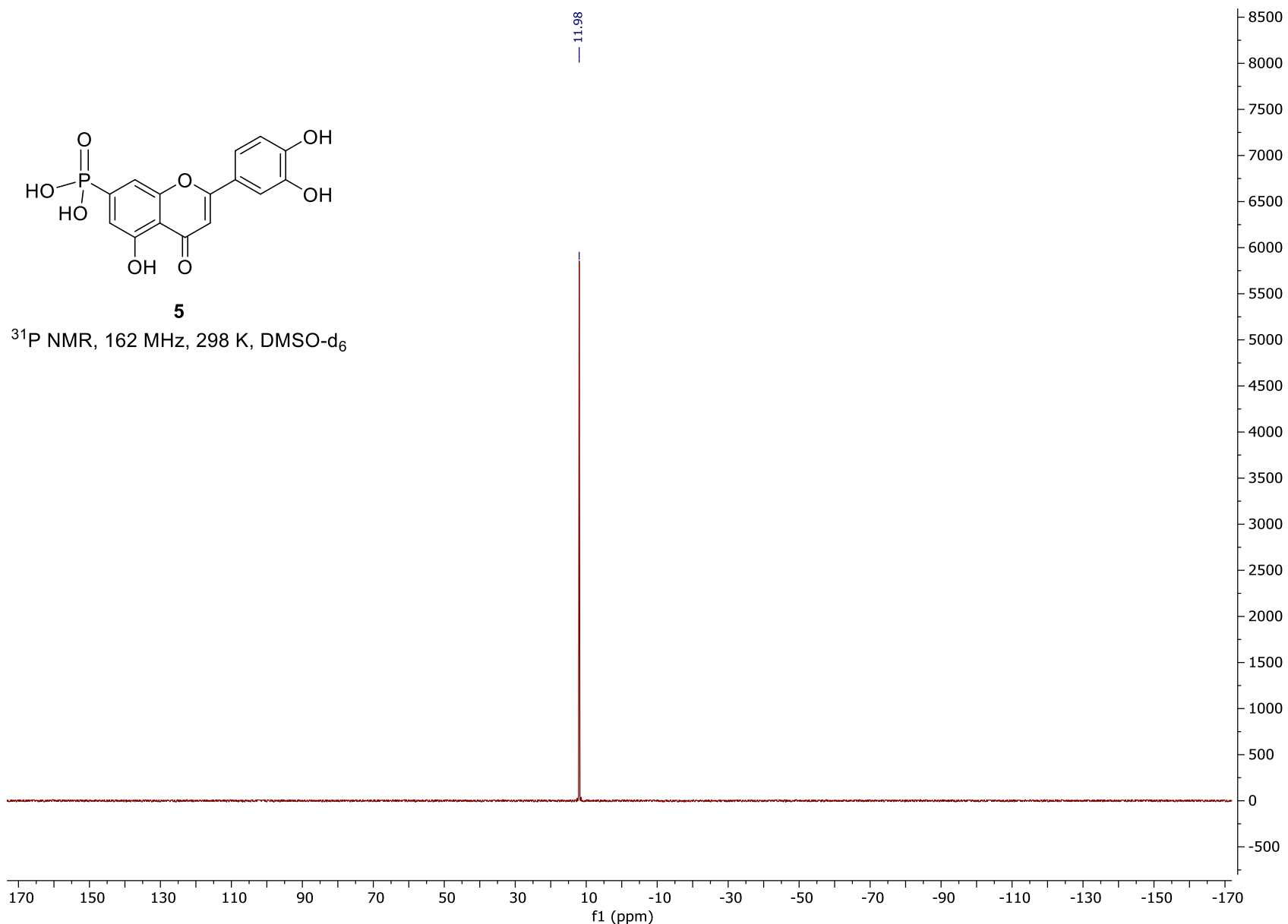


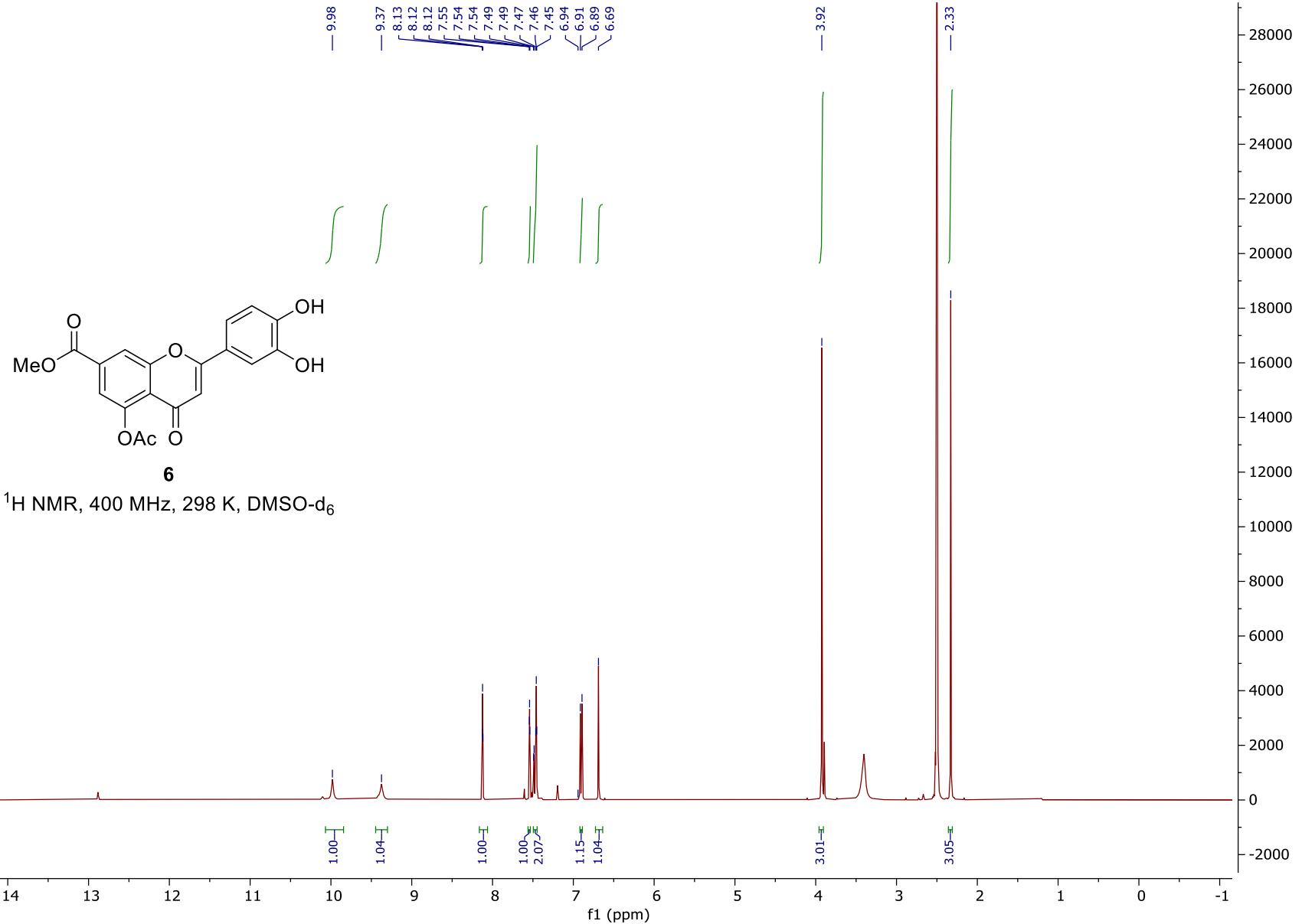


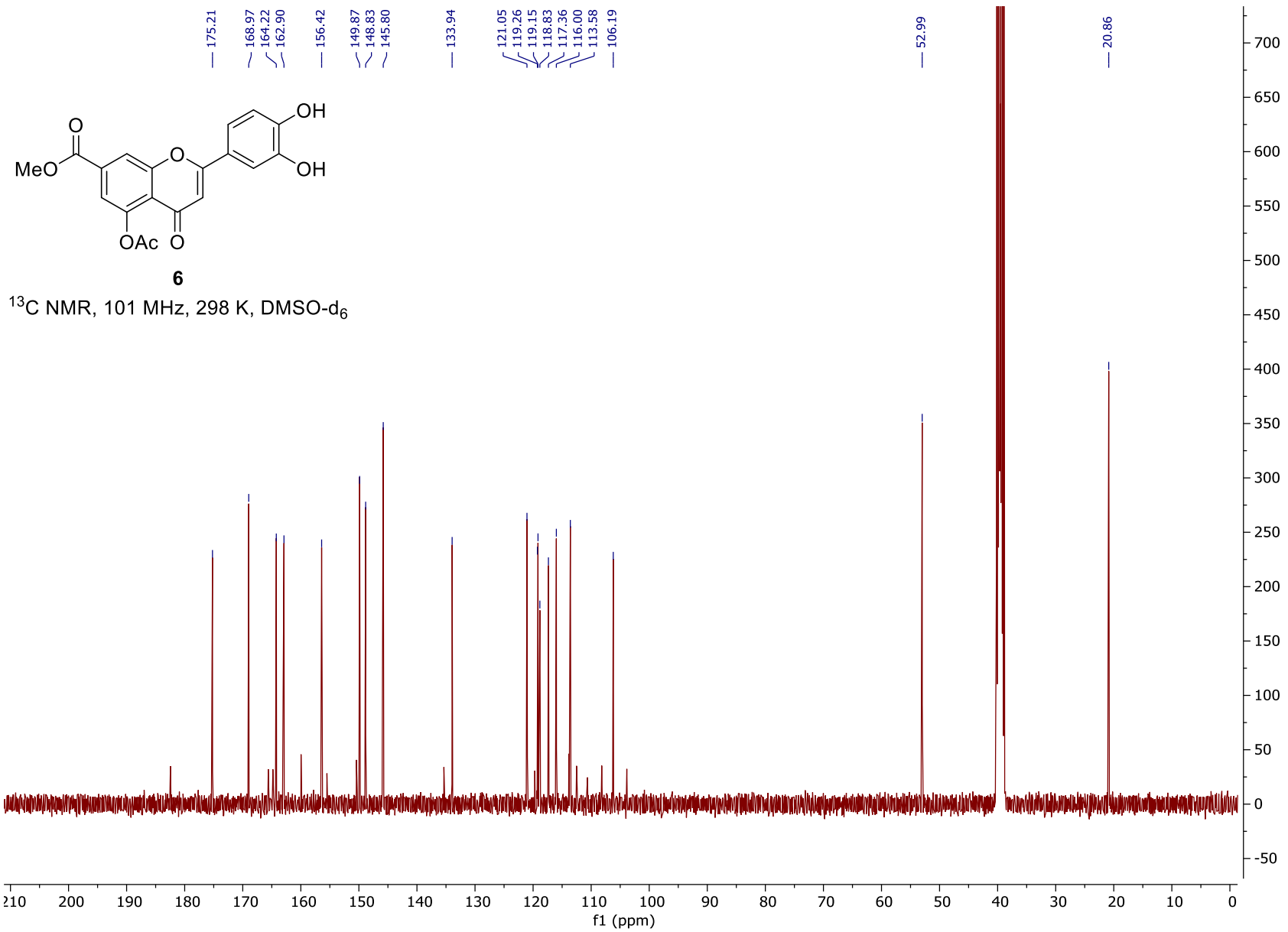


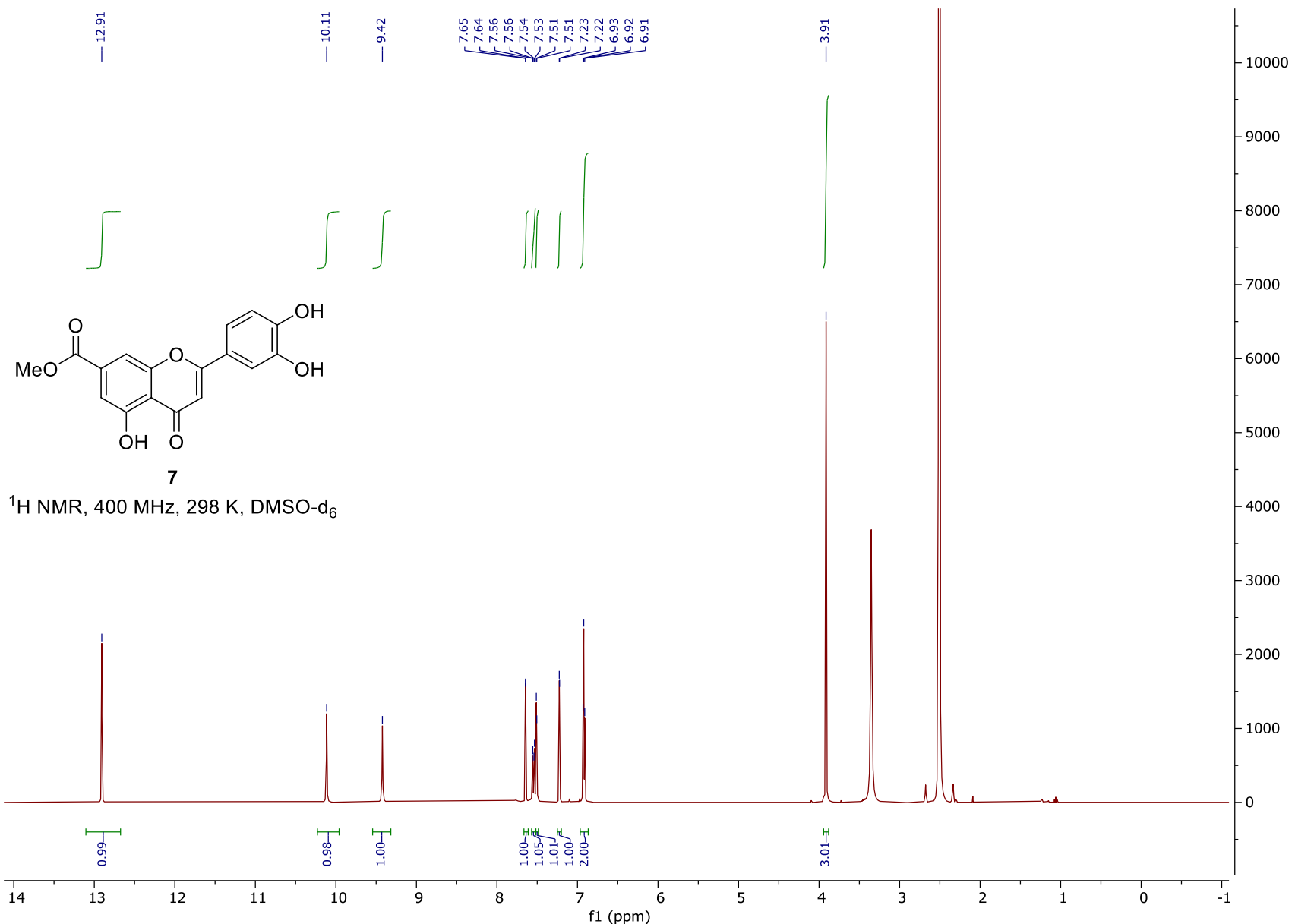
5

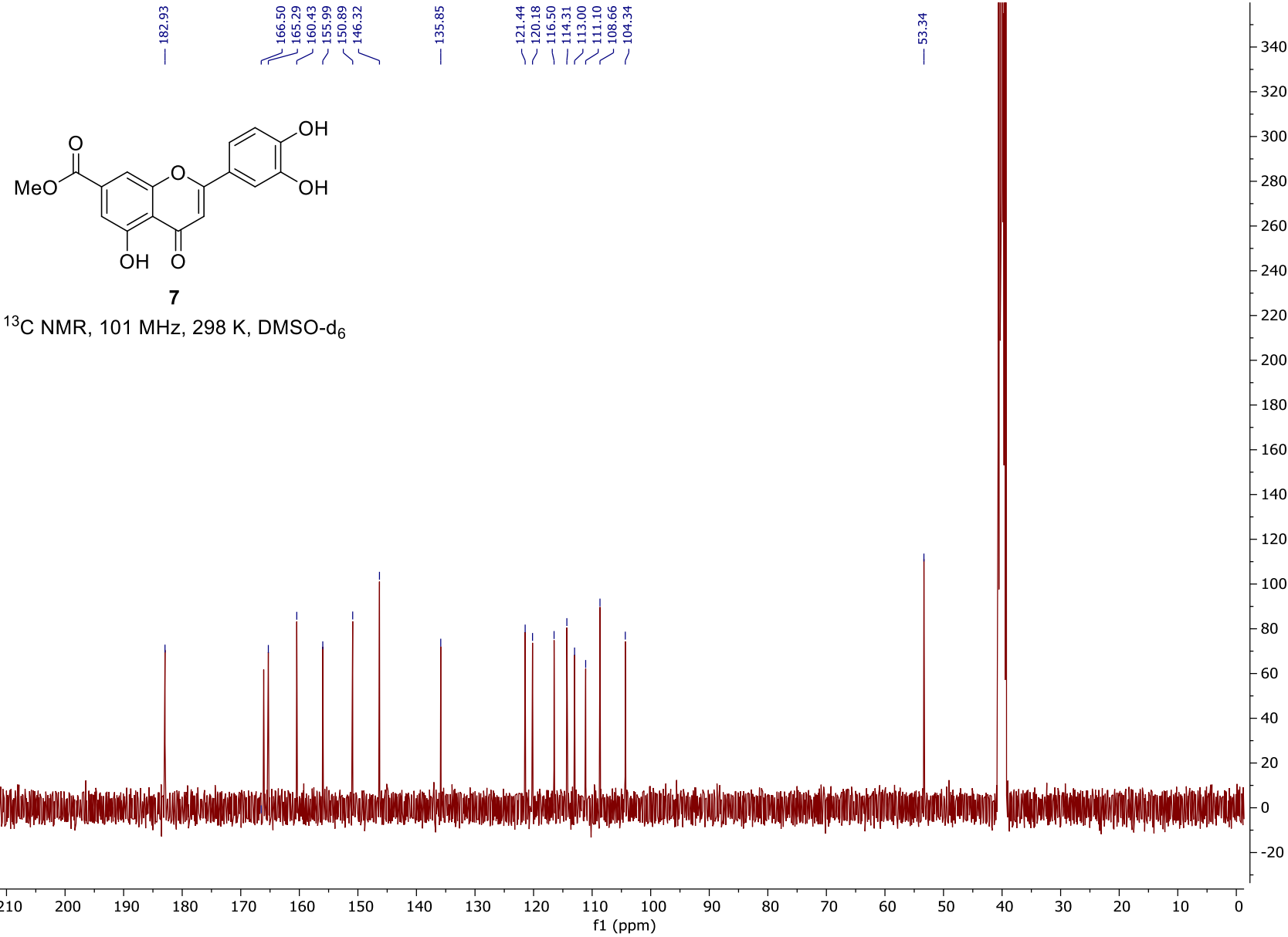
^{31}P NMR, 162 MHz, 298 K, DMSO- d_6

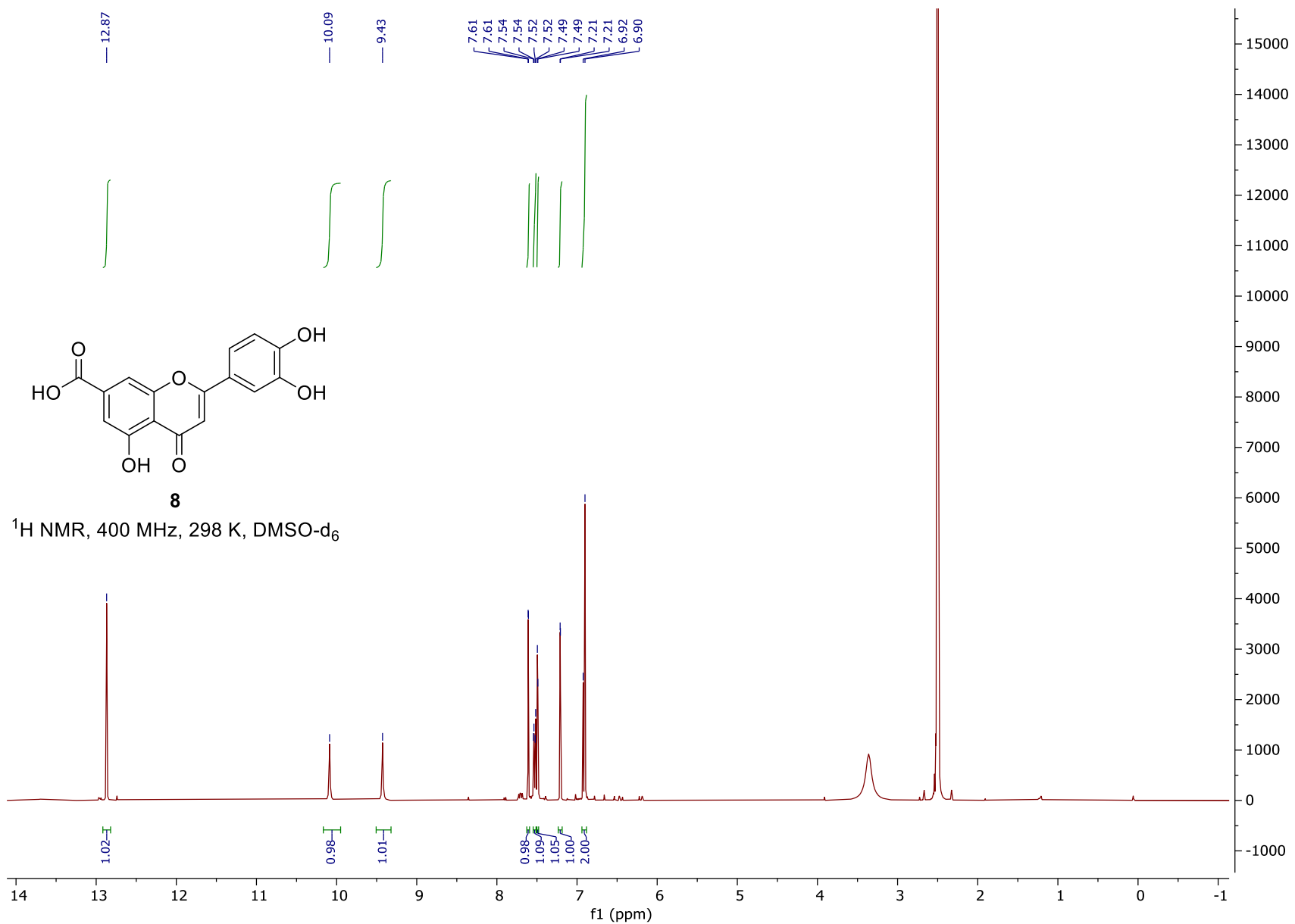


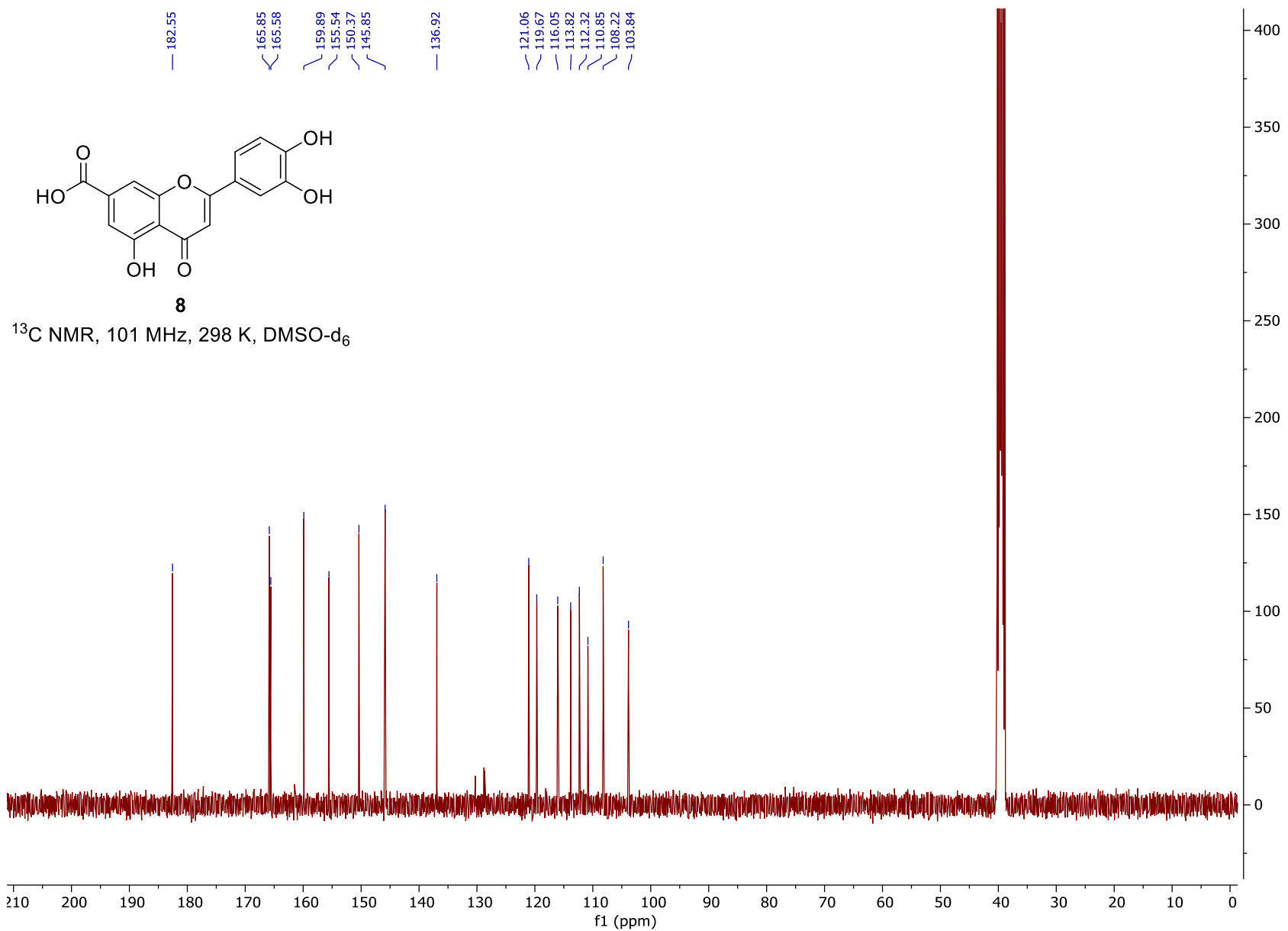


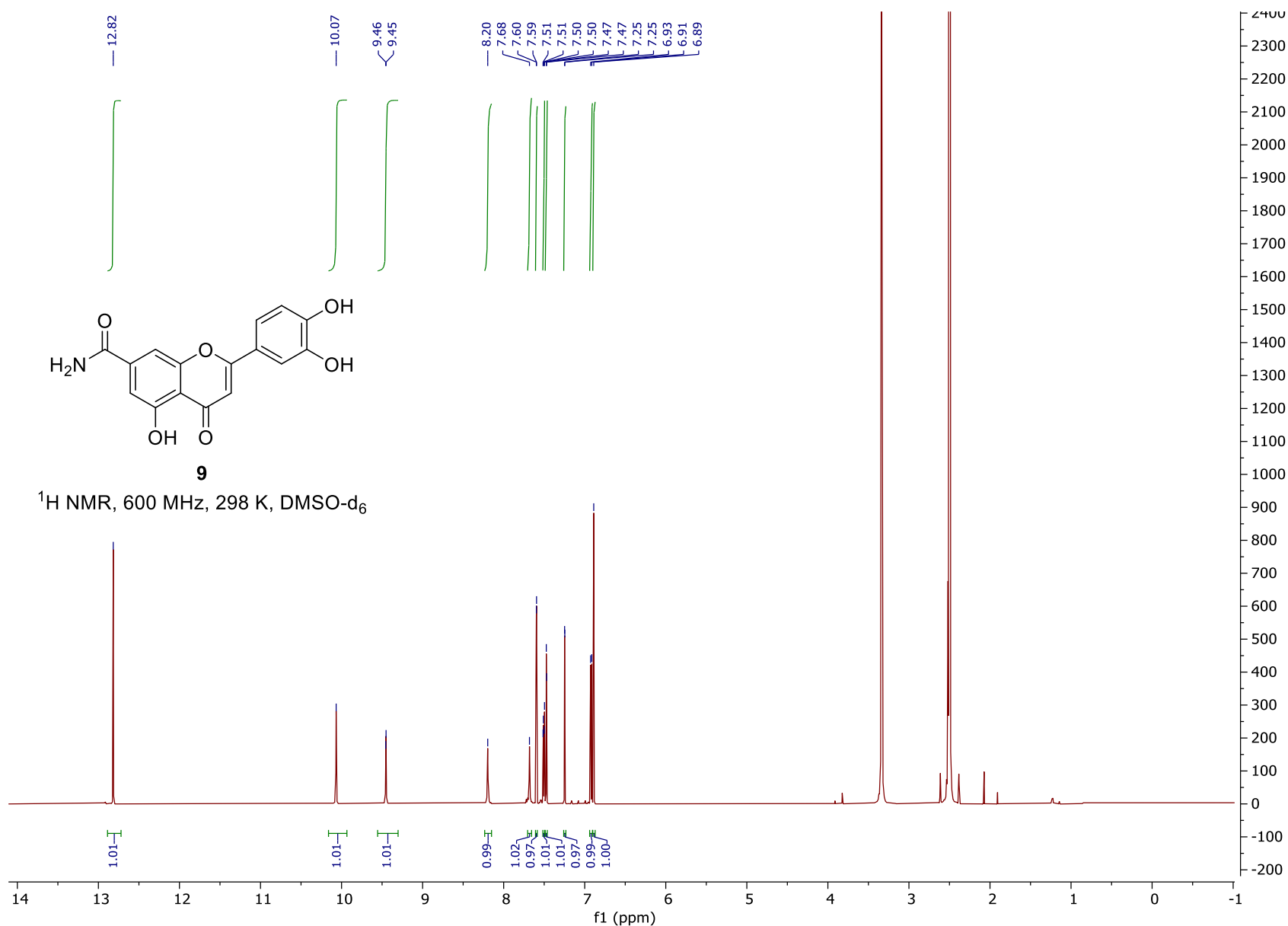


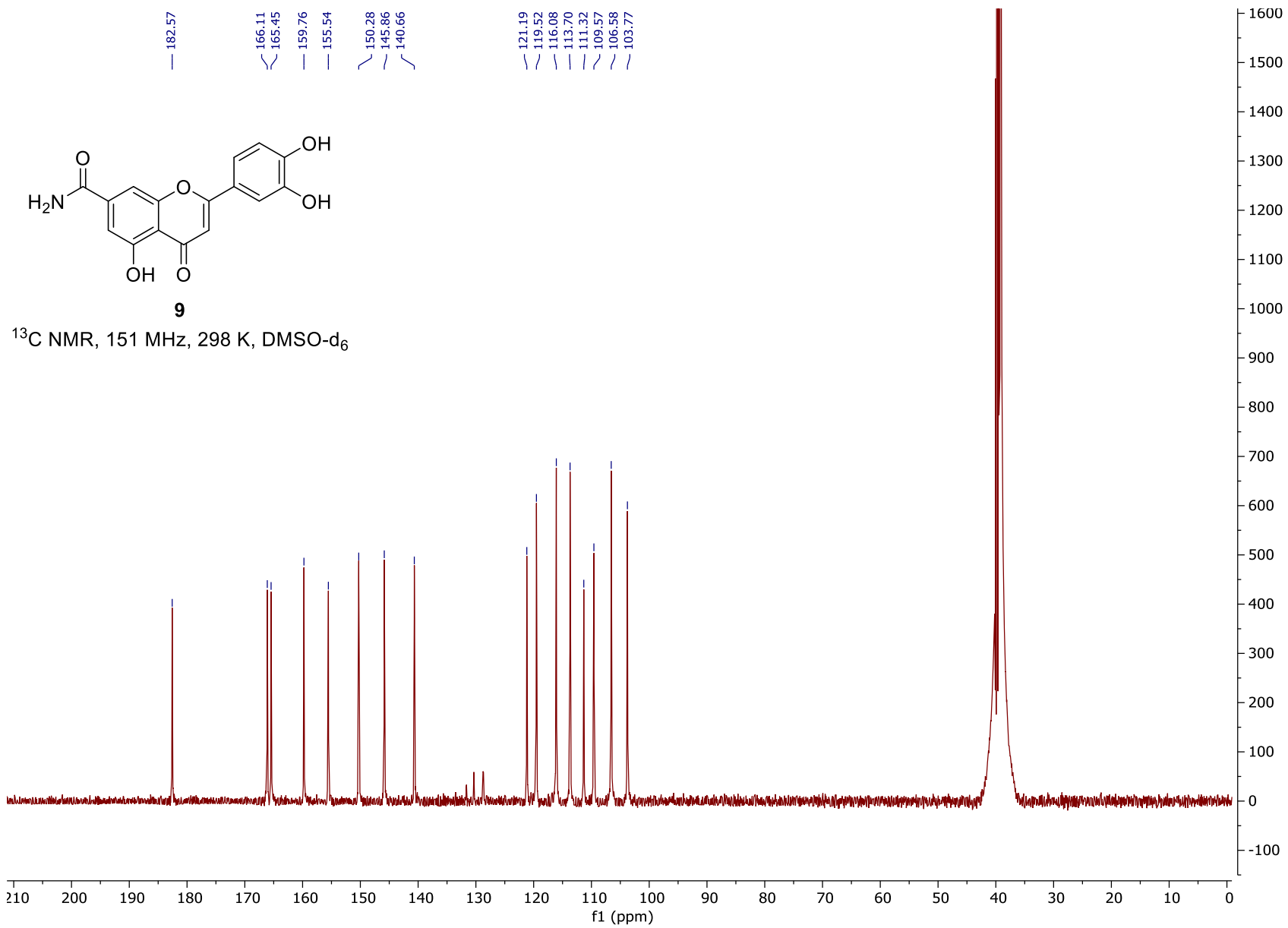


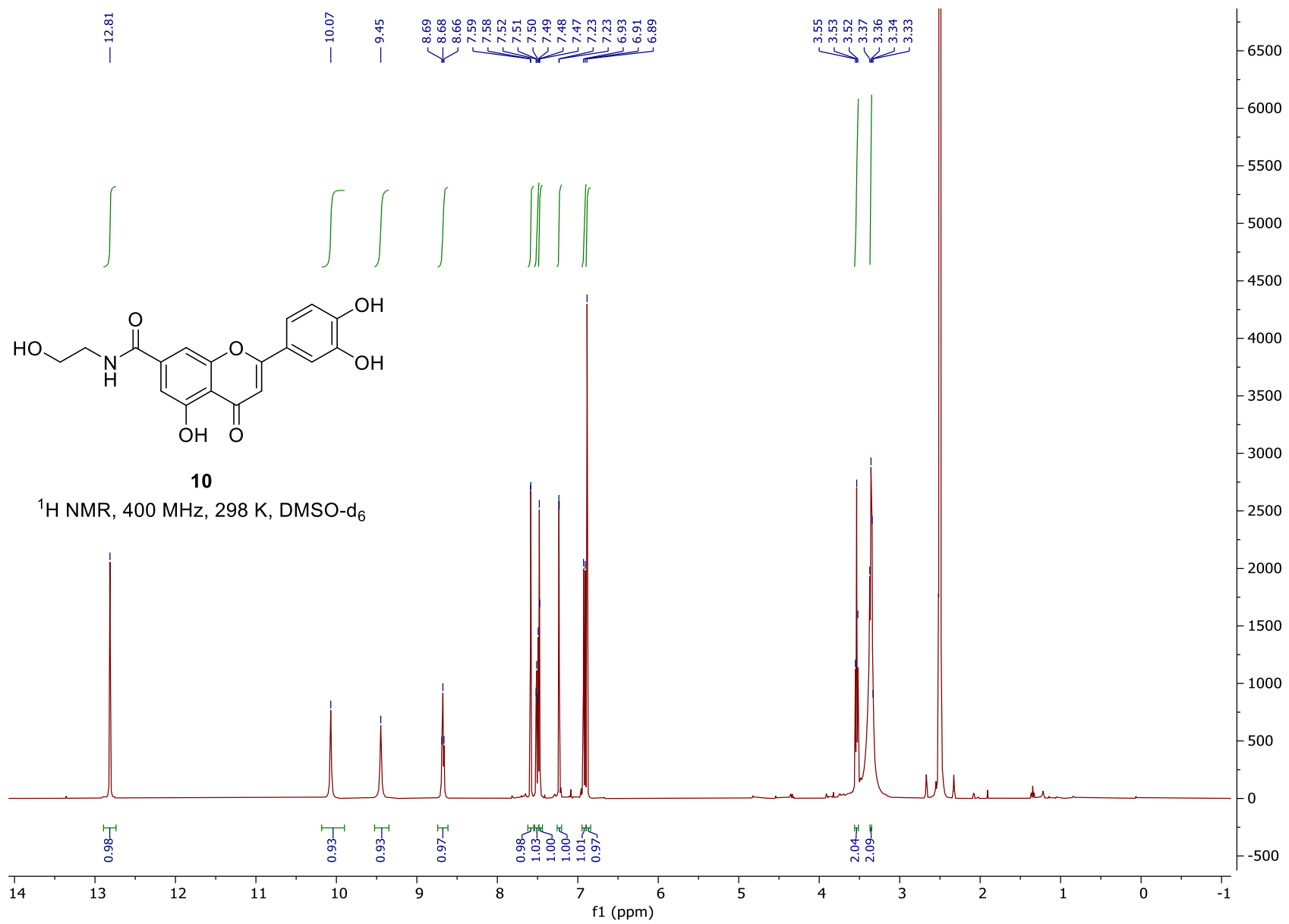


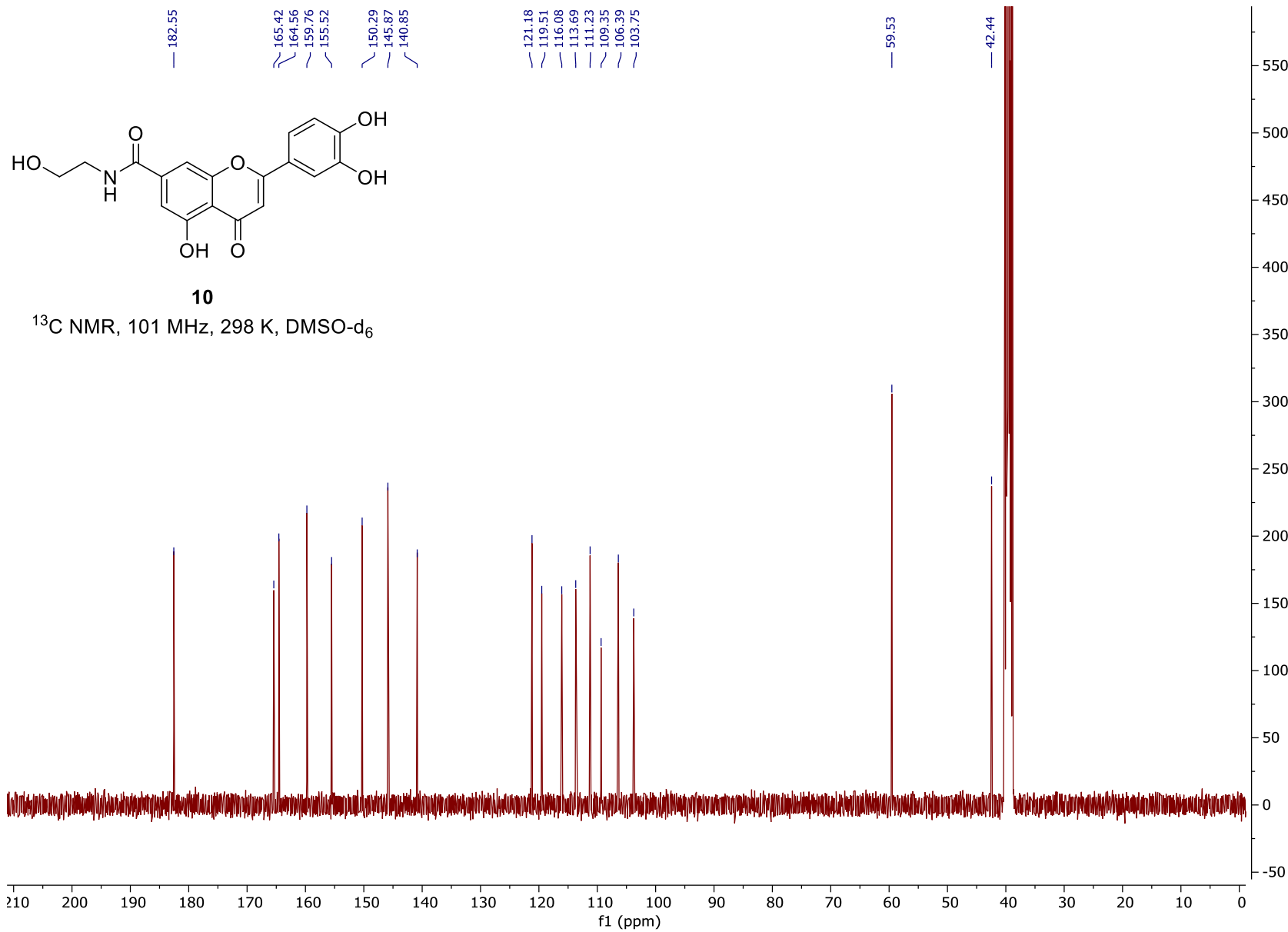


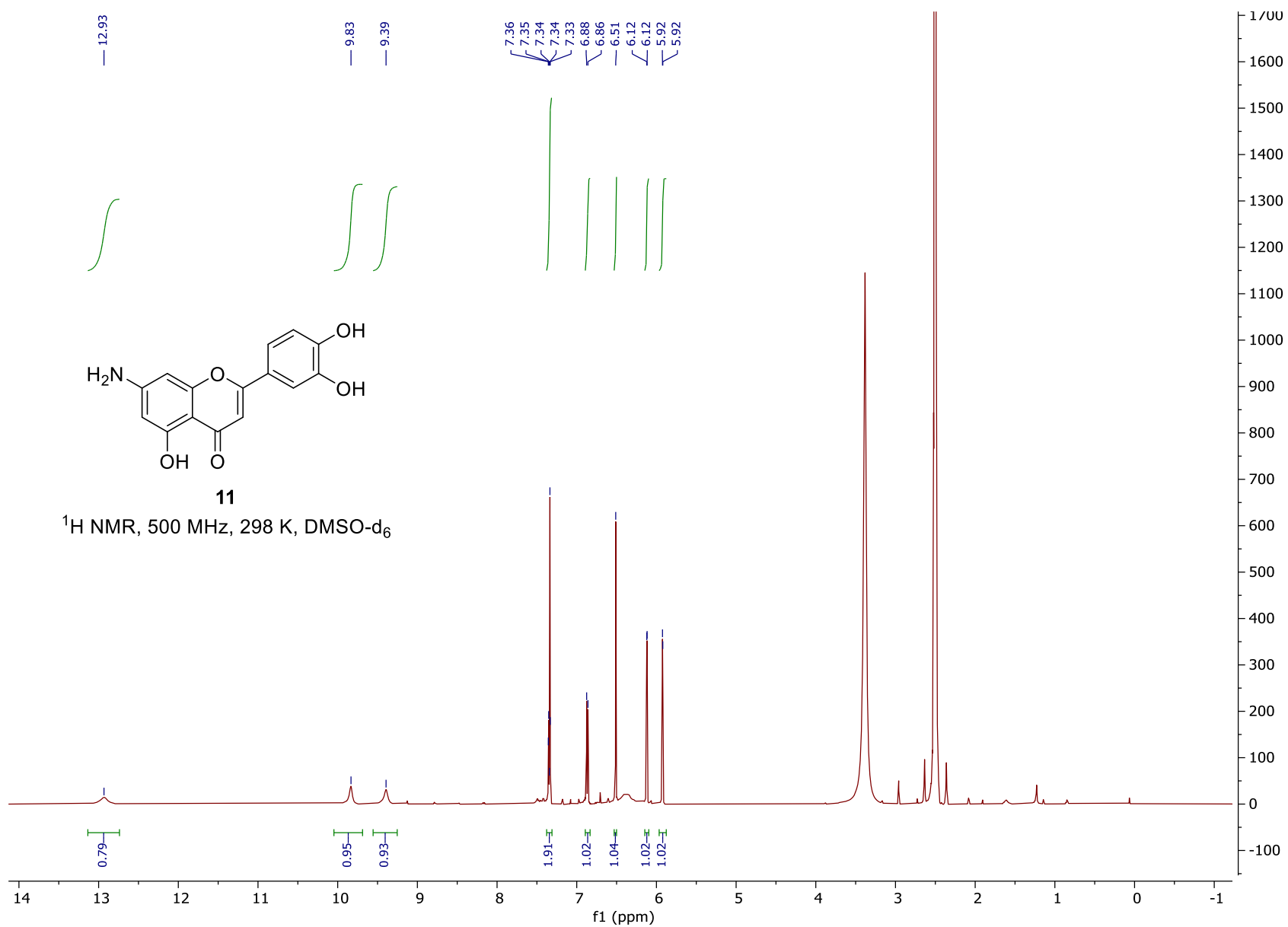


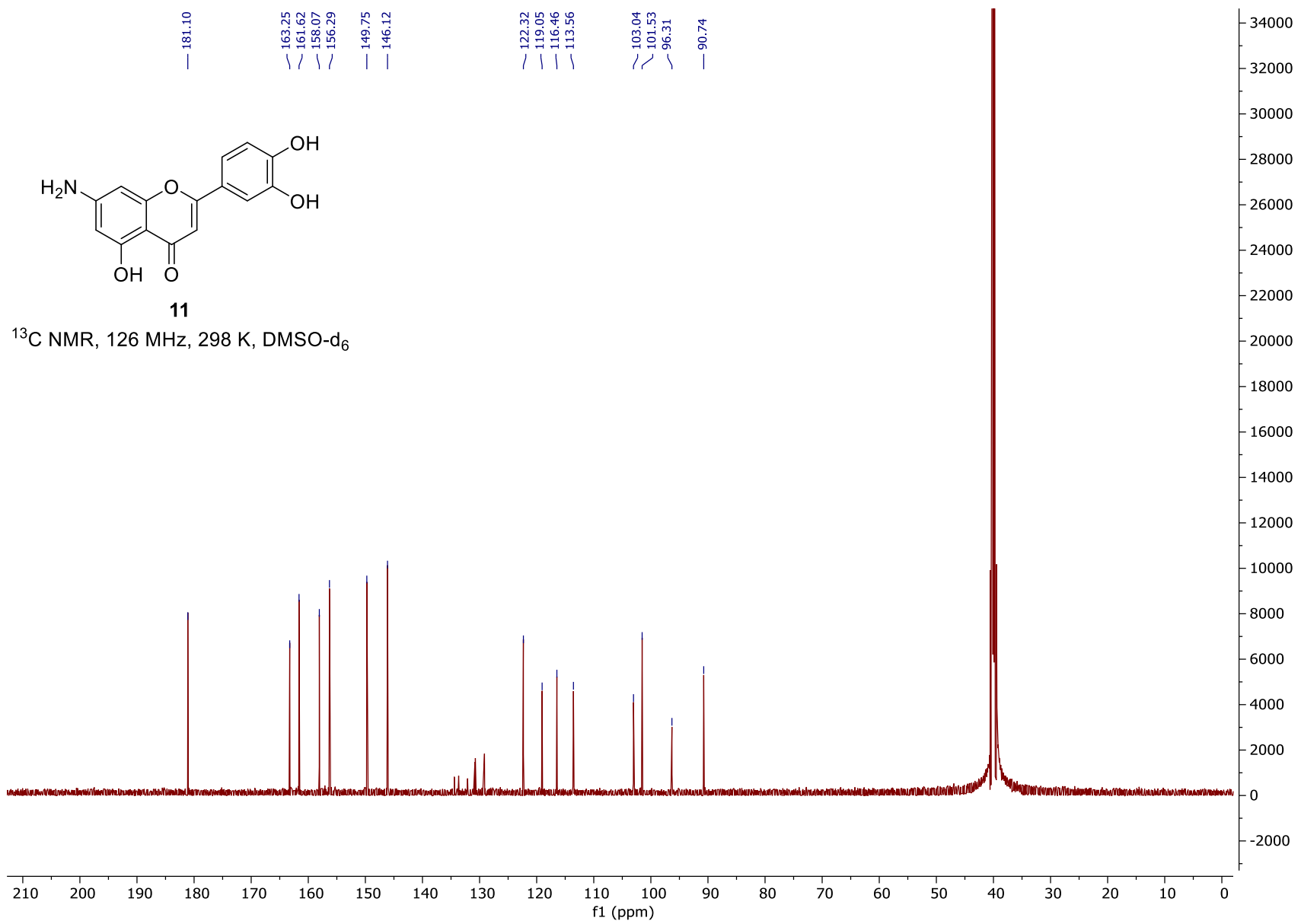


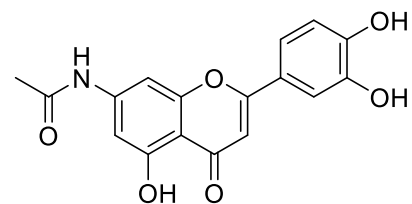






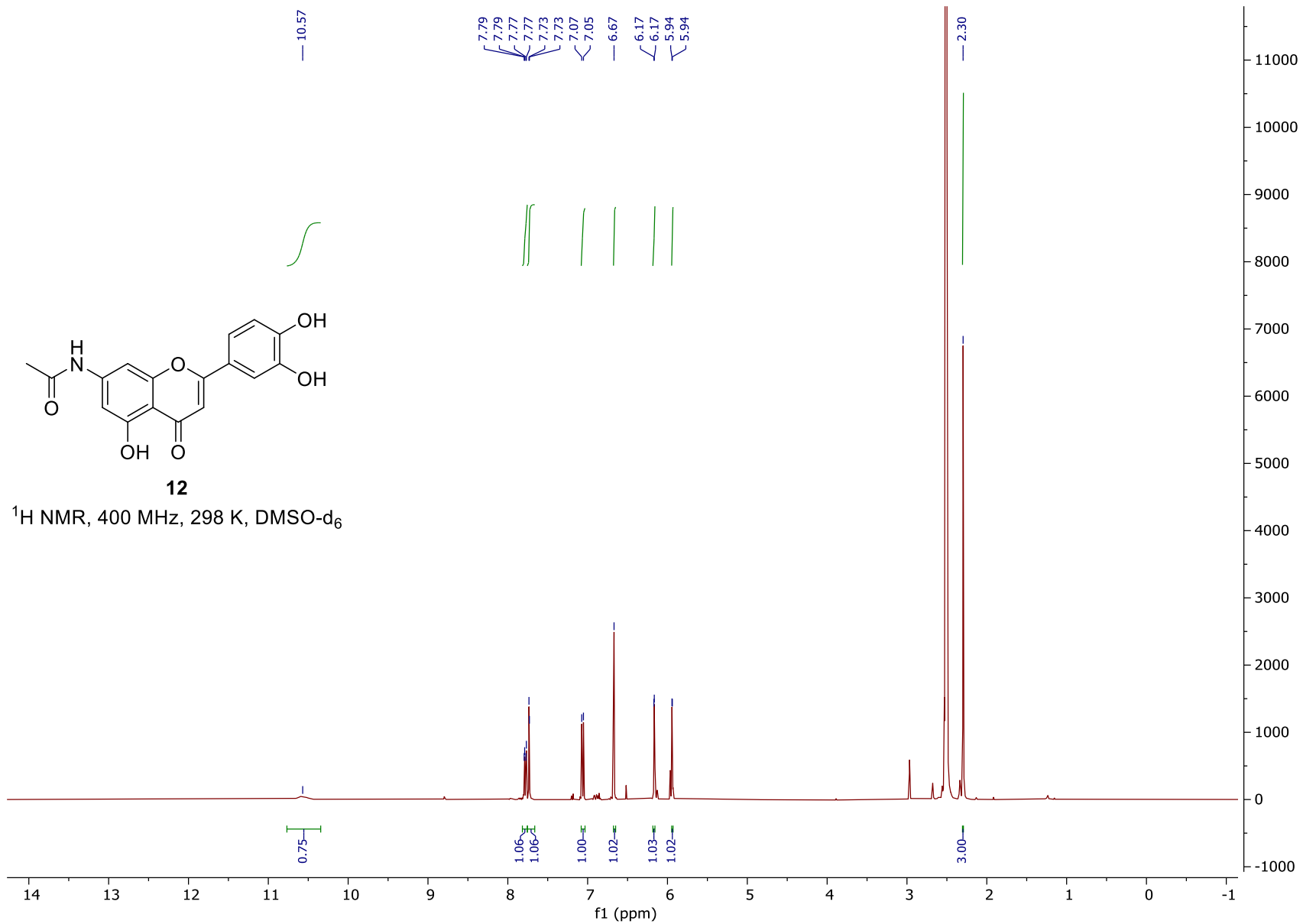


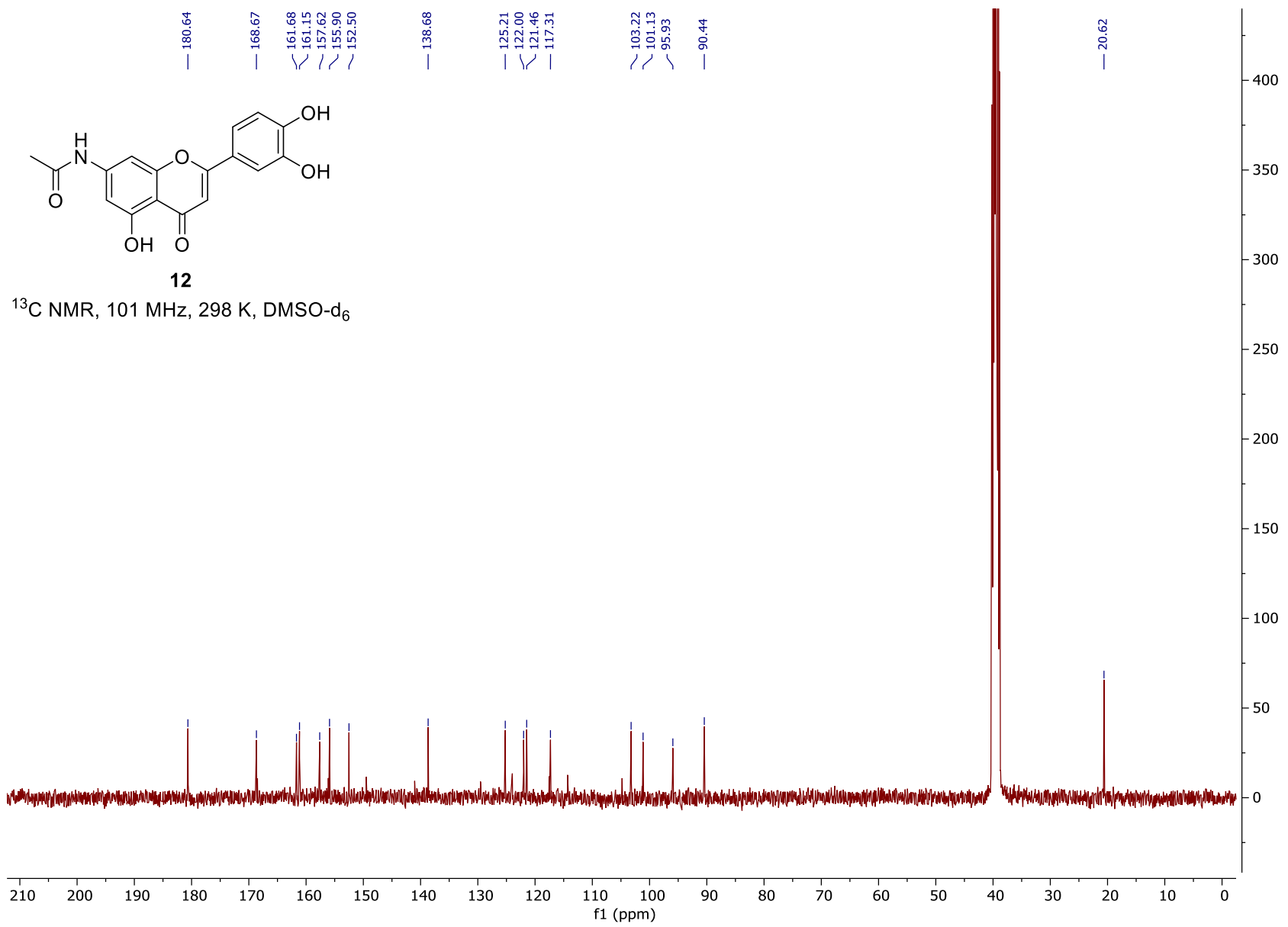


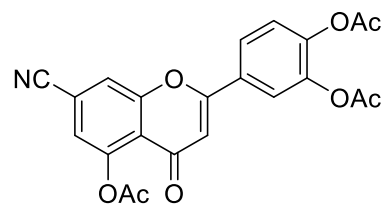


12

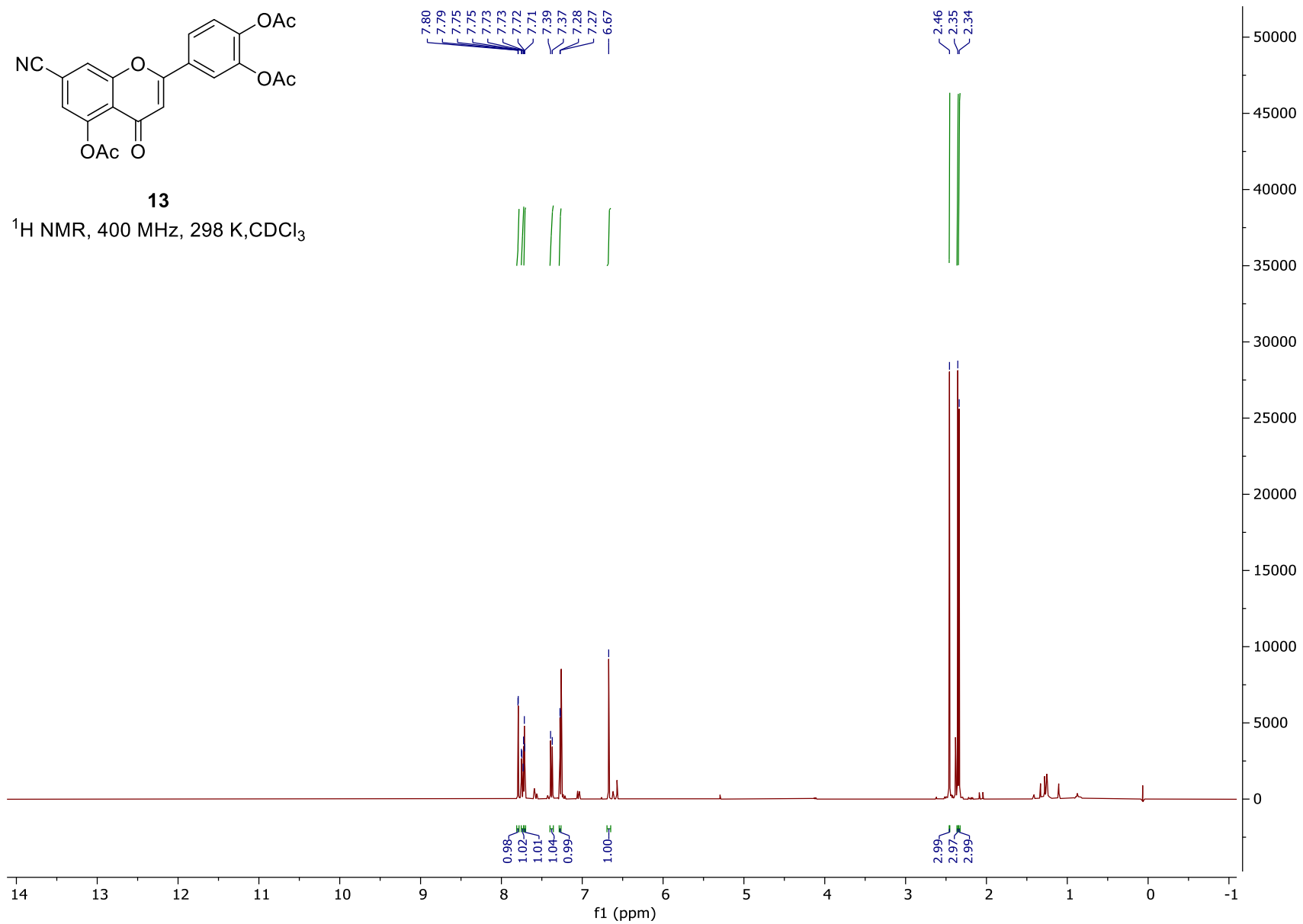
^1H NMR, 400 MHz, 298 K, DMSO-d₆

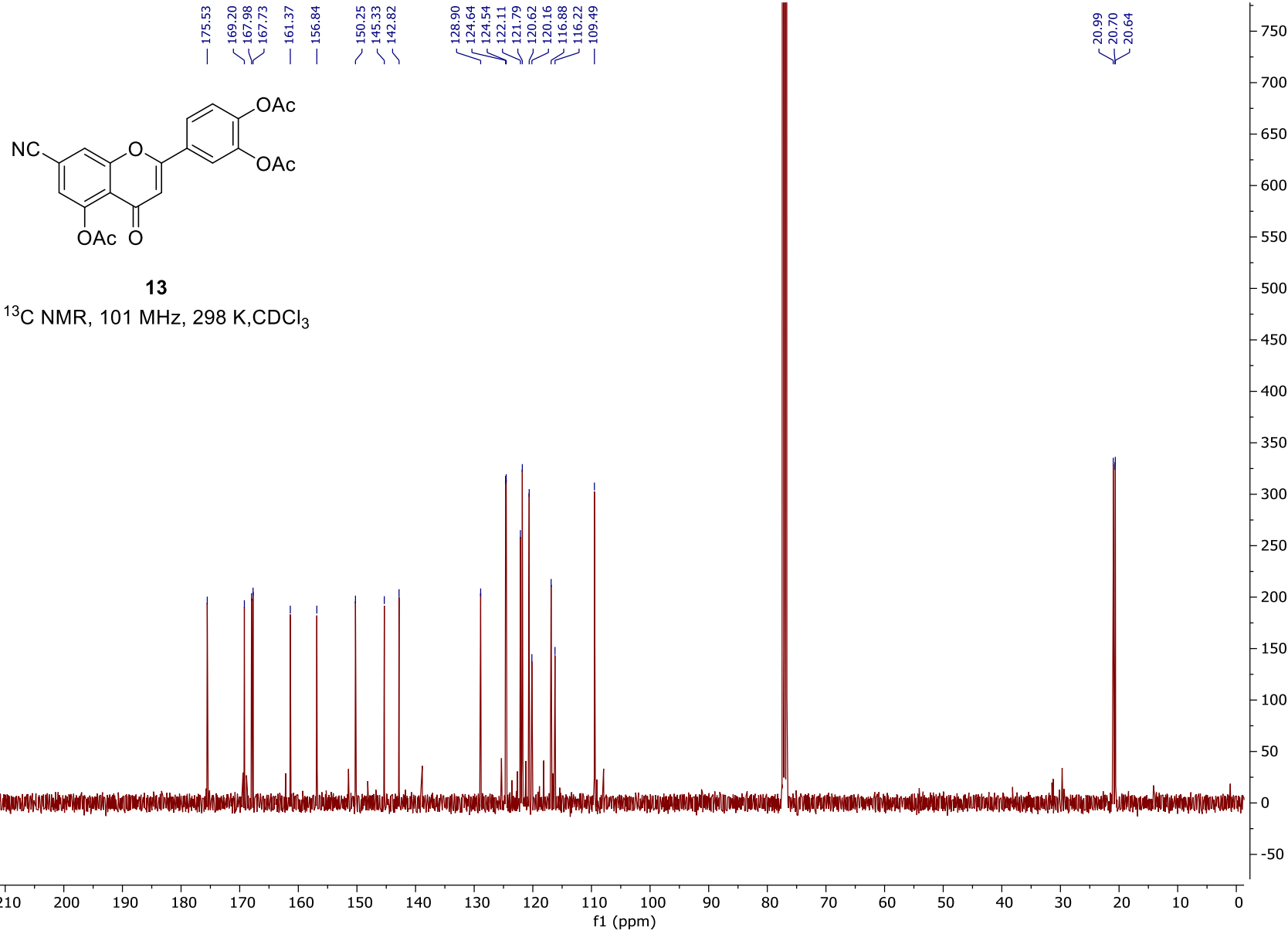


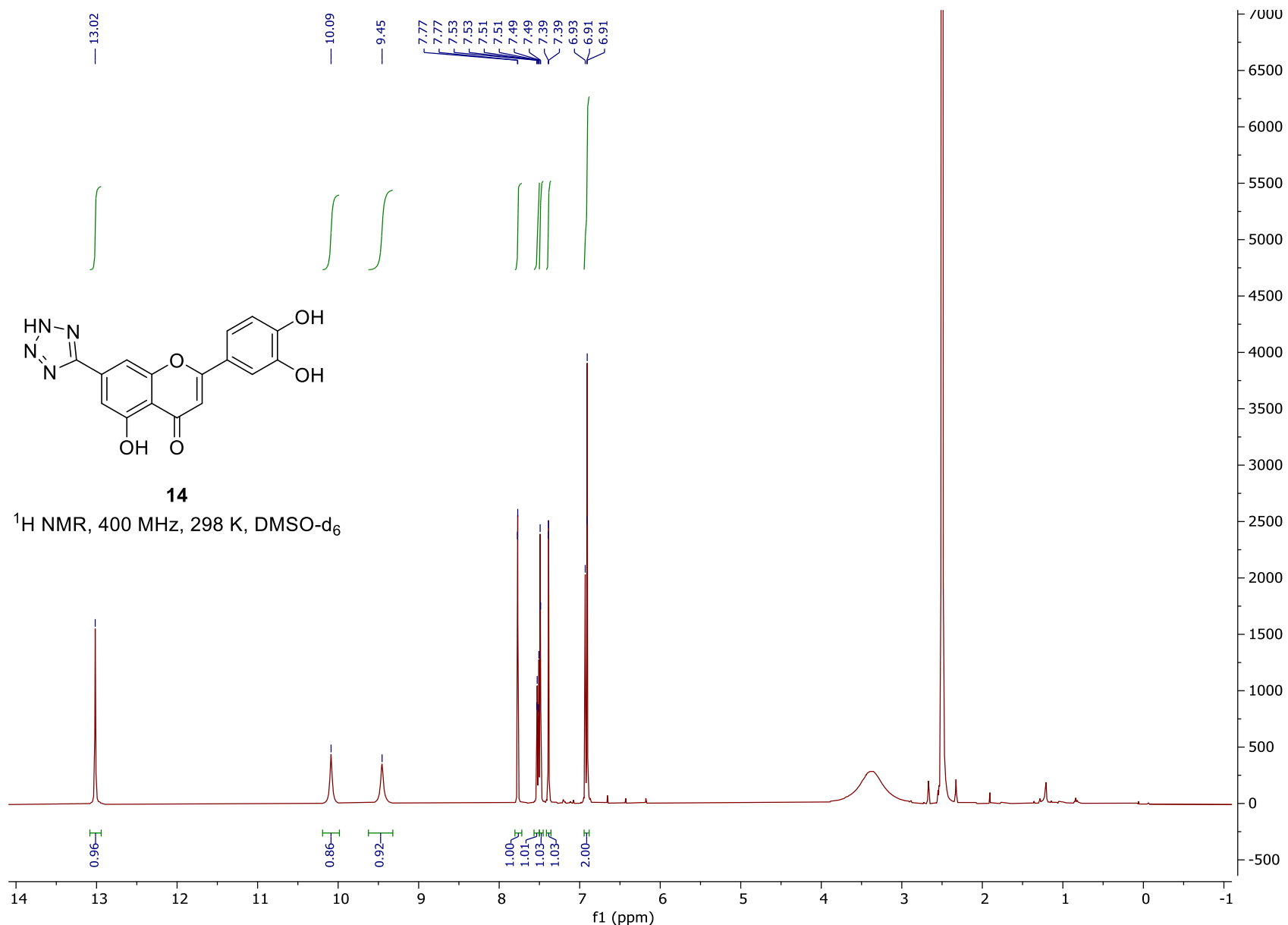


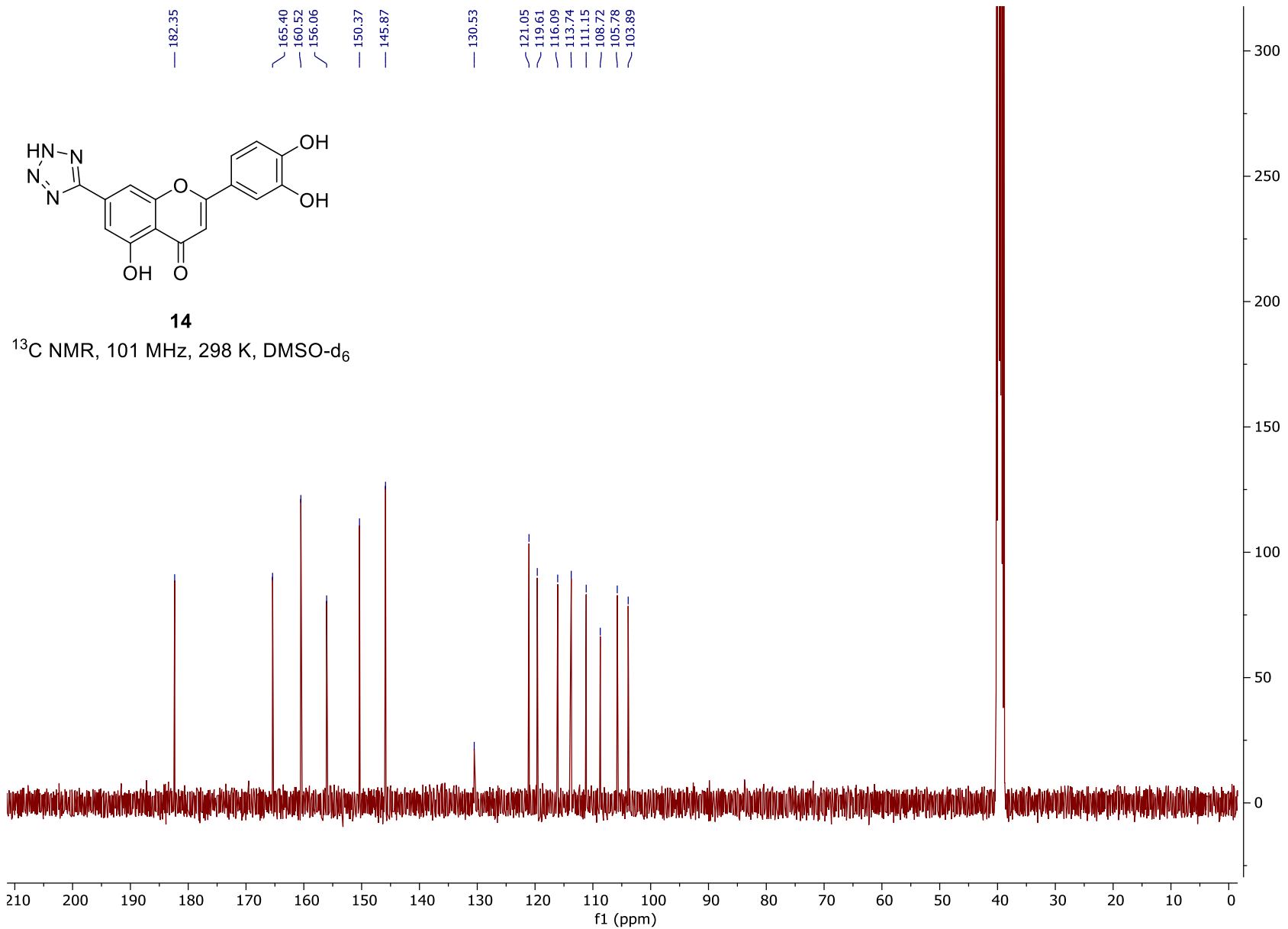


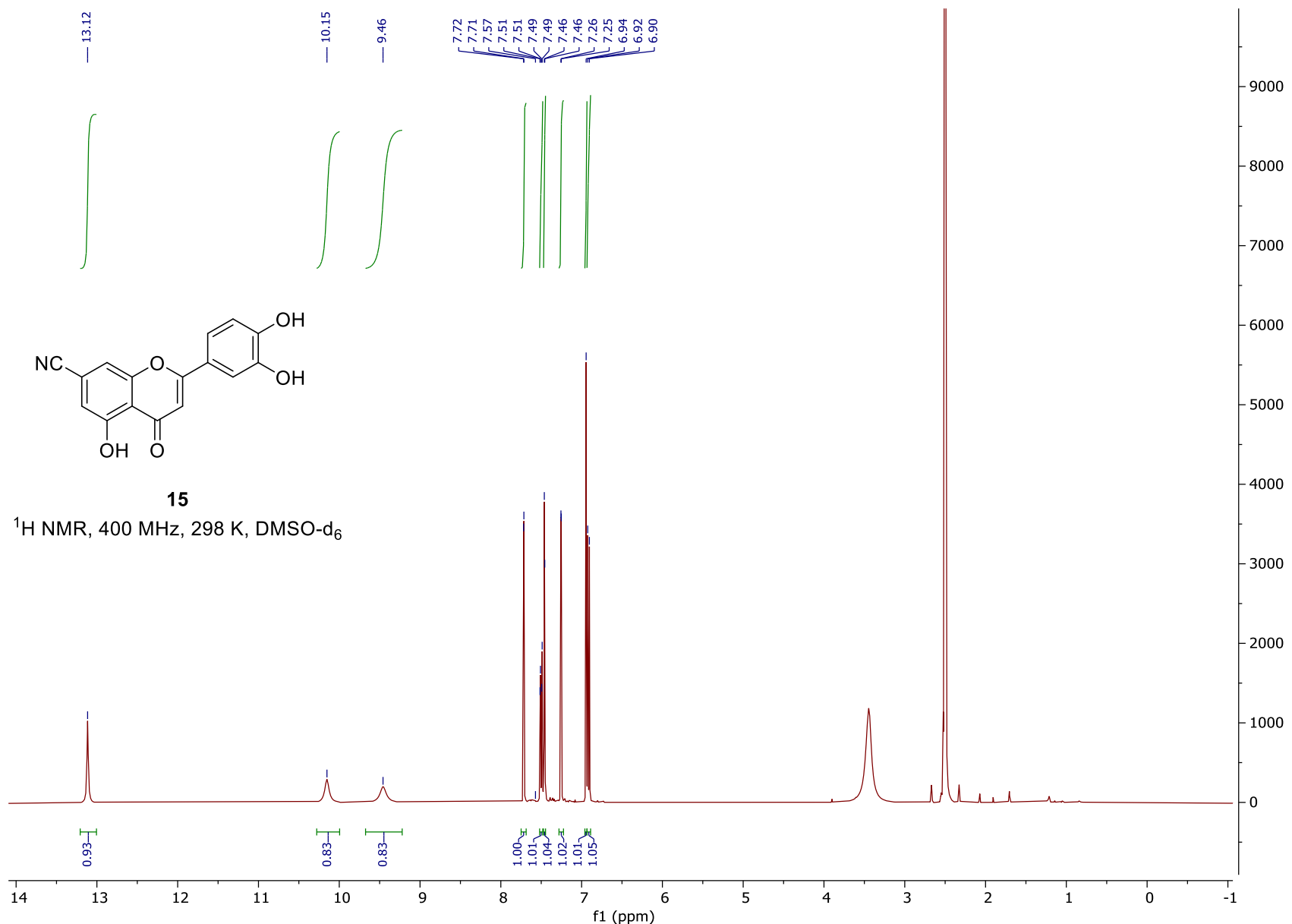
^1H NMR, 400 MHz, 298 K, CDCl_3

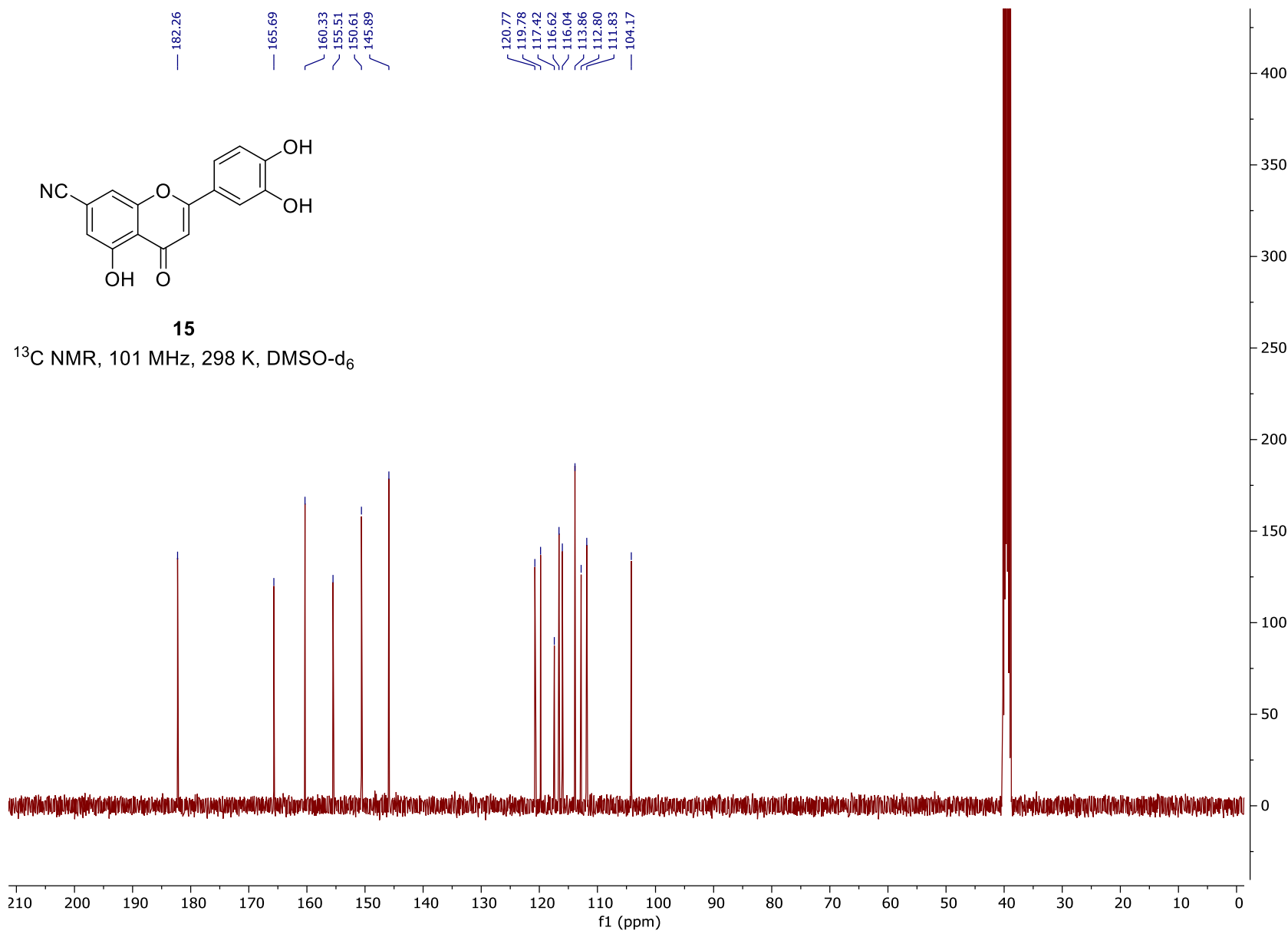


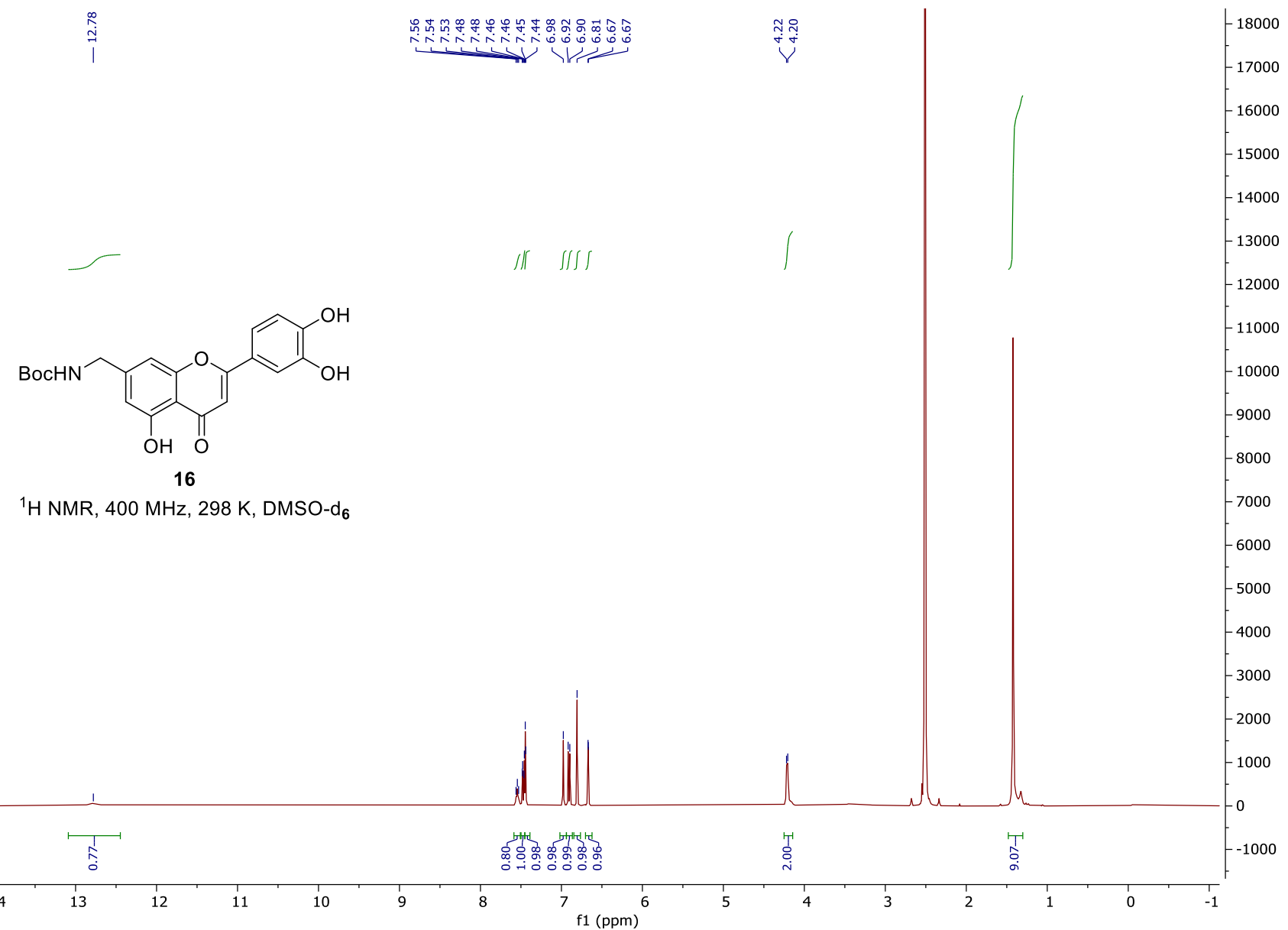


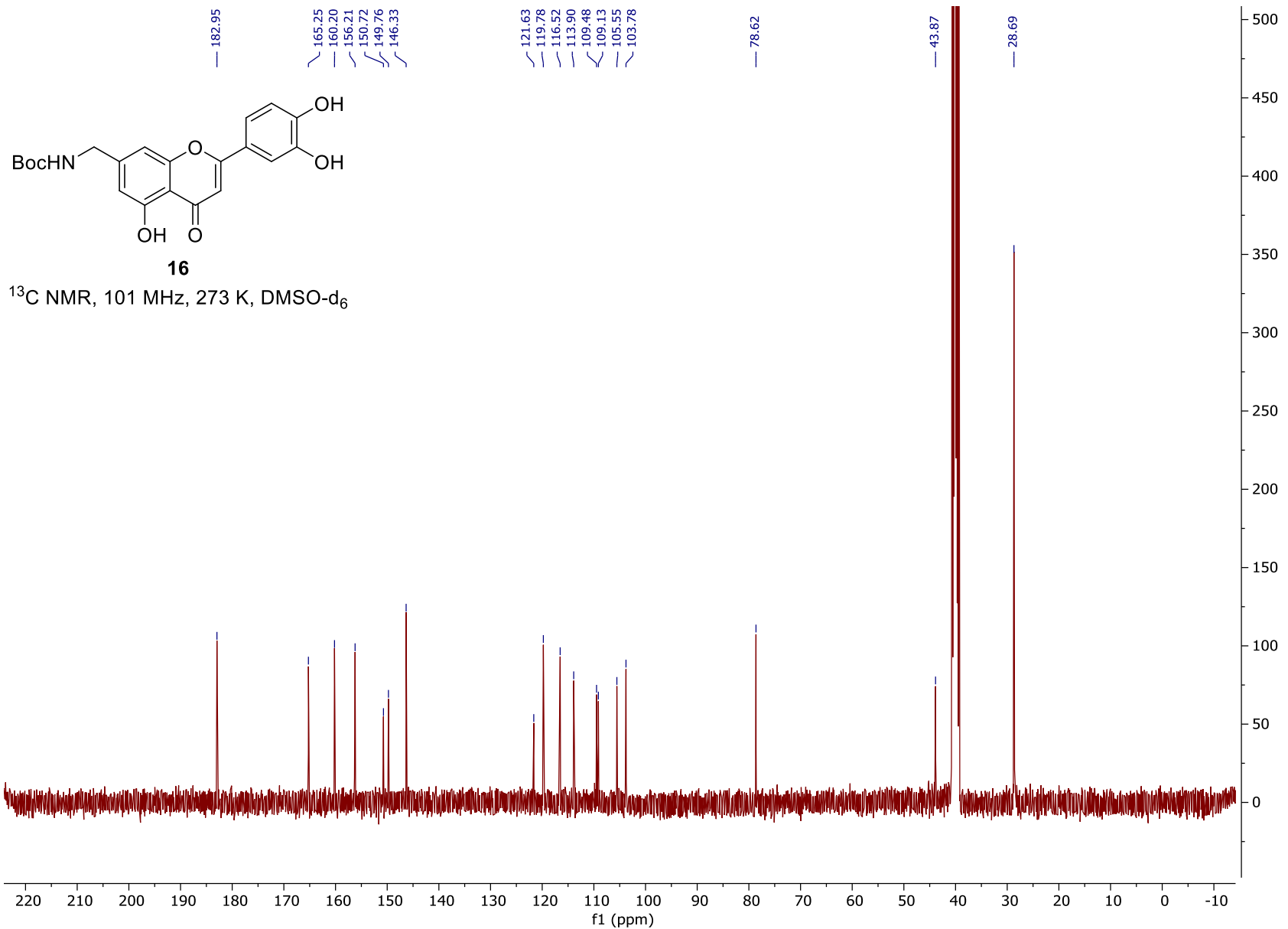


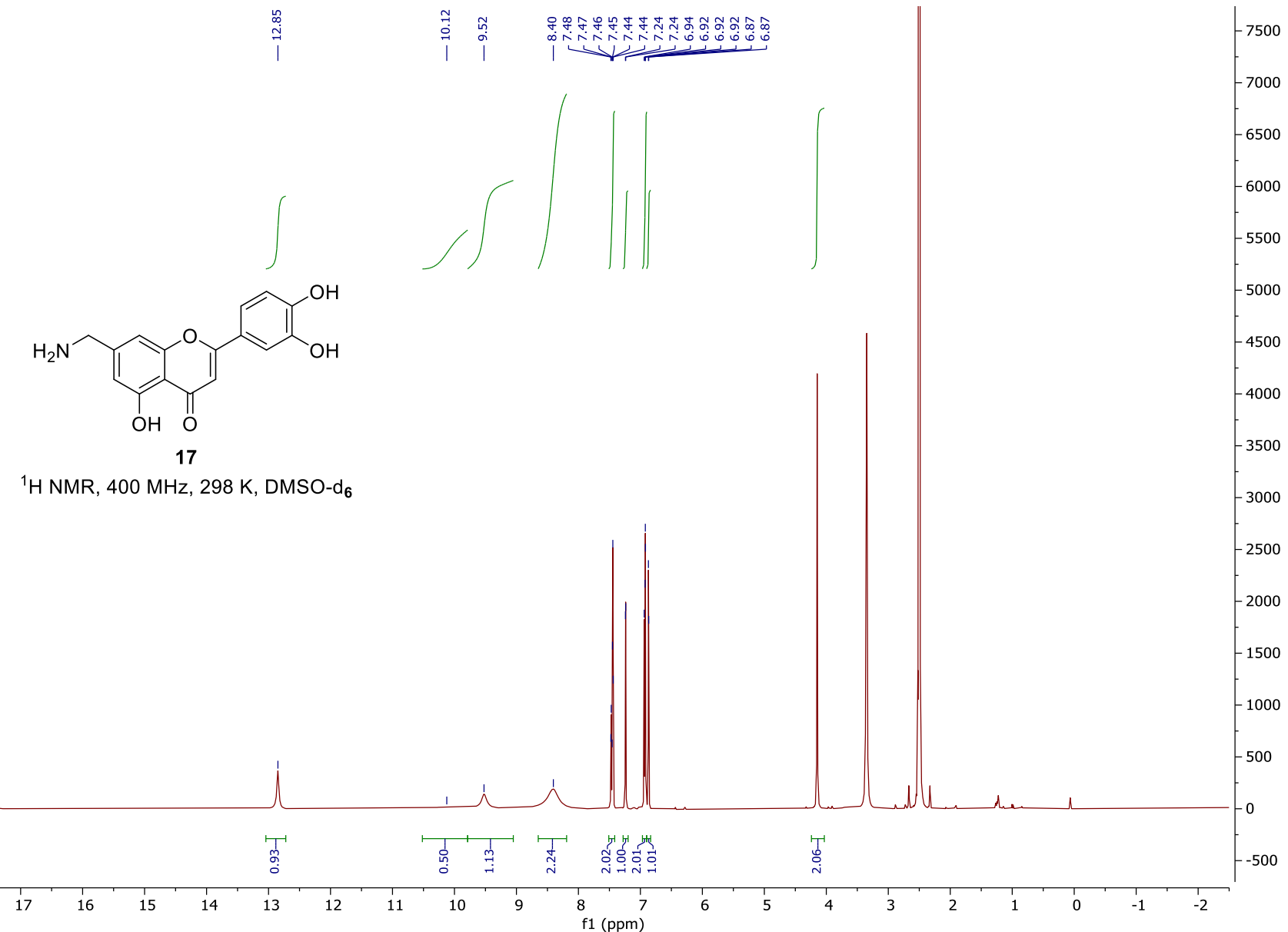


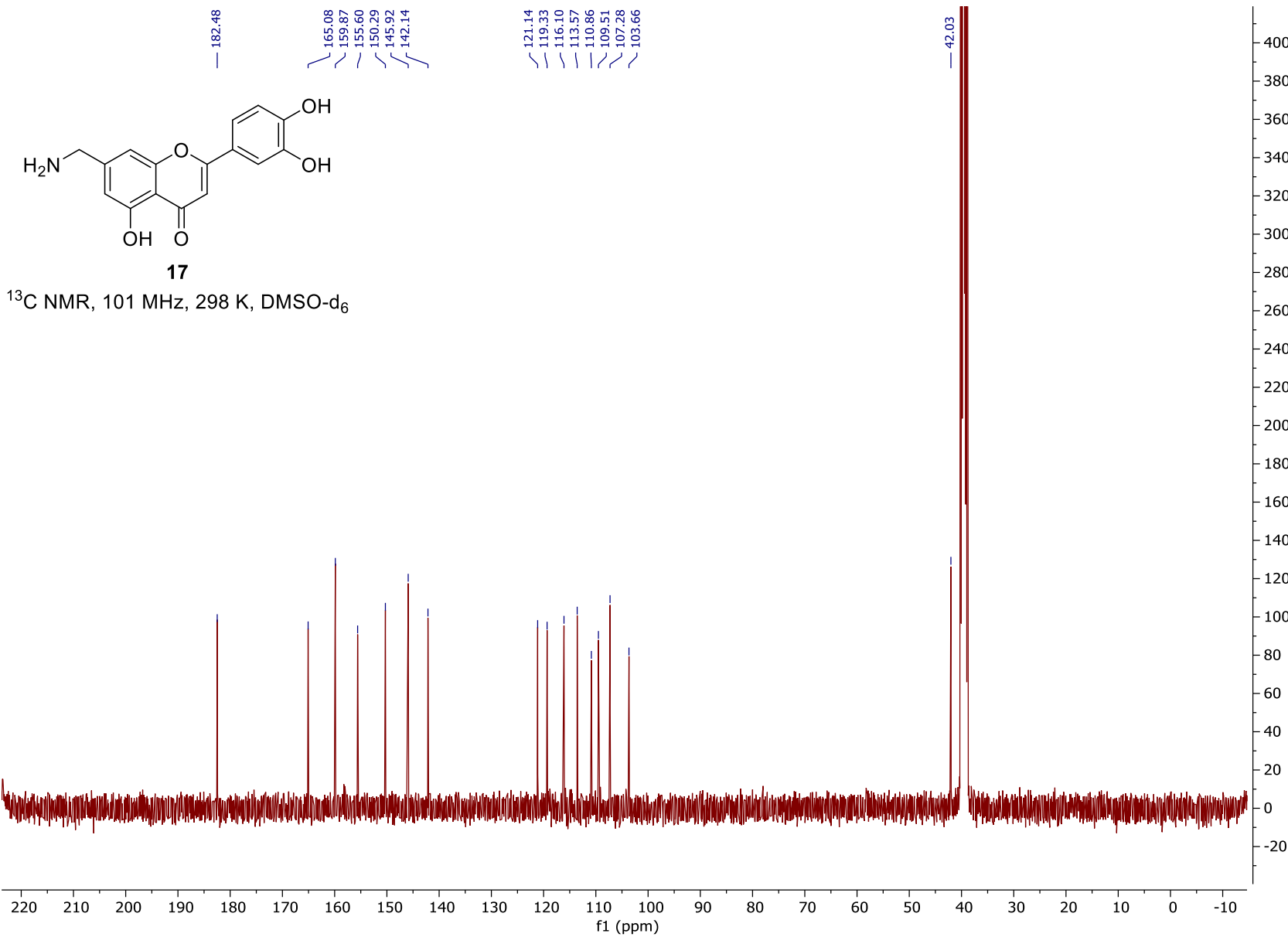


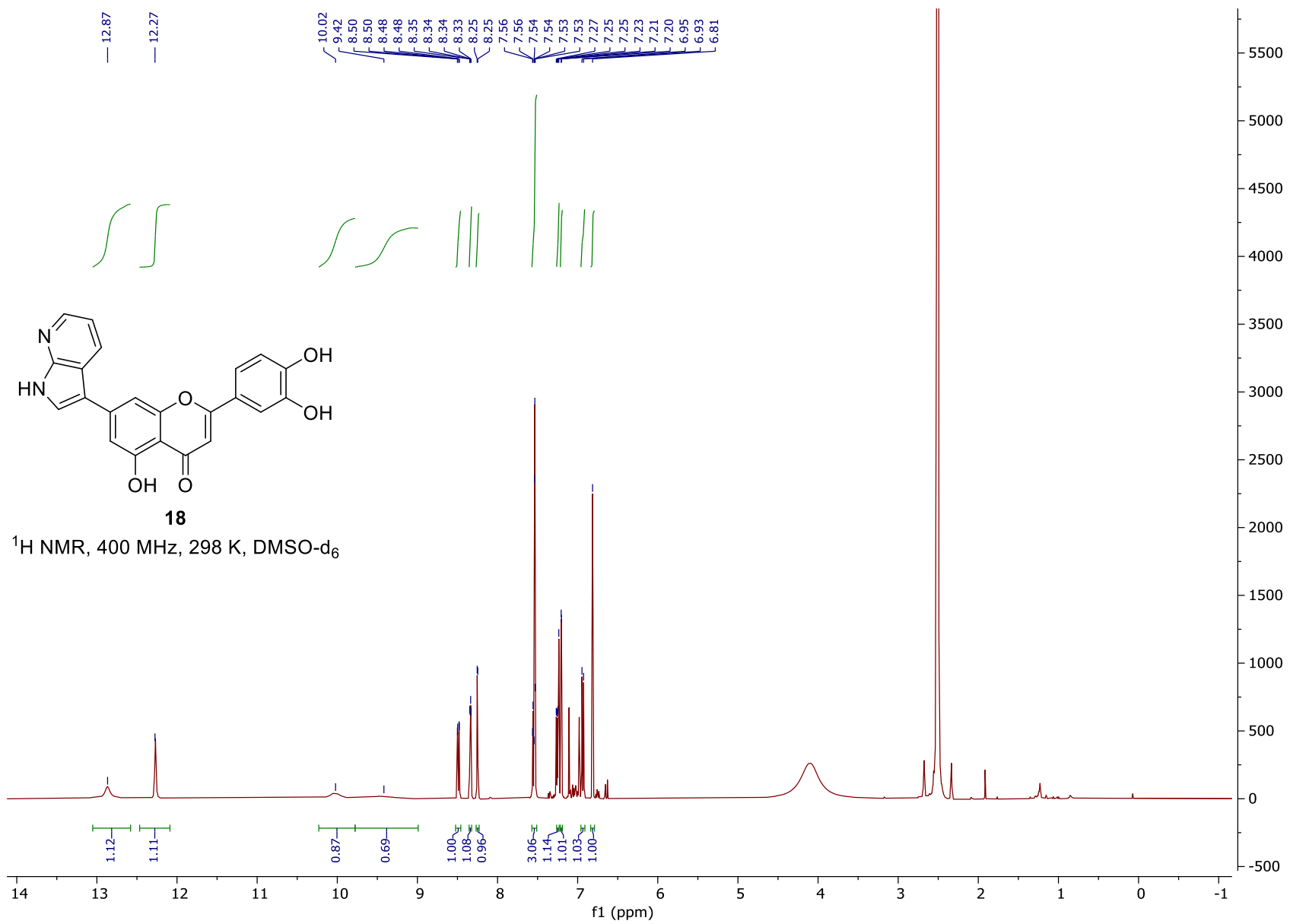


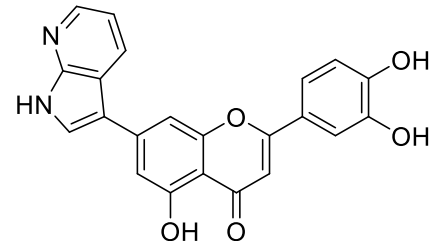






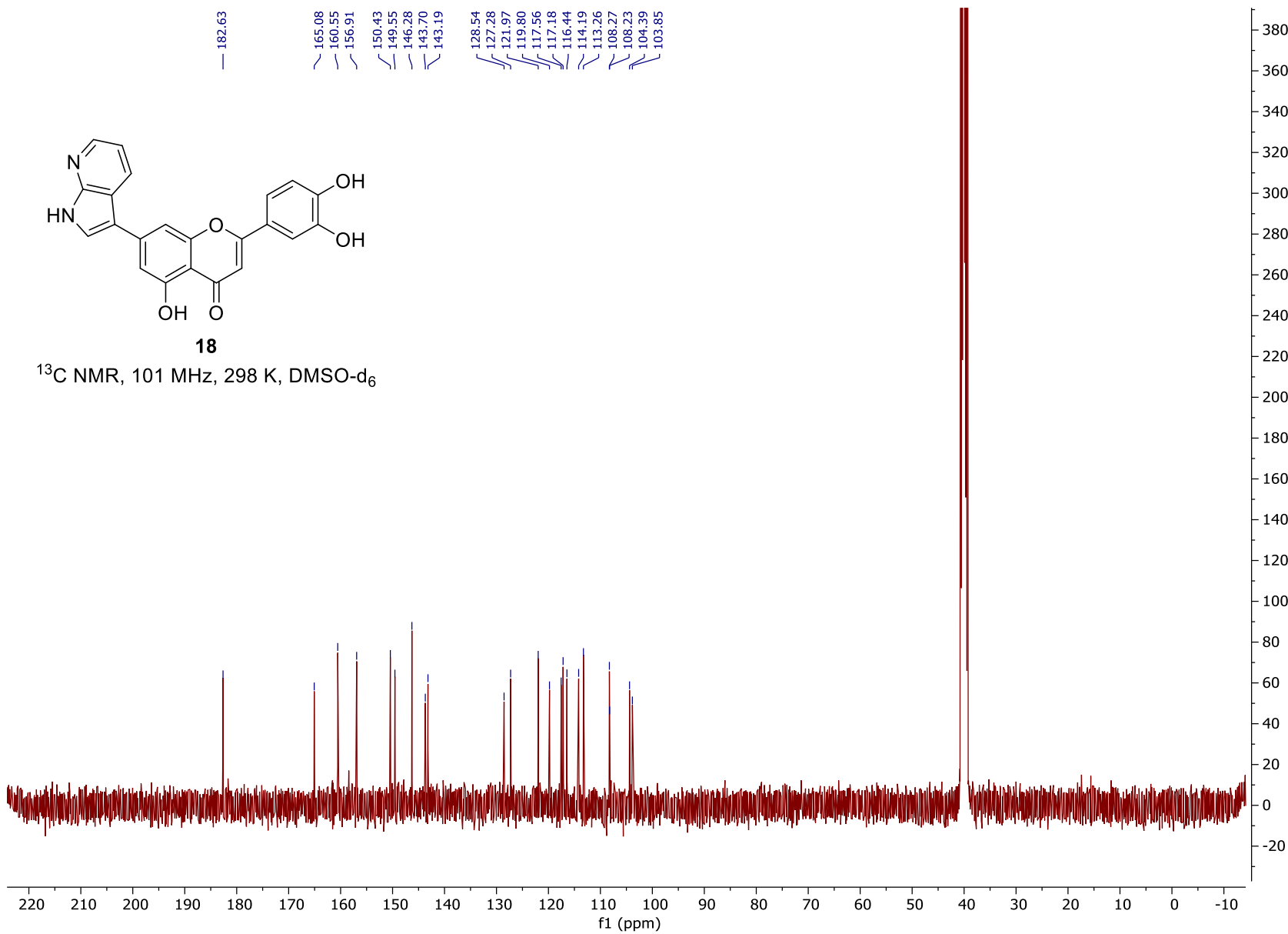


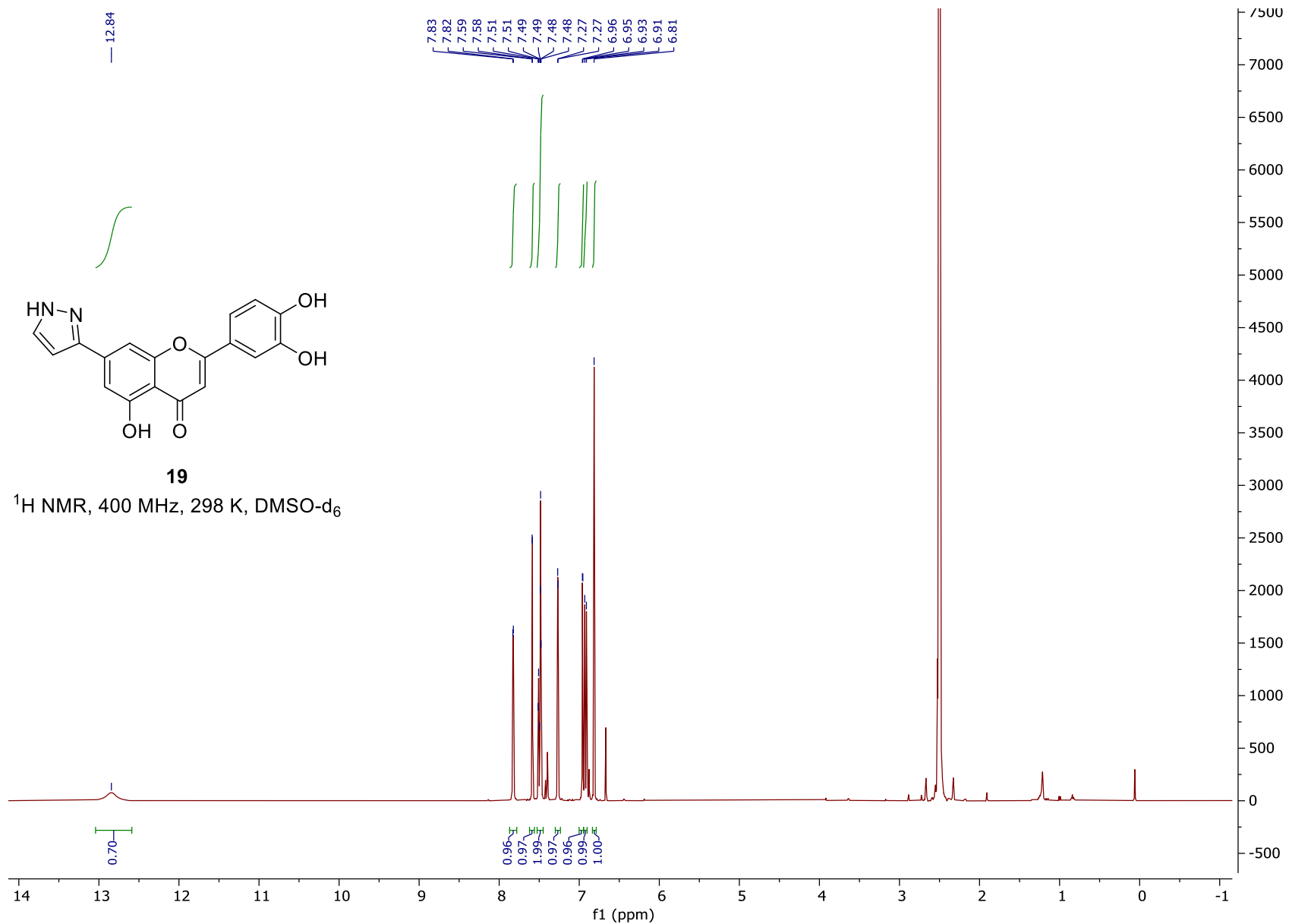


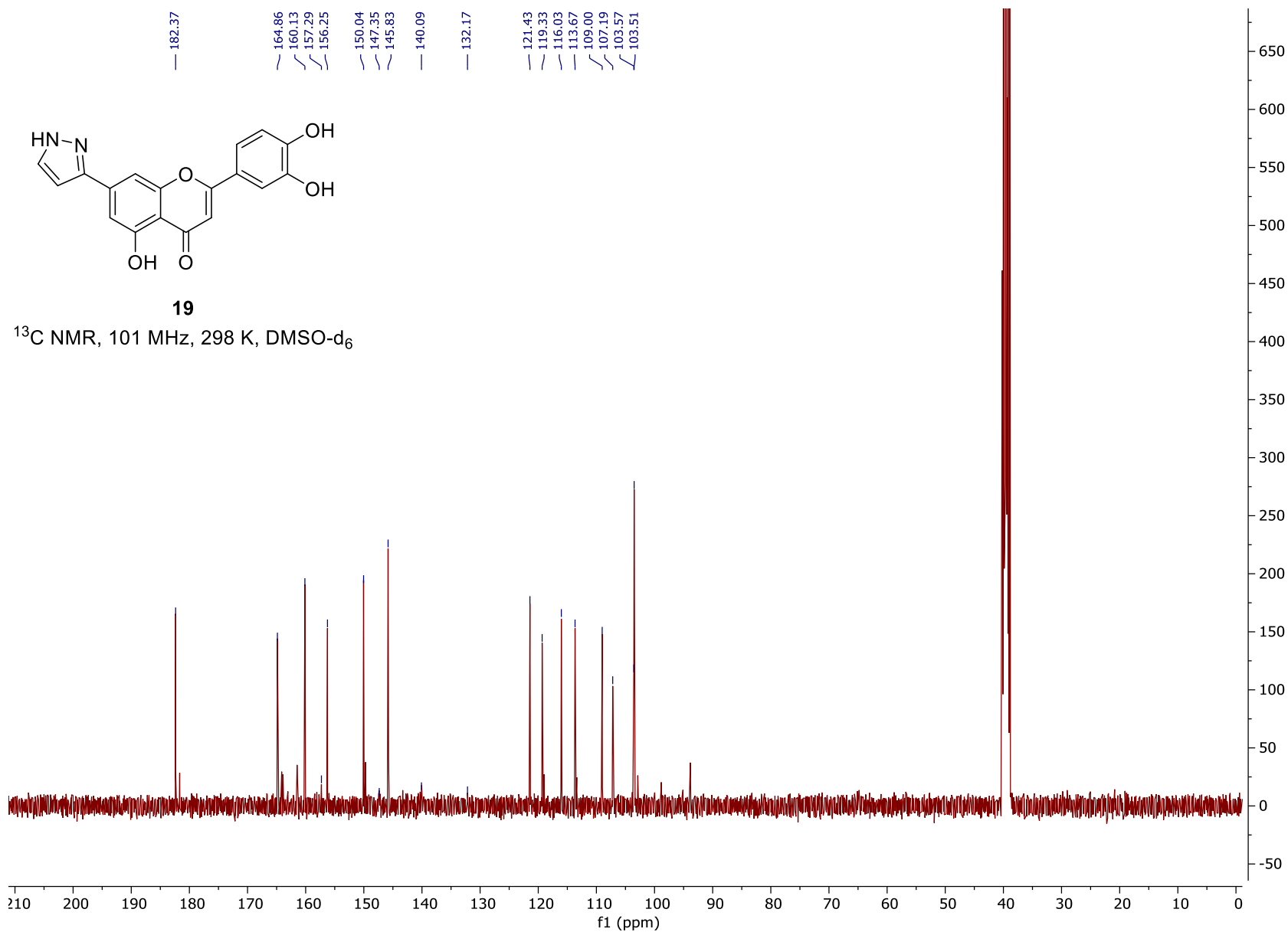


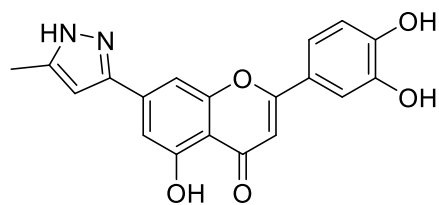
18

^{13}C NMR, 101 MHz, 298 K, DMSO-d₆



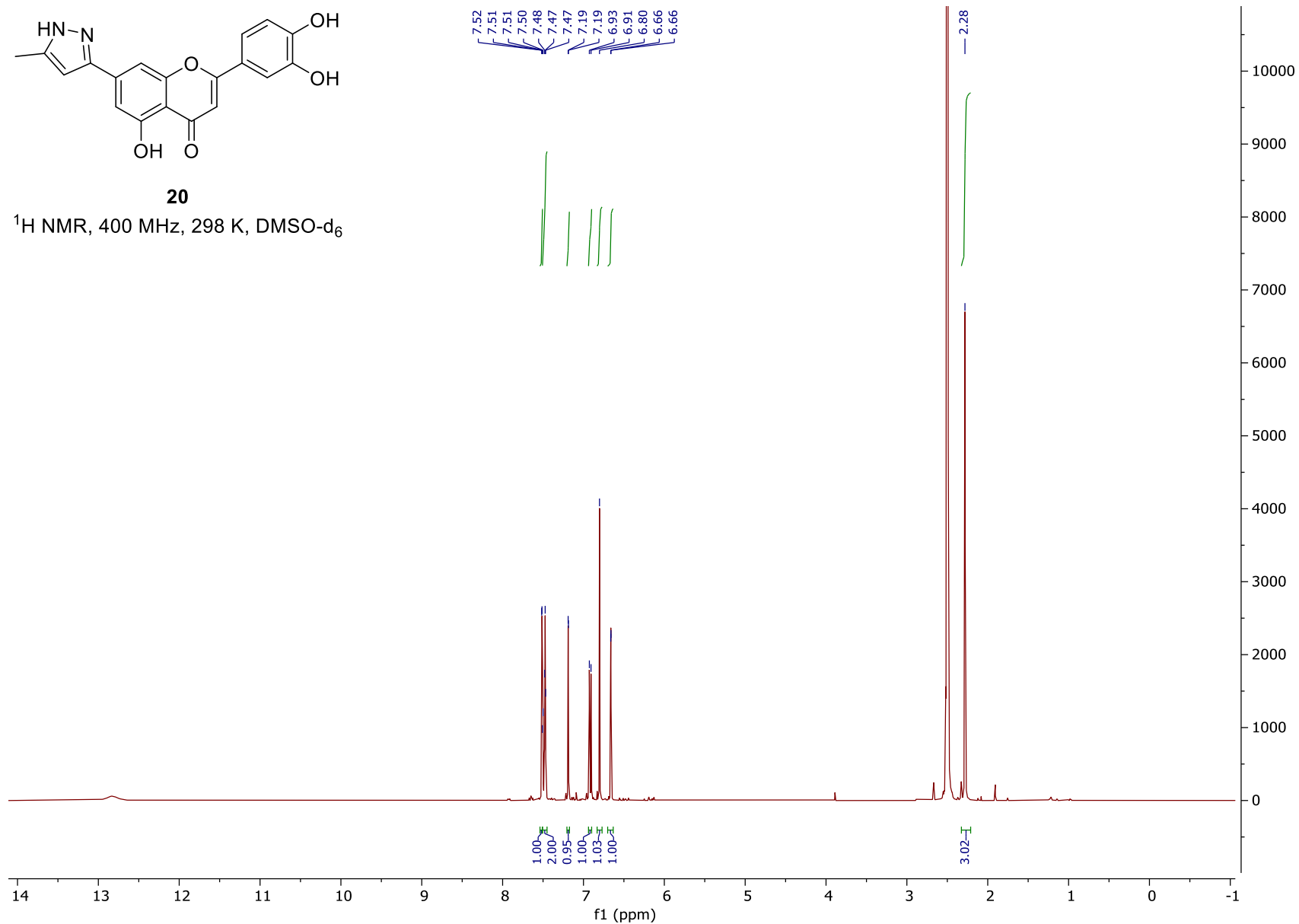


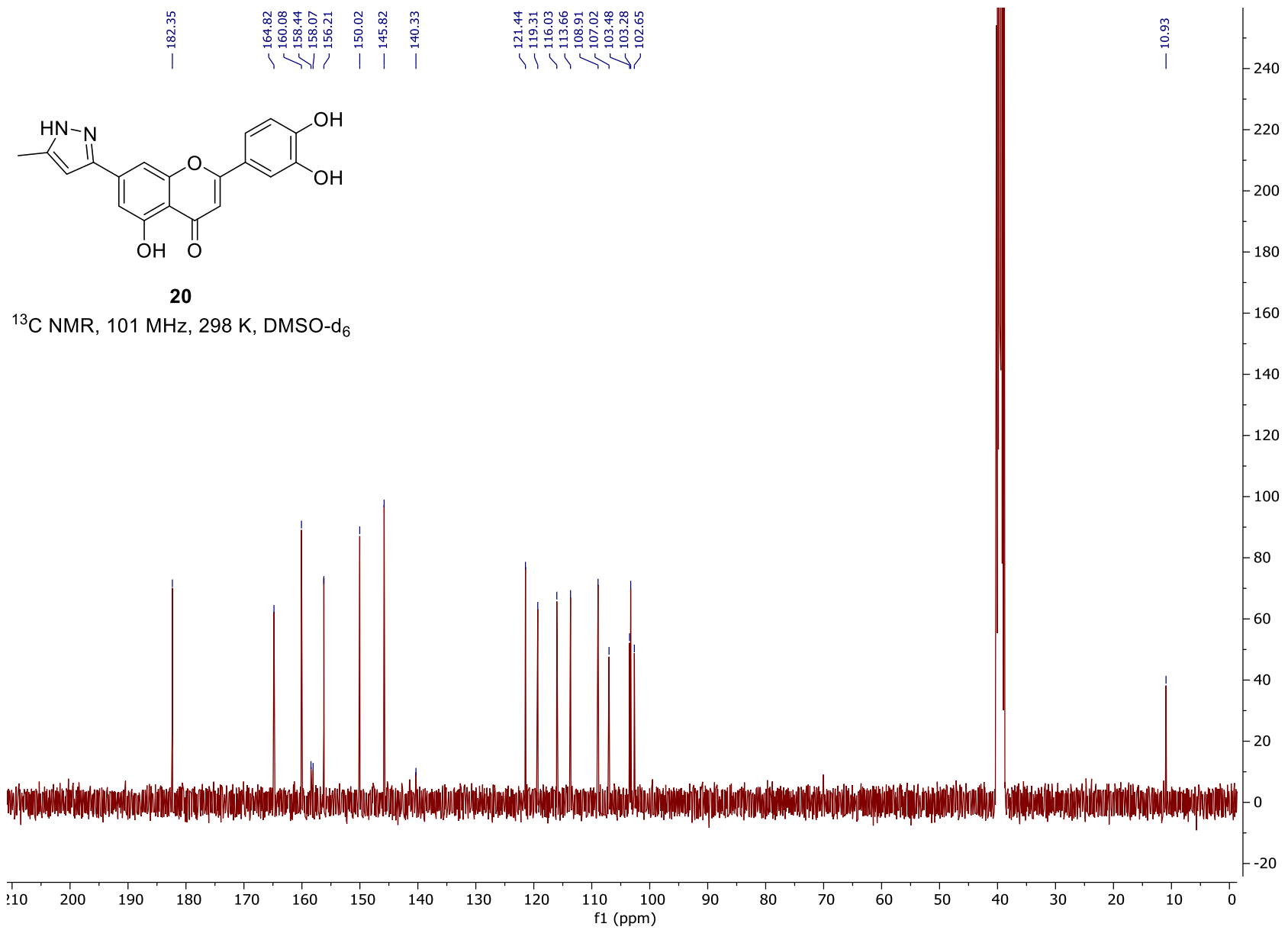


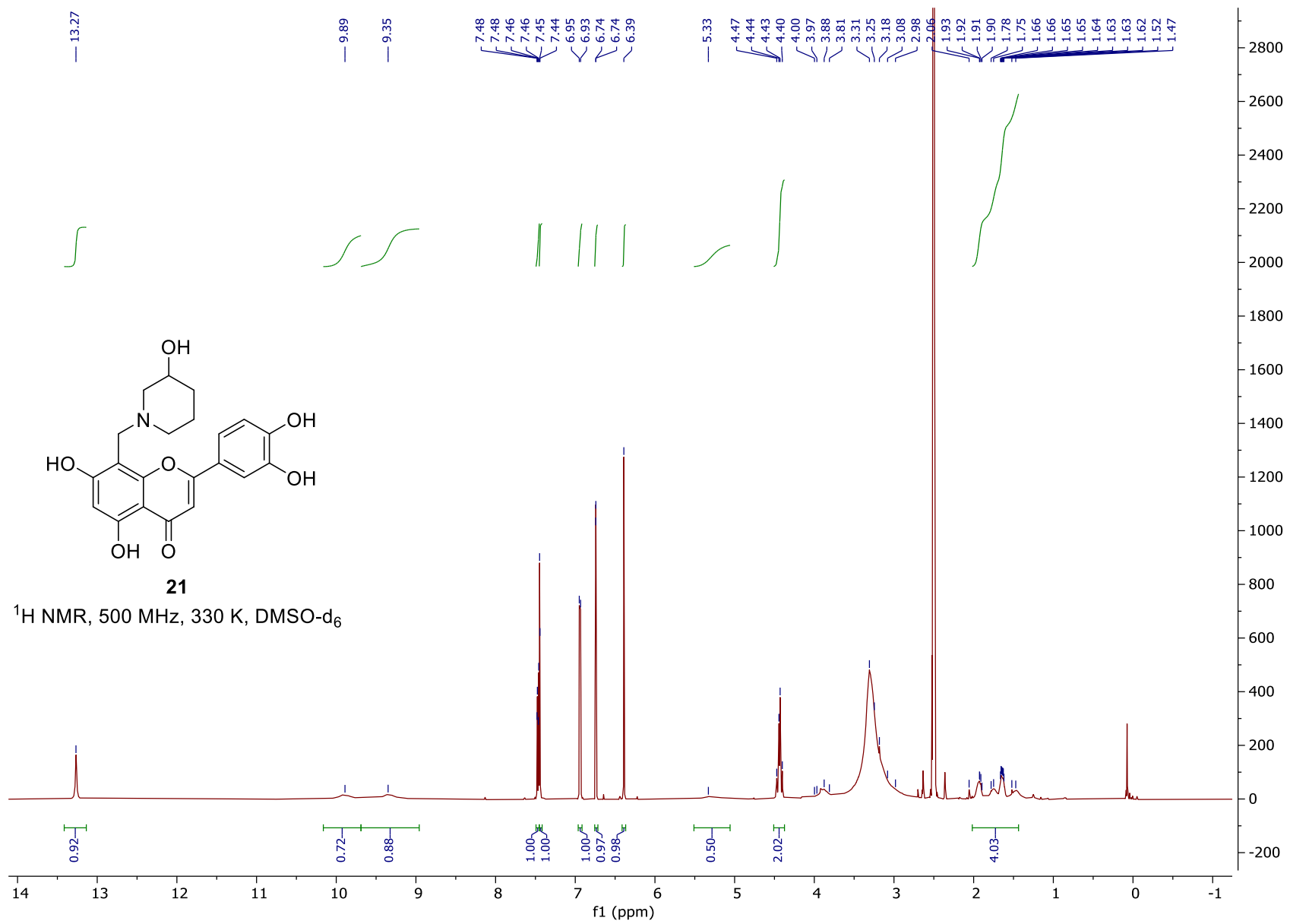


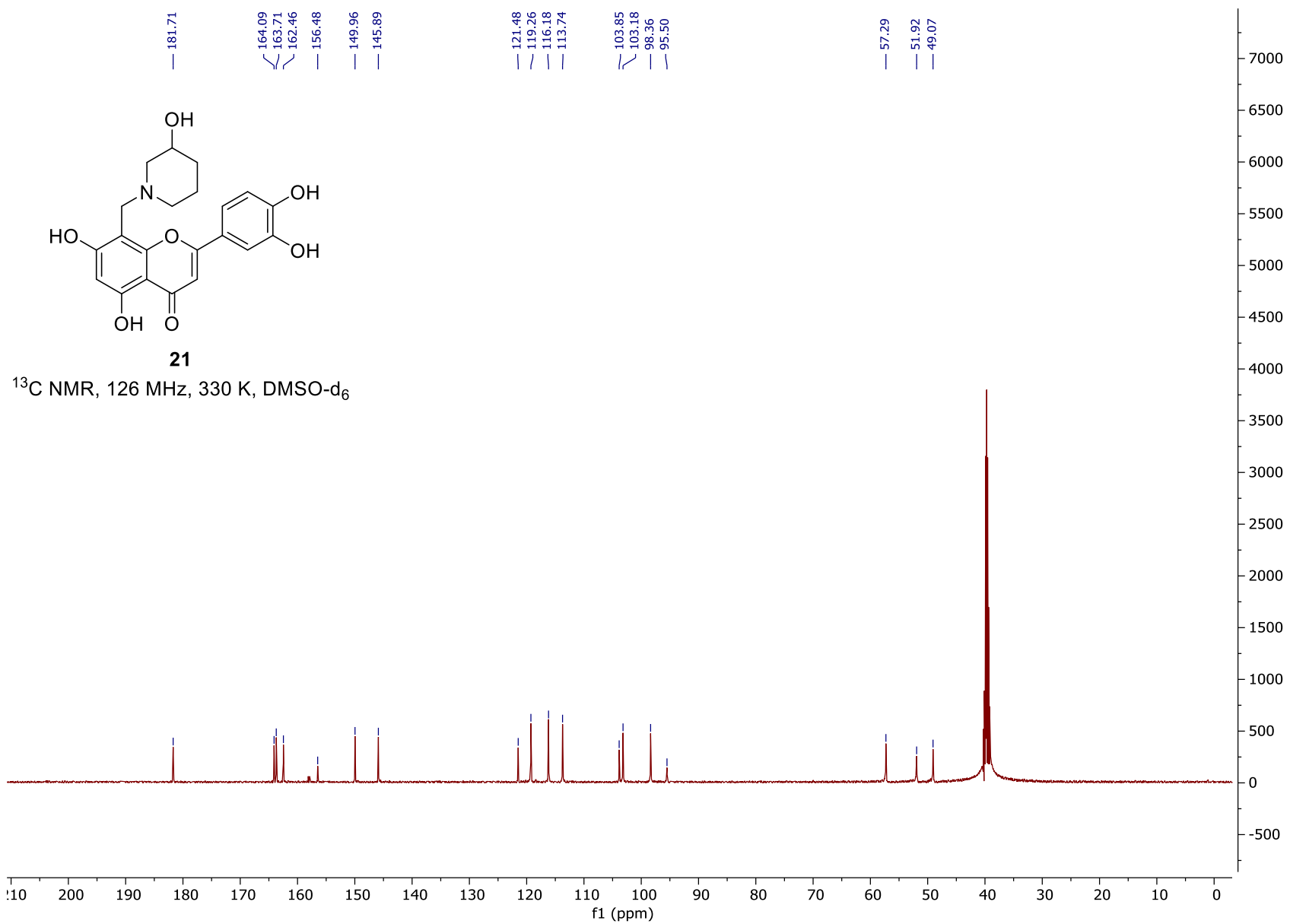
20

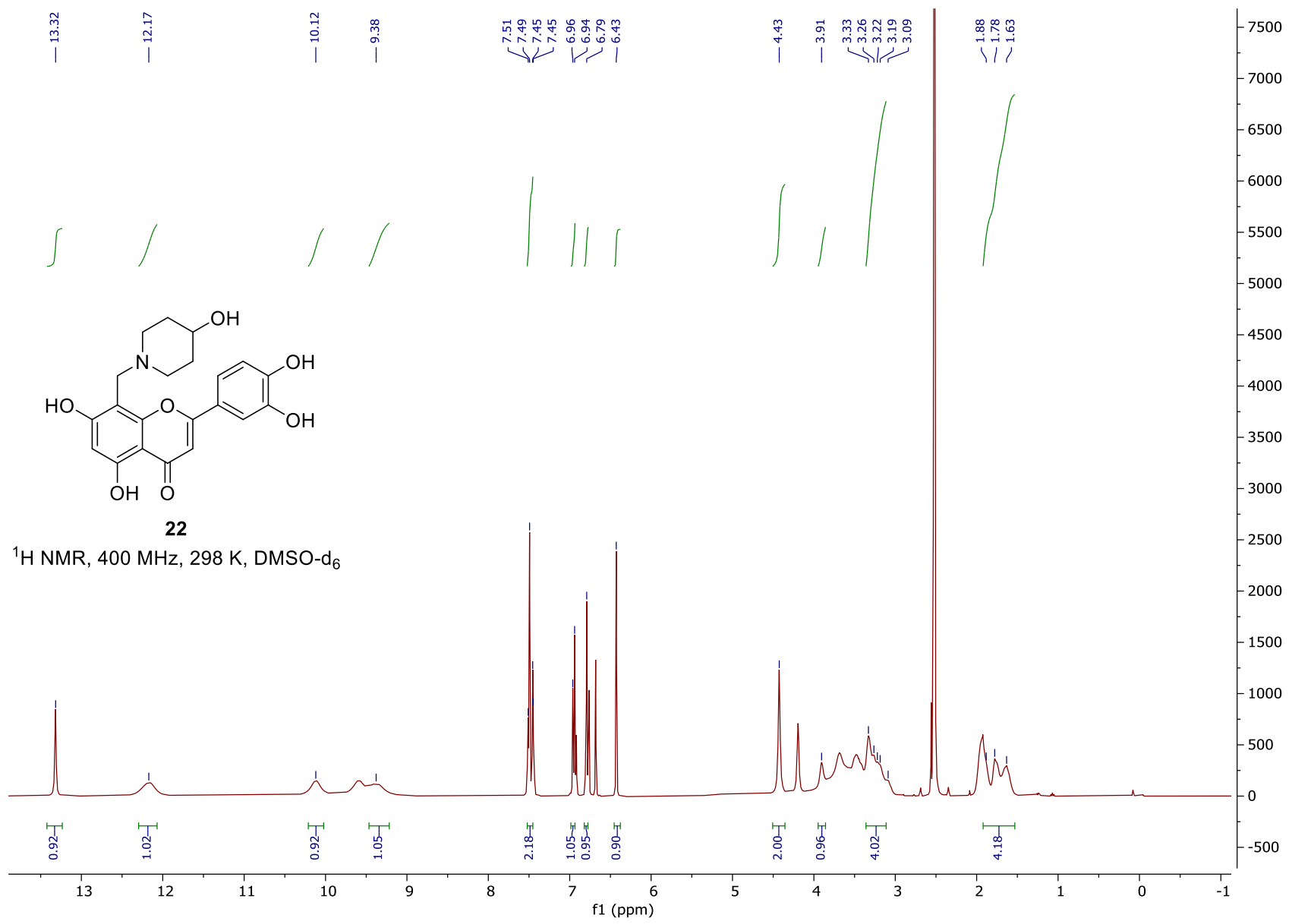
^1H NMR, 400 MHz, 298 K, DMSO-d₆

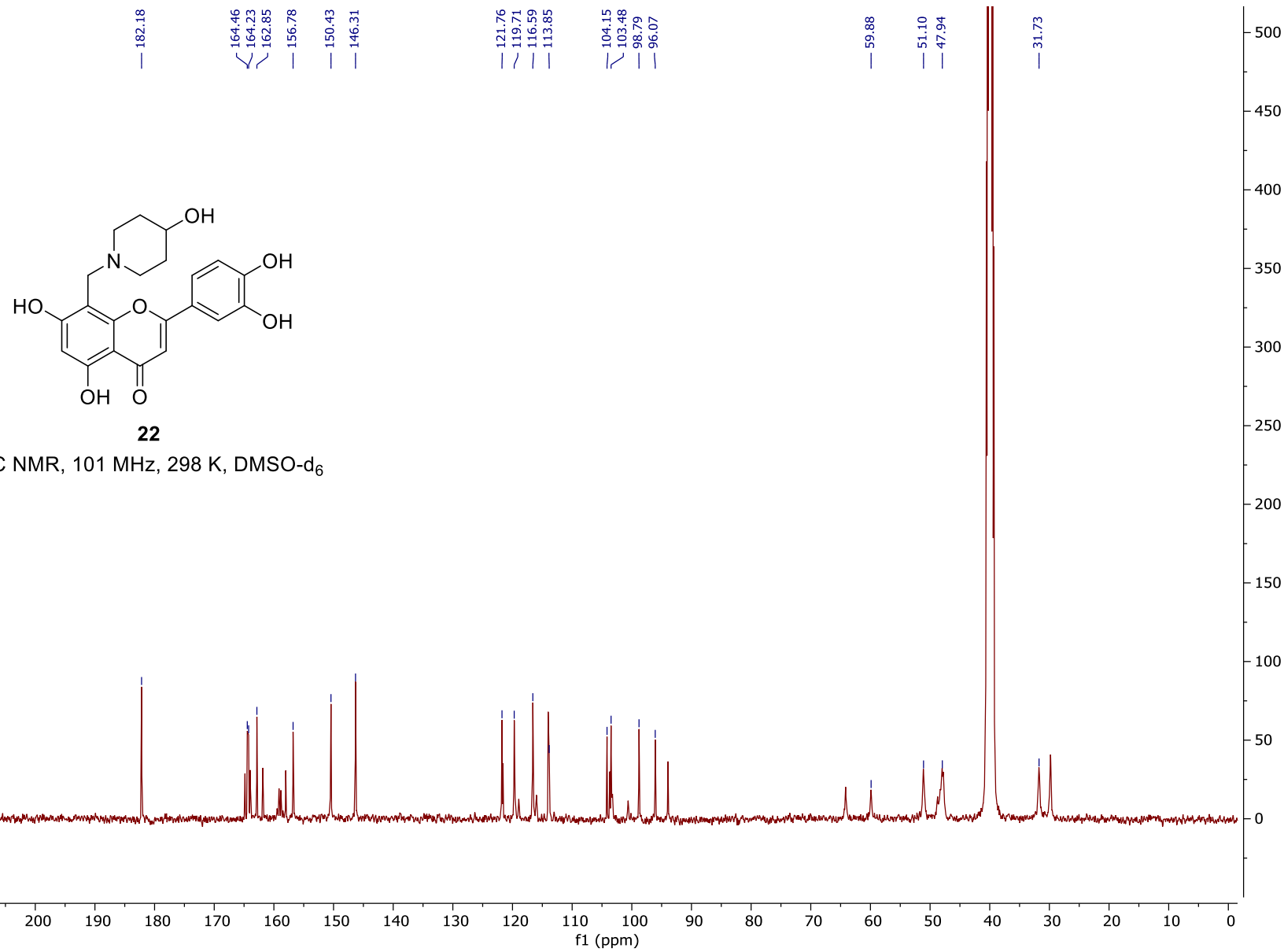


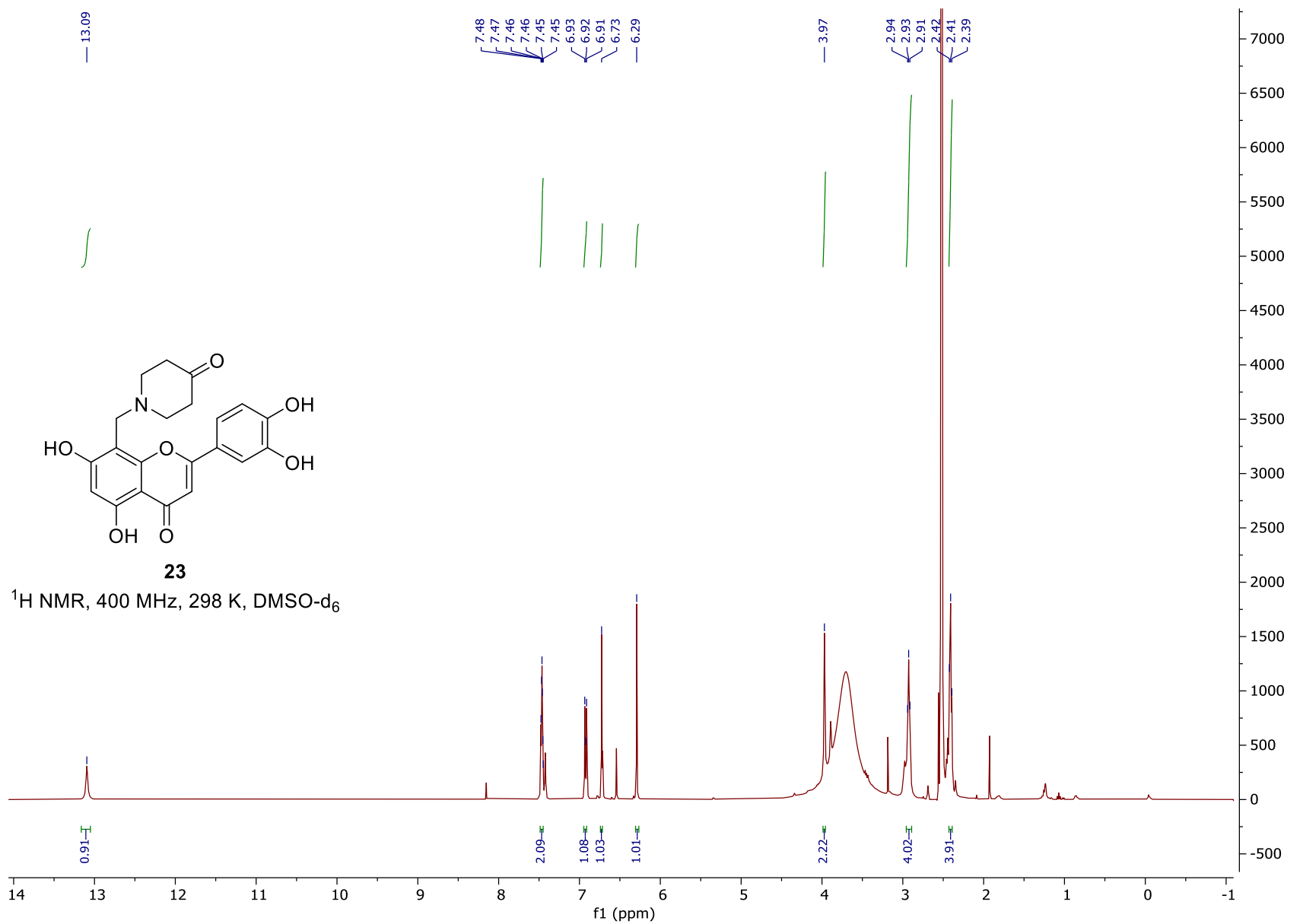


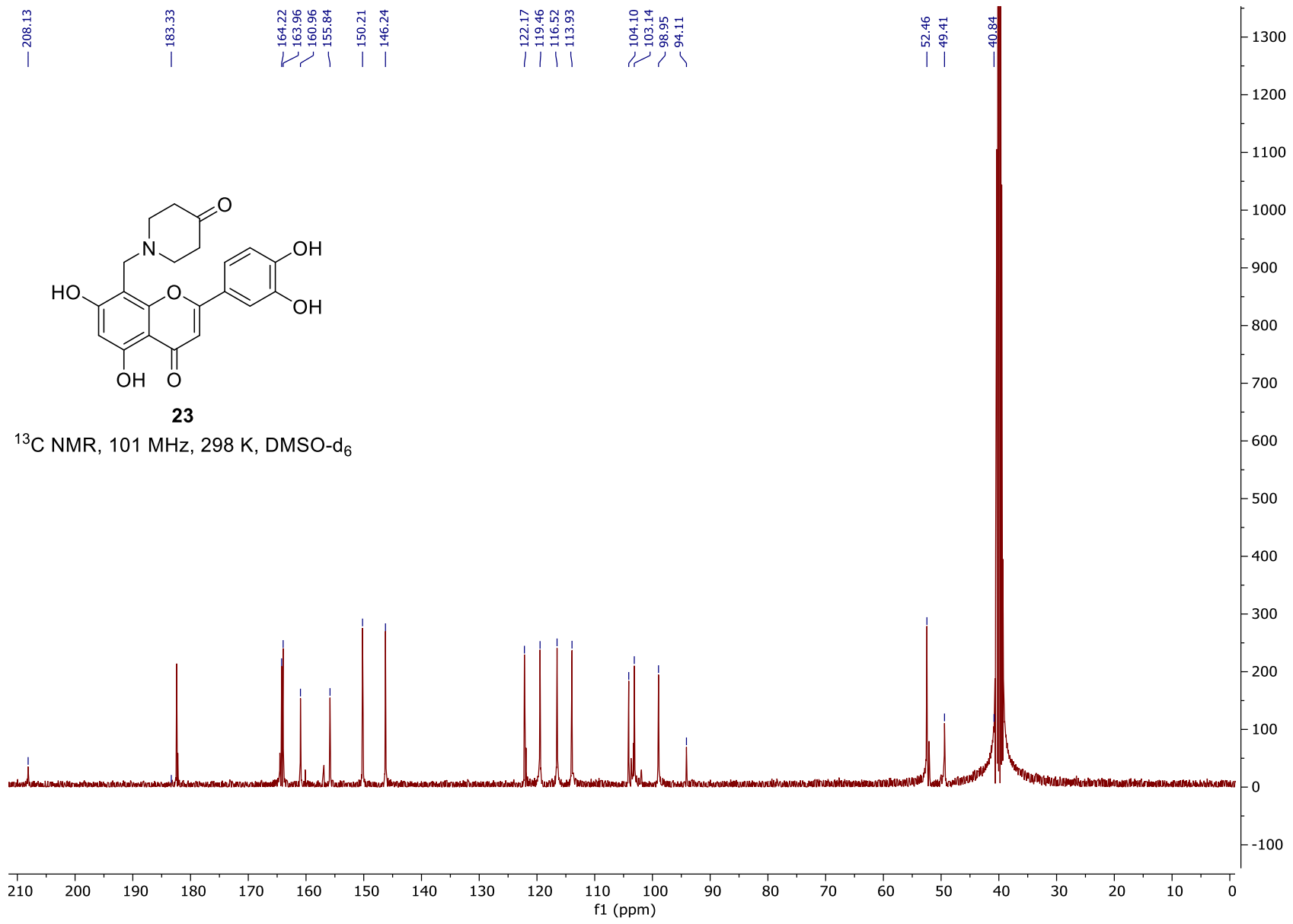


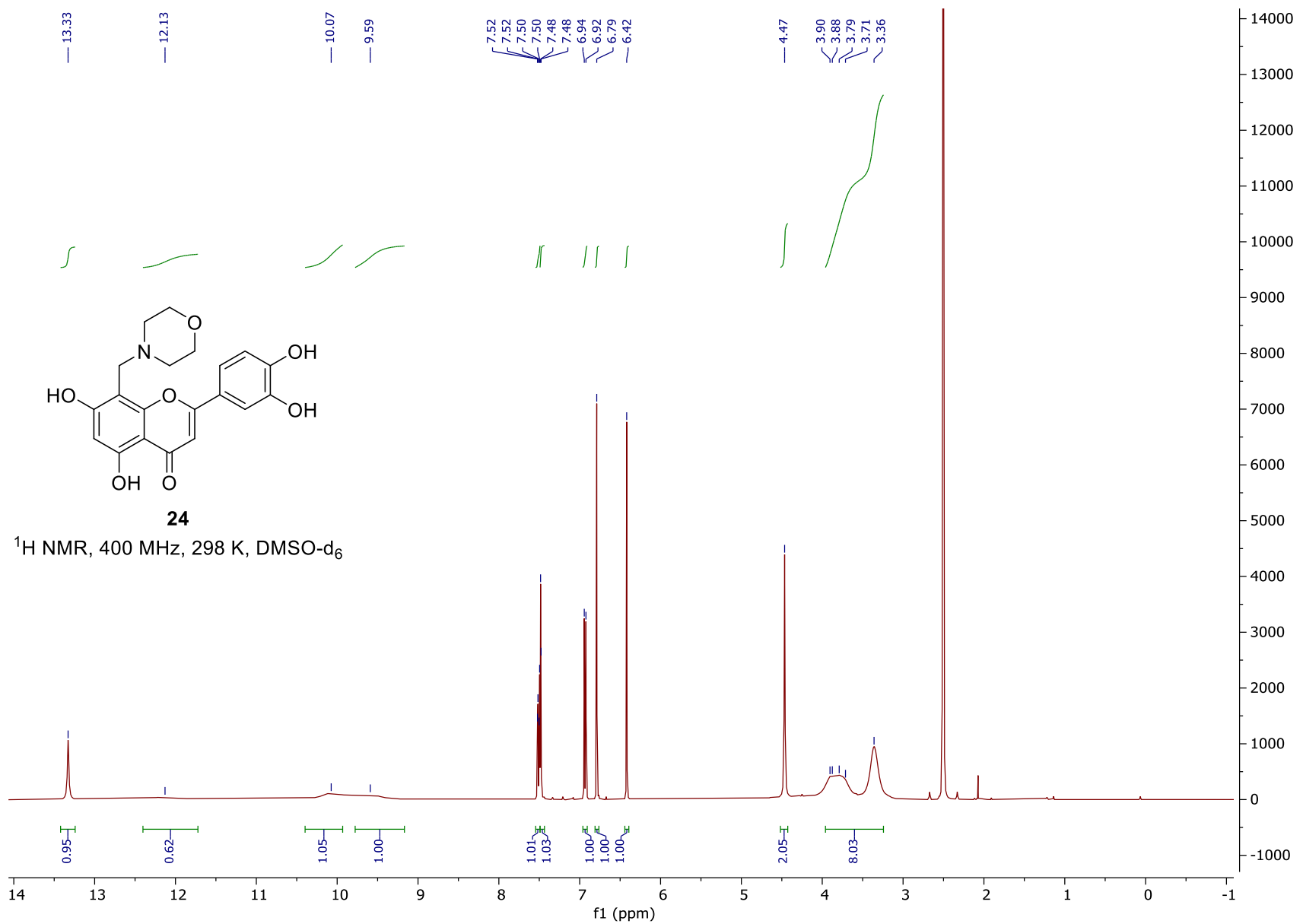


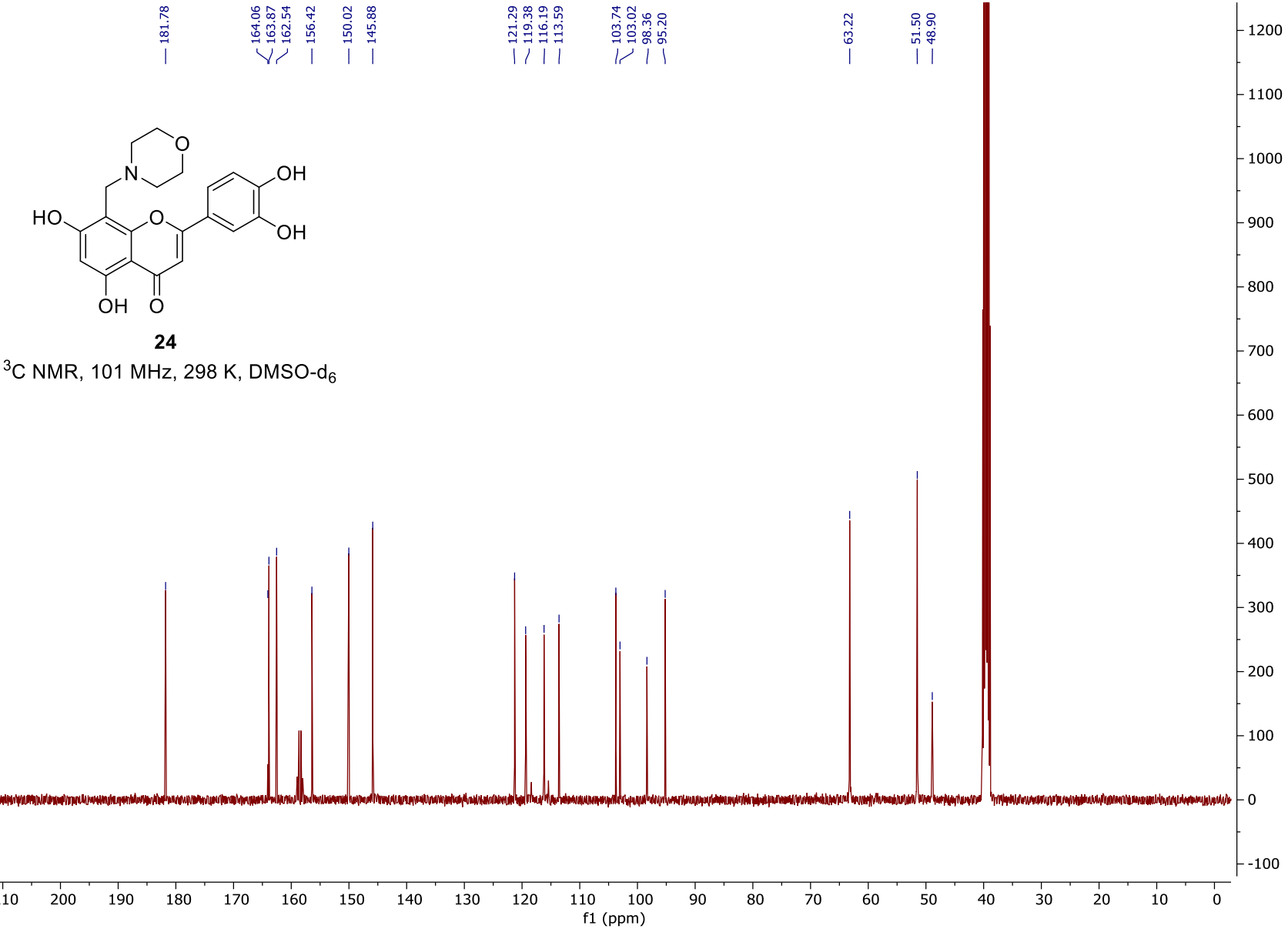


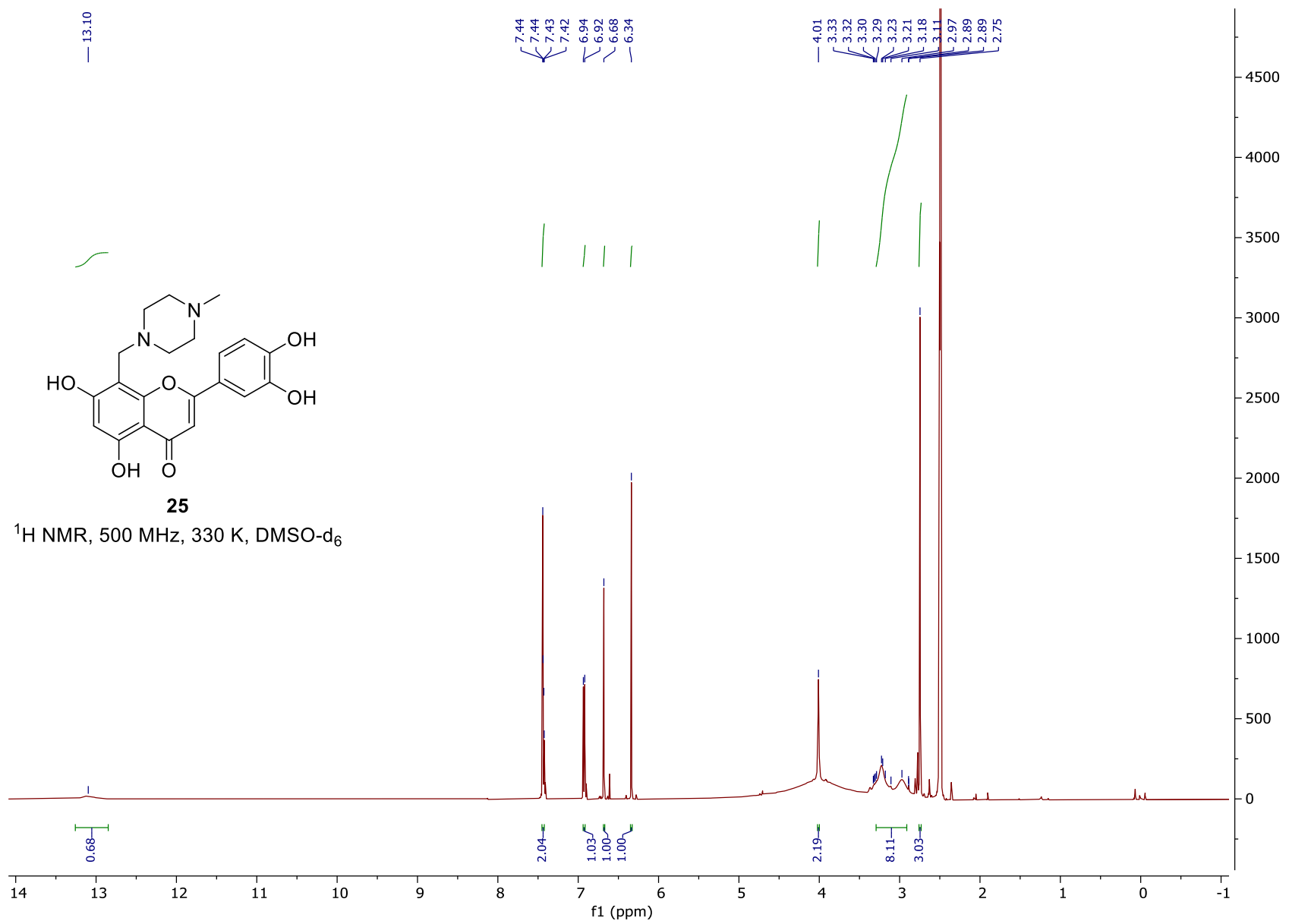


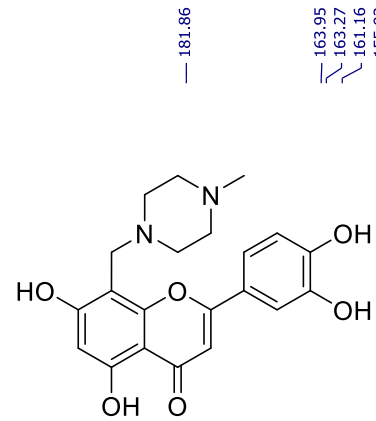




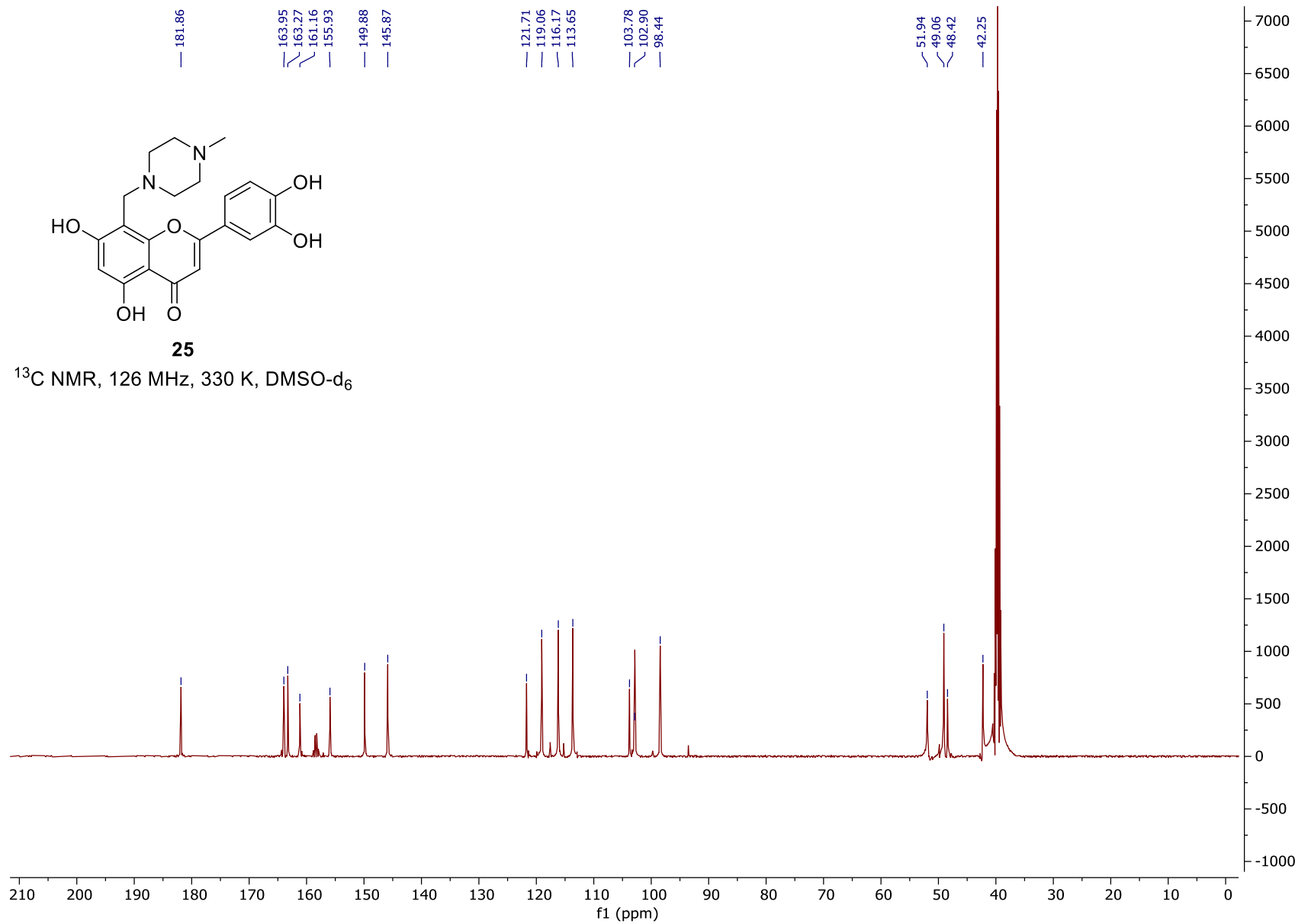


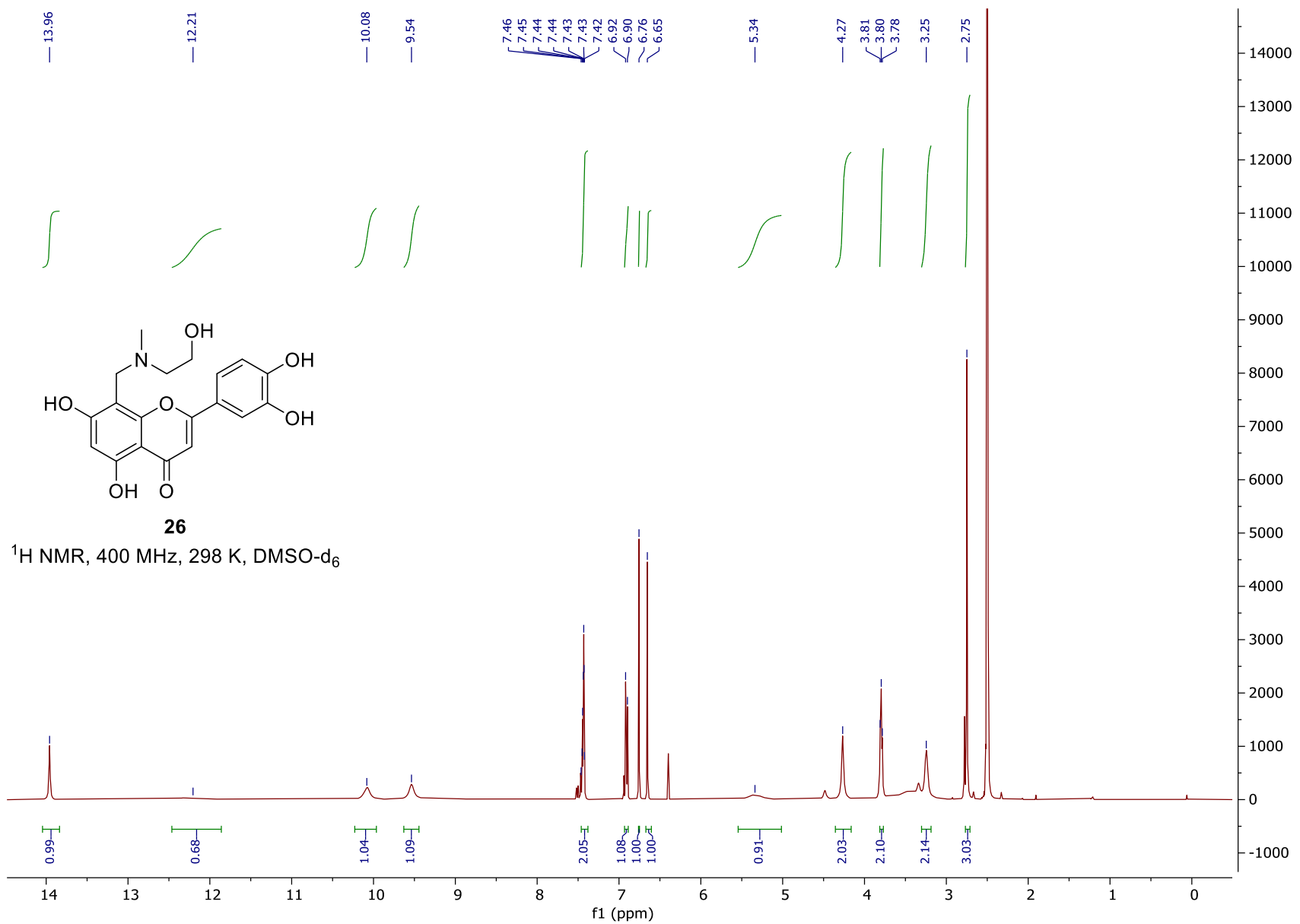


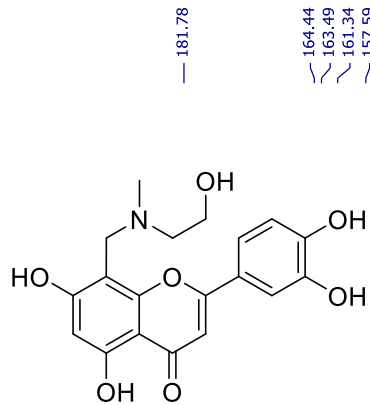




^{13}C NMR, 126 MHz, 330 K, DMSO-d₆

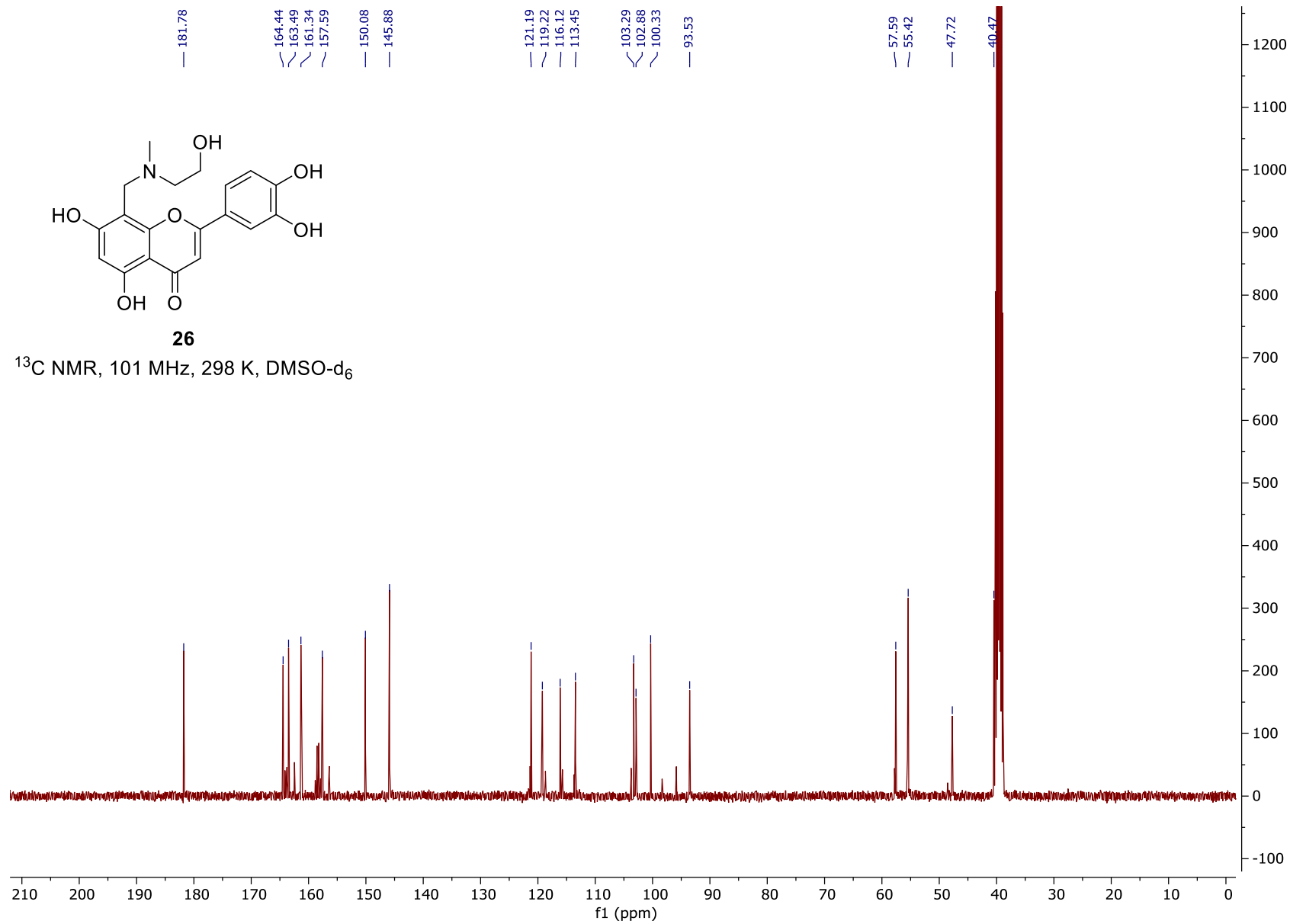


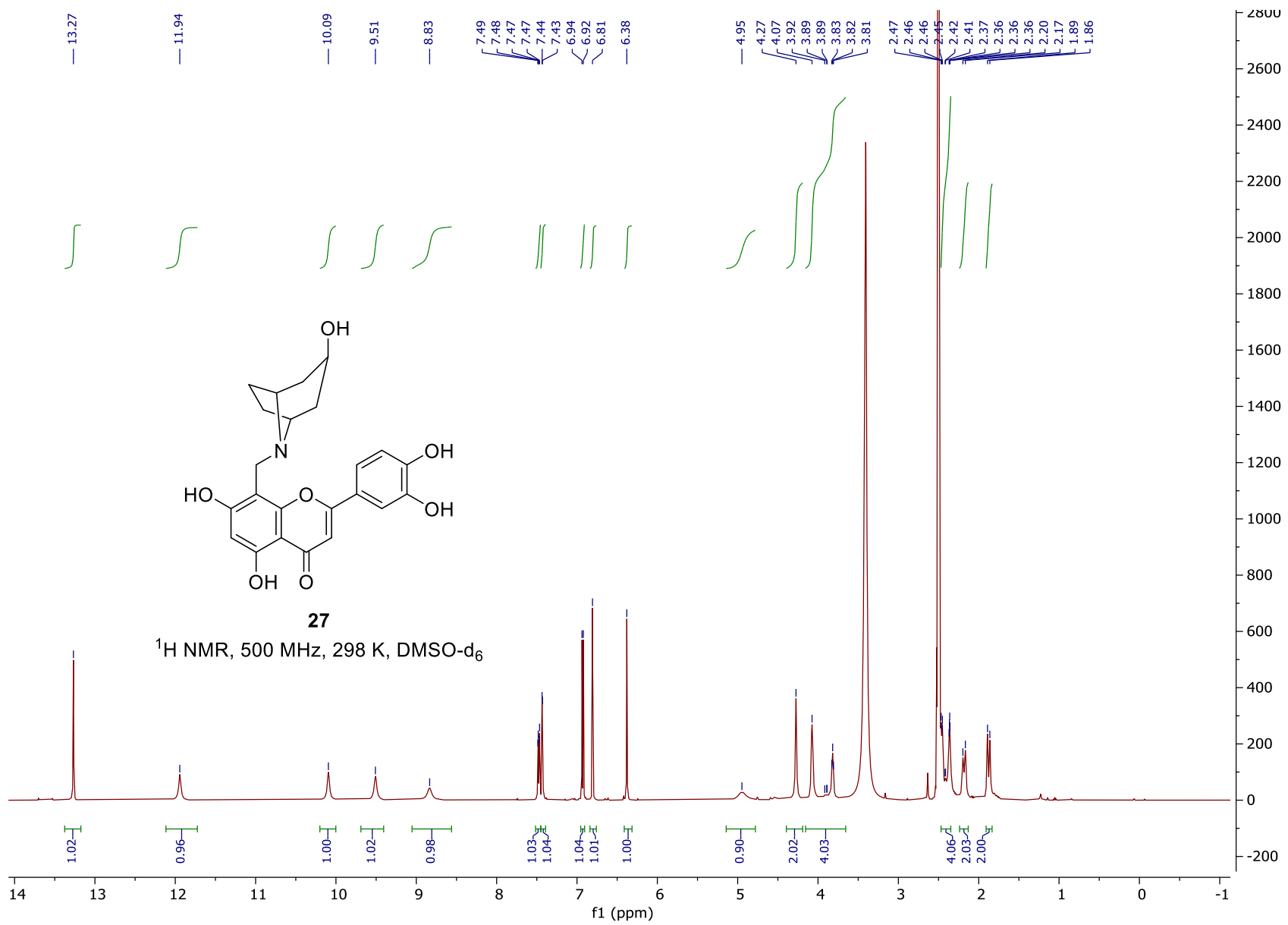


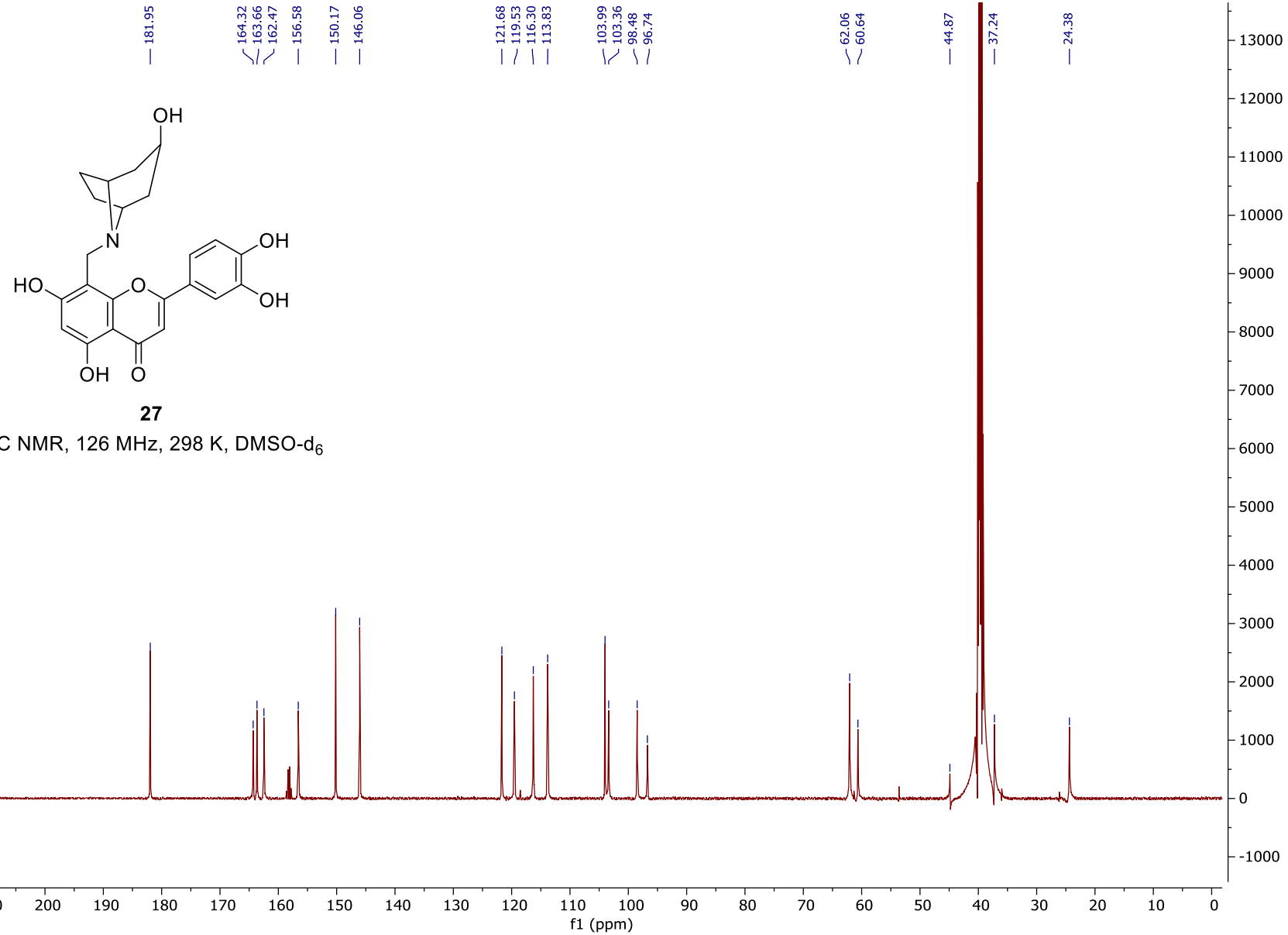


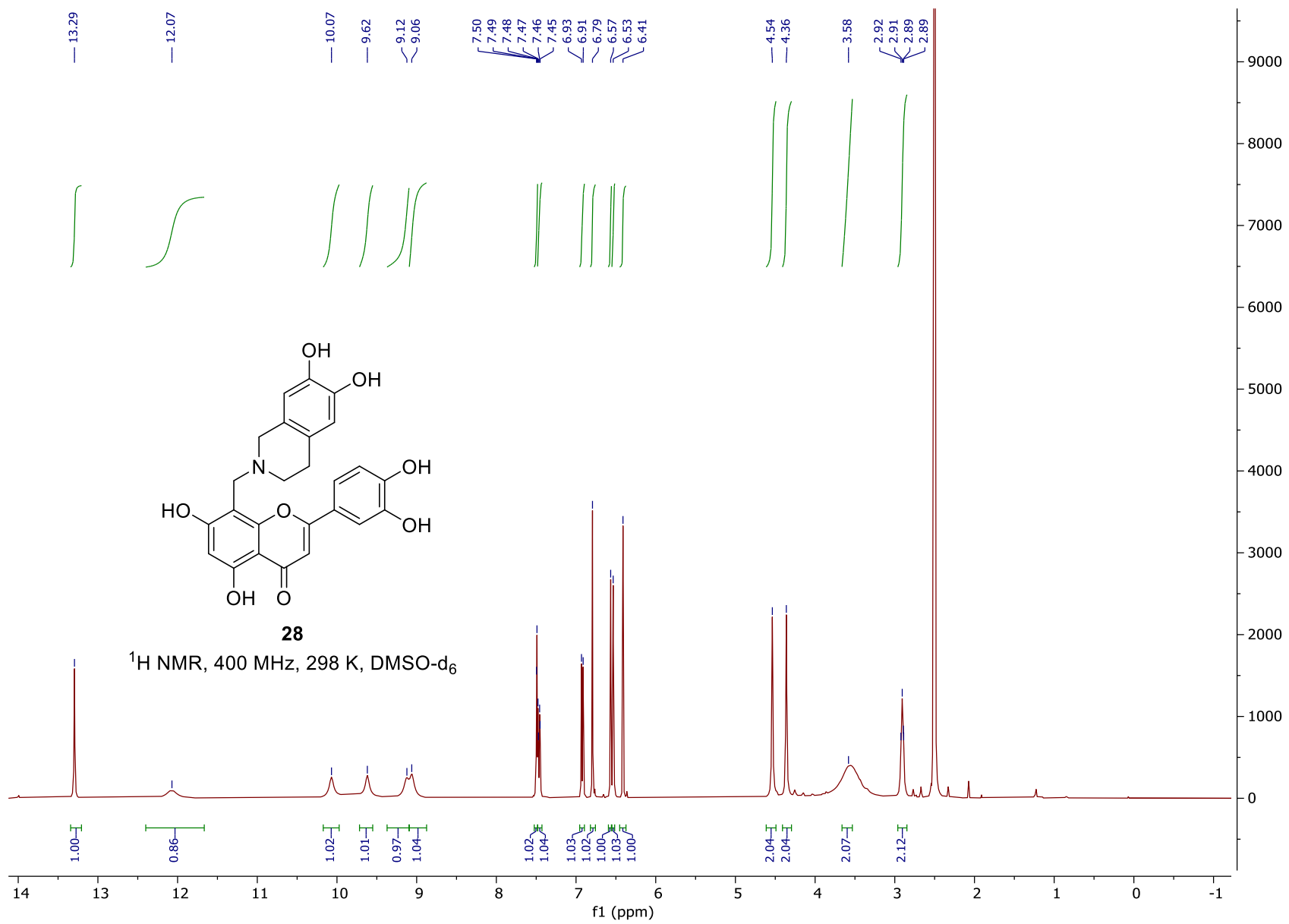
26

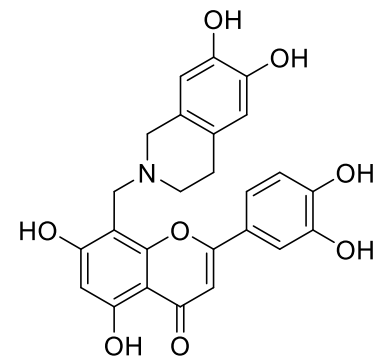
¹³C NMR, 101 MHz, 298 K, DMSO-d₆





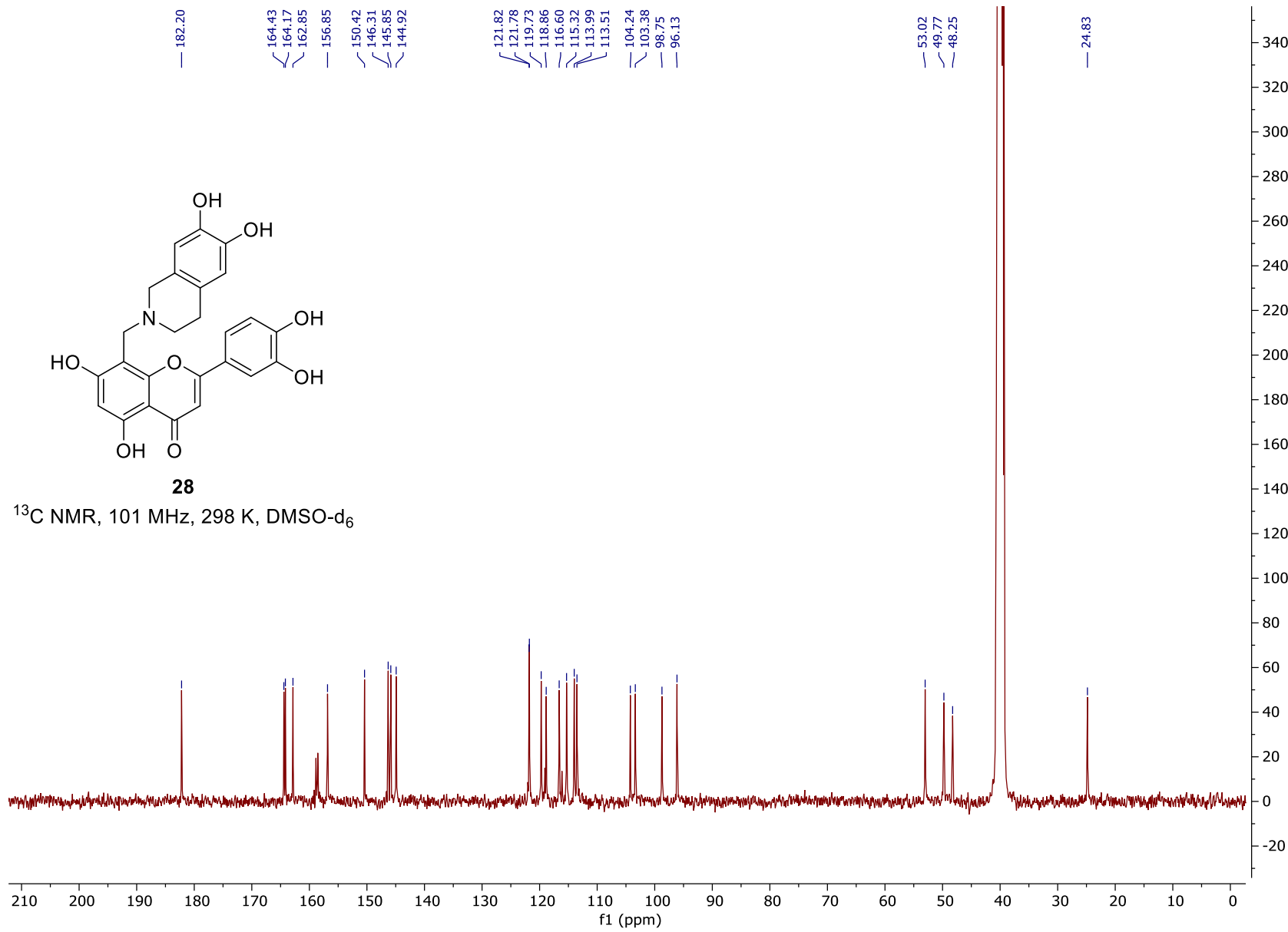


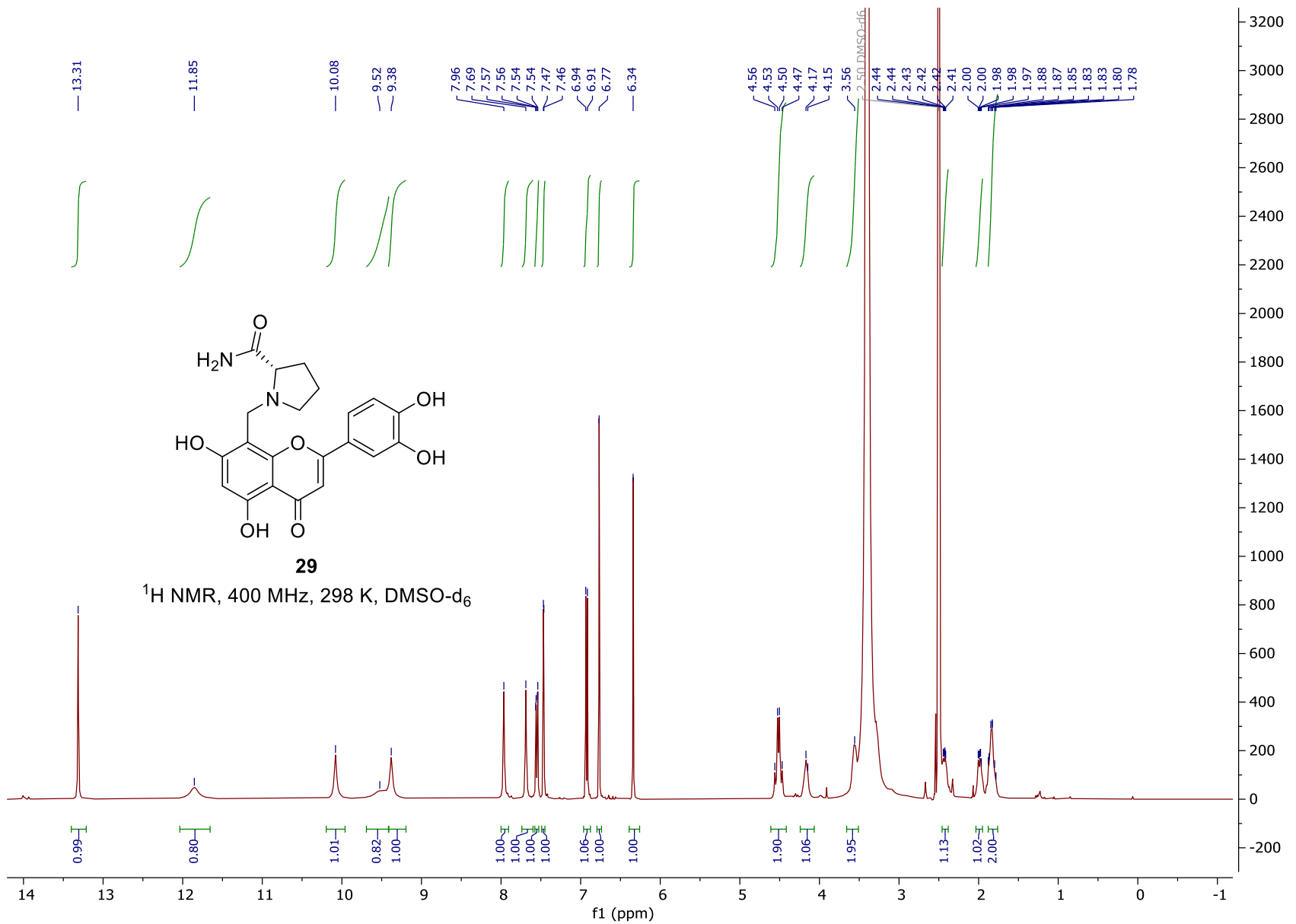


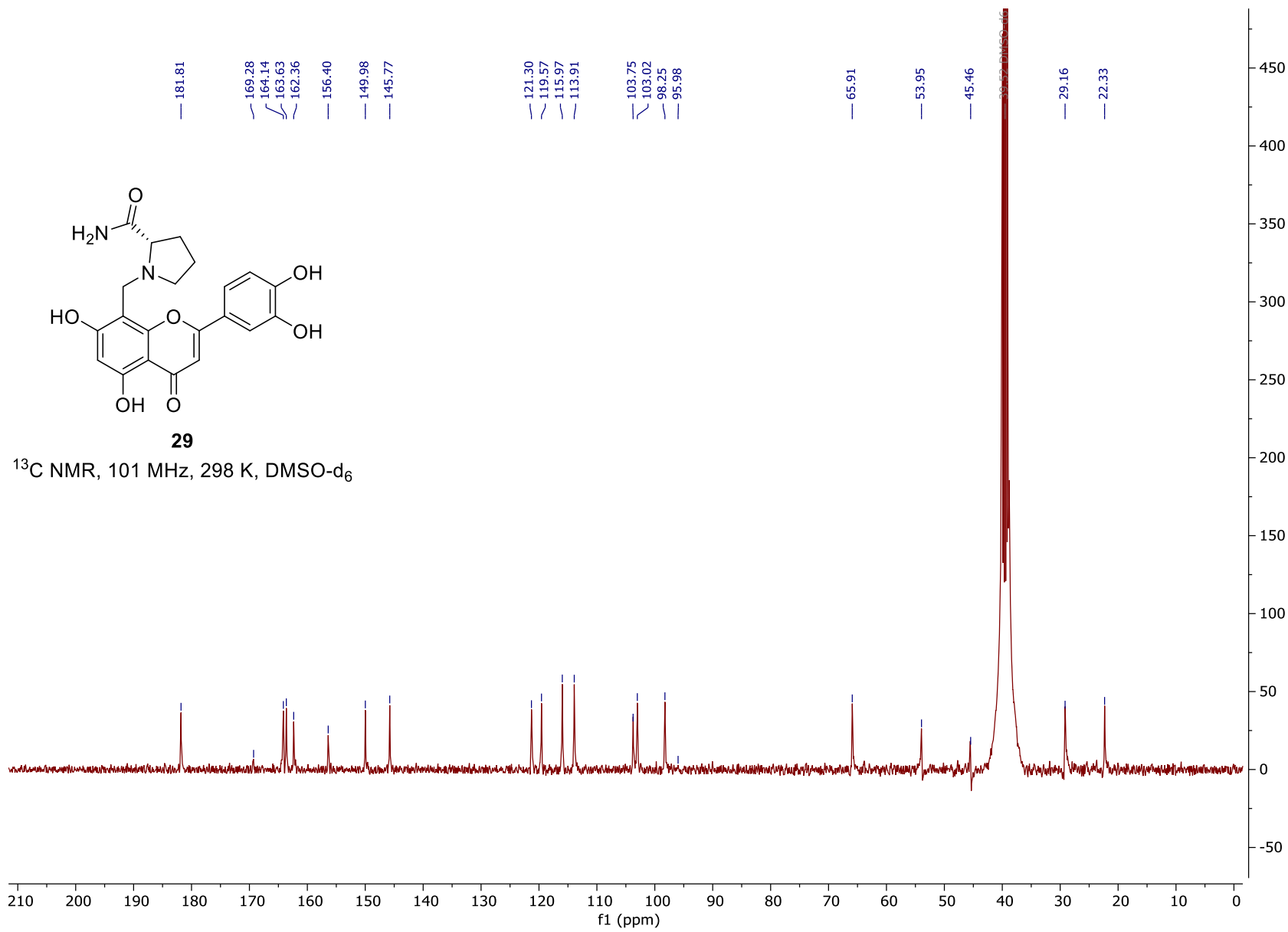


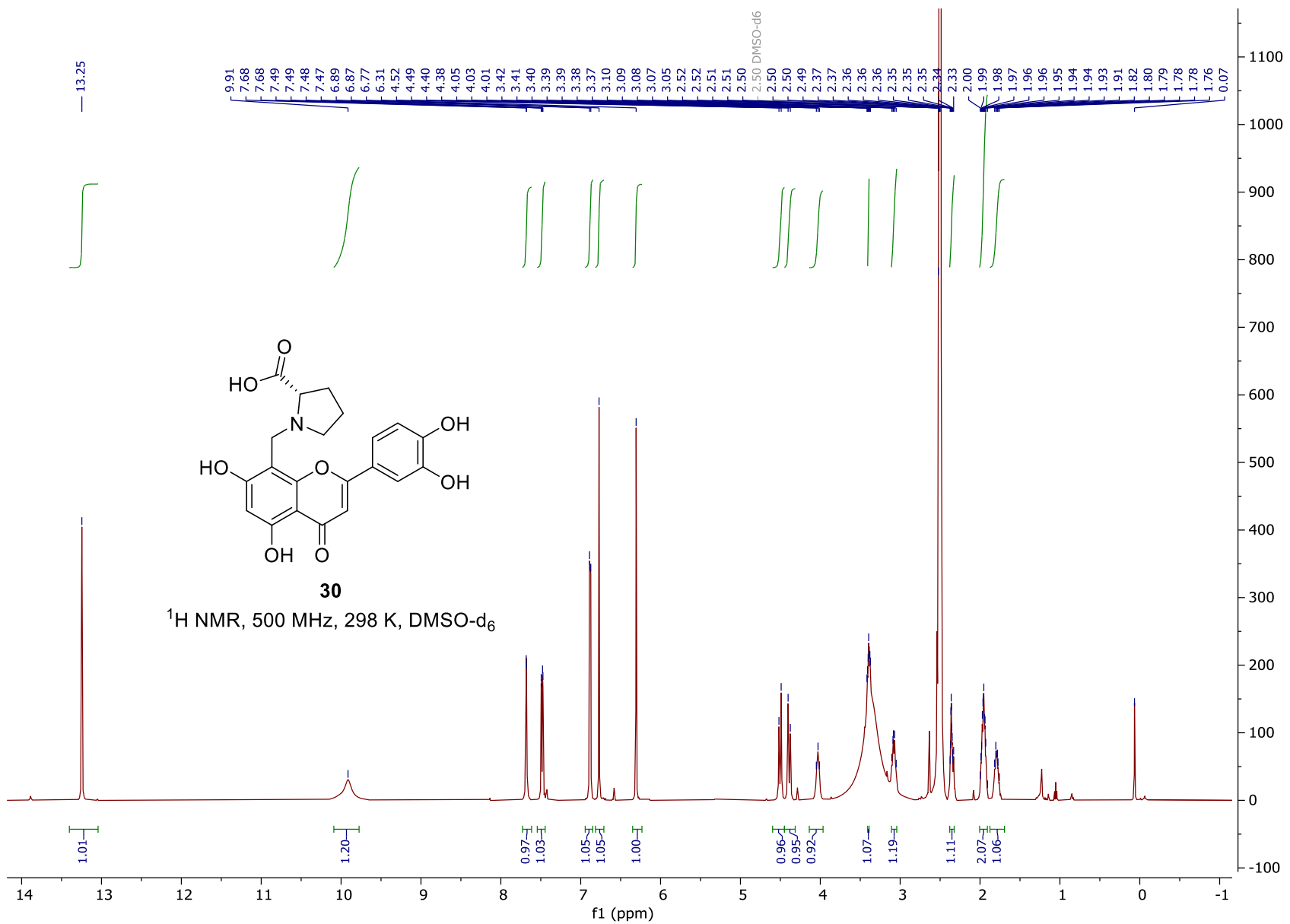
28

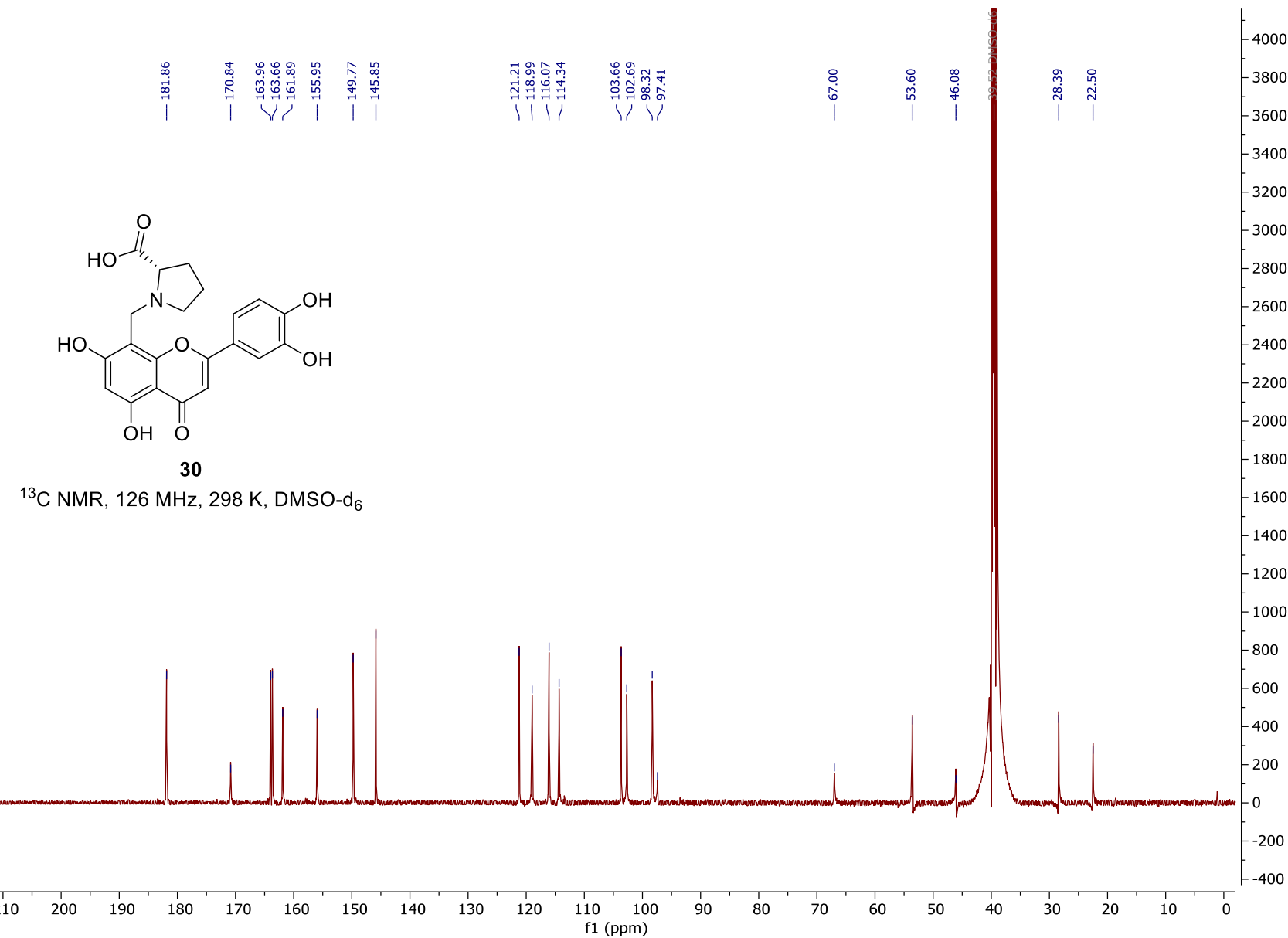
^{13}C NMR, 101 MHz, 298 K, DMSO-d₆

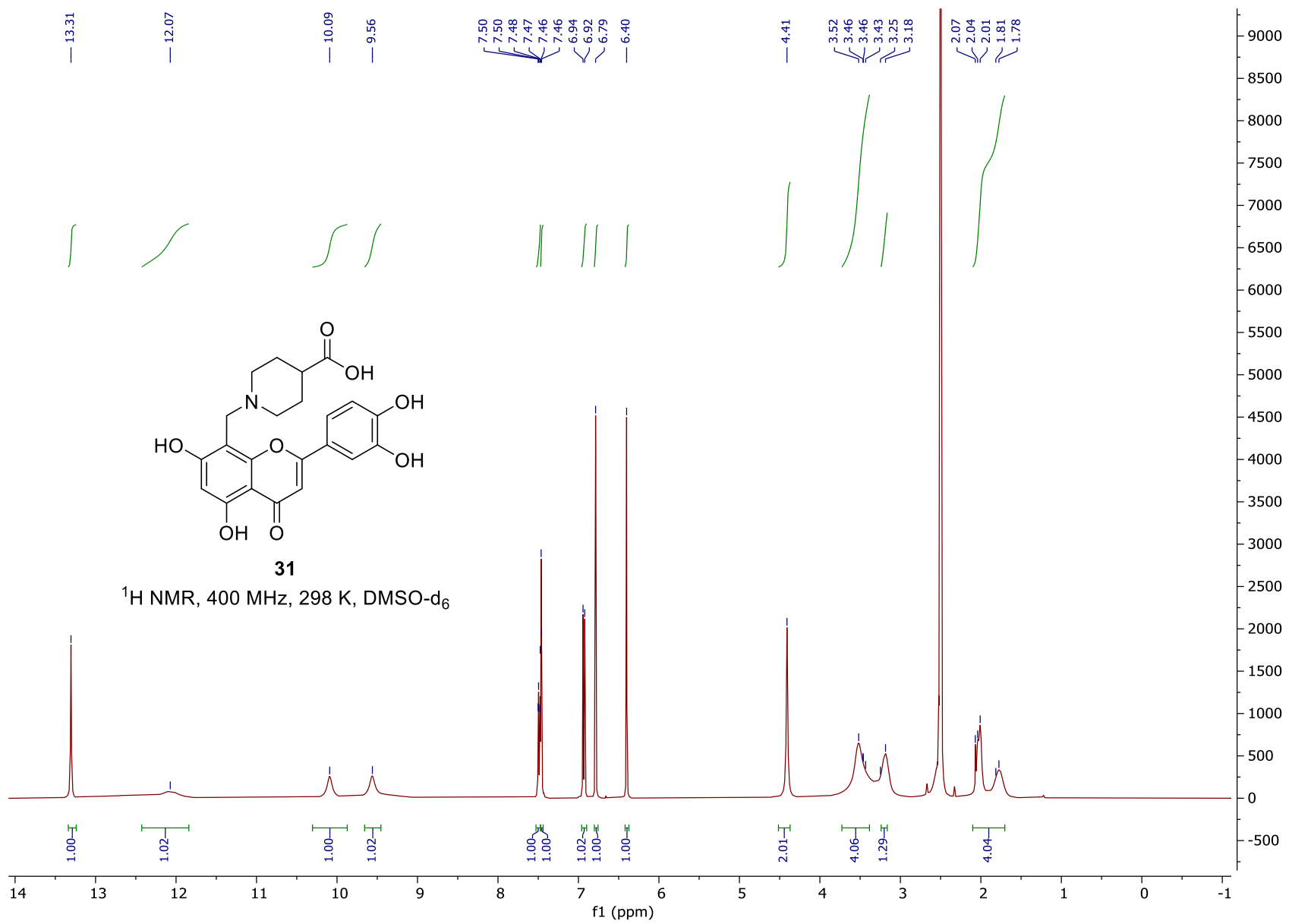


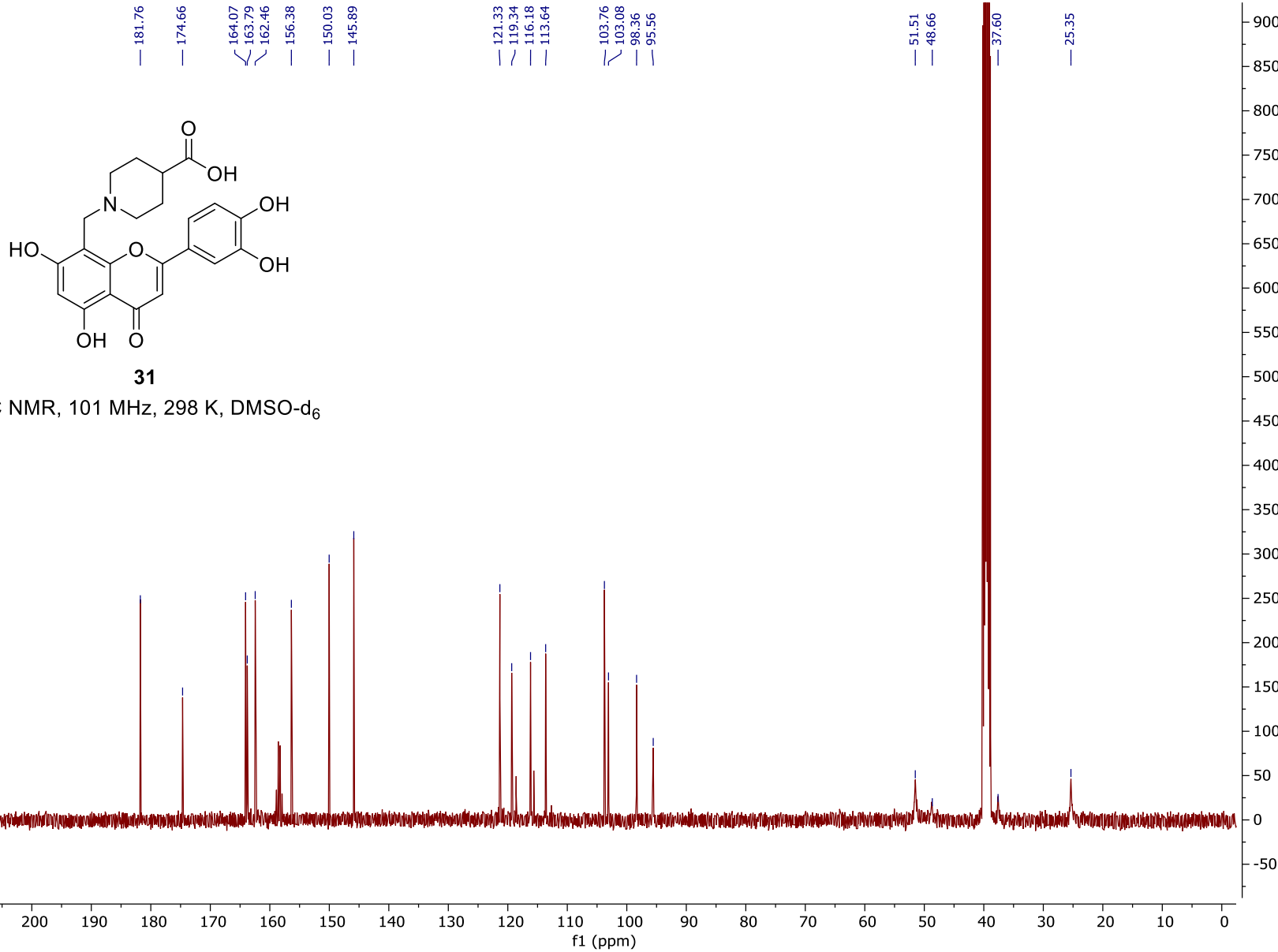


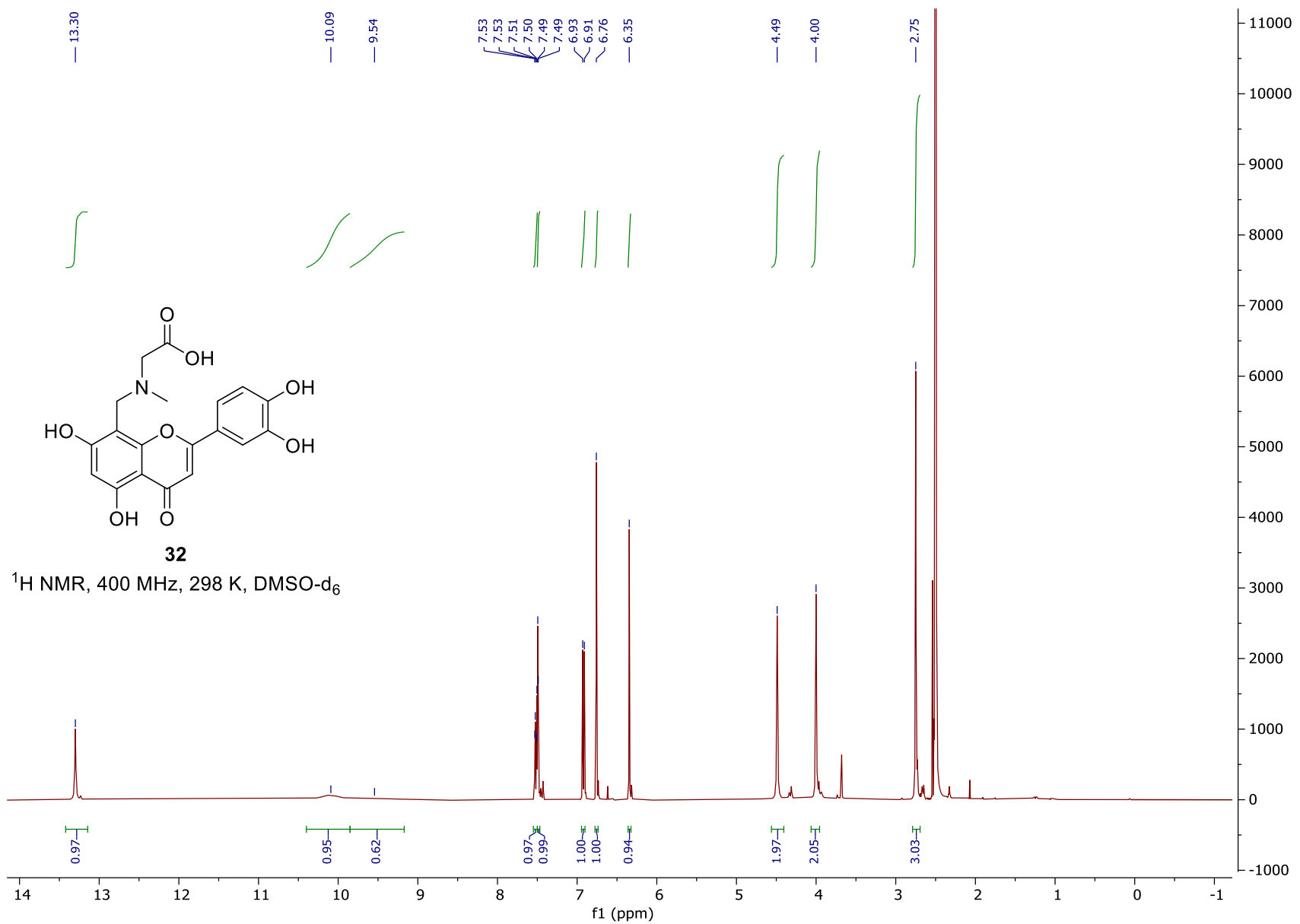


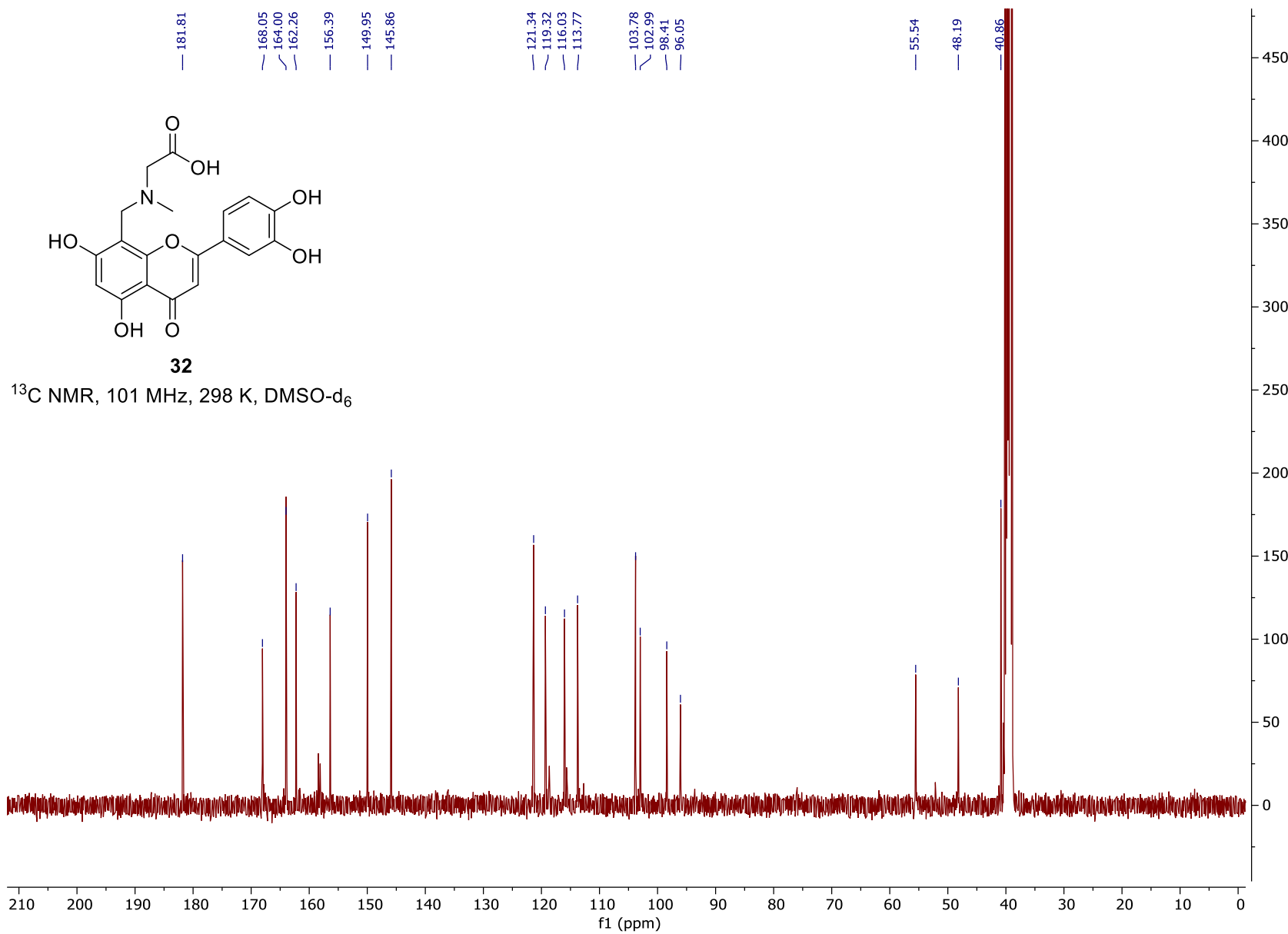












HPLC analysis of final compounds

